Title
Studies of Chromosome Damage Induced by Topoisomerase II Inhibitors in Human Cells

Permalink
https://escholarship.org/uc/item/8f84d89w

Author
Gollapudi, Pavan

Publication Date
2019

Peer reviewed|Thesis/dissertation

UNIVERSITY OF CALIFORNIA
RIVERSIDE

Studies of Chromosome Damage Induced by Topoisomerase II Inhibitors
in Human Cells

A Dissertation submitted in partial satisfaction
of the requirements for the degree of

Doctor of Philosophy

in

Environmental Toxicology

by

Pavan Gollapudi

June 2019

Dissertation Committee:
      Dr. David A. Eastmond, Chairperson
      Dr. Yinsheng Wang
      Dr. Carl Cranor

The Dissertation of Pavan Gollapudi is approved:

_____

_____

_____

Committee Chairperson

University of California, Riverside

ACKNOWLEDGEMENTS

I would like to first thank my advisor, Dr. David Eastmond, for his support, guidance, encouragement, and patience over the years. I would also like to thank the members of my dissertation committee, Dr. Yinsheng Wang and Dr. Carl Cranor, for their support in helping me complete this dissertation. My sincere gratitude goes to Leslie Hasegawa for her assistance over the years on many of the research projects included in this dissertation and somehow figuring out a way to make sure every piece of equipment in the lab worked long enough for me complete my research. Similar thanks must go to all current and former members of the Eastmond lab, especially Virunya Bhat for lending her expertise in risk assessment and data analysis to this research. Lastly, I have to thank my family for always pushing me to reach my goals and my friends both in the ETOX community and at home for keeping me sane throughout this graduate school experience.

The text in Chapter 2 is a reprint of the material as it appears in *Mutation Research Genetic Toxicology and Environmental Mutagenesis* and is co-authored with LS Hasegawa and DA Eastmond, who directed and supervised the research that forms the basis for this dissertation.

ABSTRACT OF THE DISSERTATION

Studies of Chromosome Damage Induced by Topoisomerase II Inhibitors in Human
Cells

by

Pavan Gollapudi

Doctor of Philosophy, Graduate Program in Environmental Toxicology
University of California, Riverside, June 2019
Dr. David A. Eastmond, Chairperson

Topoisomerase II (topo II) is an essential nuclear enzyme that plays a role in

maintaining DNA topology during several cellular processes such as DNA

replication, transcription, DNA repair, and mitosis. While topo II inhibitors are

commonly used in chemotherapy, their use is limited by their causal association

with therapy-related acute myeloid leukemias. Similarly, several environmental

toxicants, including flavonoids, have been reported to inhibit topo II in cell free

assays. Topo II poisons, such as etoposide, act to stabilize the cleavage complex and

inhibit the religation step, an important step which when inhibited leads to the

formation of unprotected double stranded breaks. Catalytic inhibitors affect other

parts of the topo II catalytic cycle and can act either prior to the cleavage step or

after religation of the DNA strand break. The focus of this dissertation research was to more thorough investigate the types of genotoxic effects caused by topo II poisons, catalytic inhibitors, as well as flavonoids fisetin and genistein.

Fisetin, a flavonoid, has previously been reported to inhibit both topo II as well as Aurora kinases. In a comparative study, between fisetin and two Aurora kinase inhibitors, VX-680 and ZM-447439, all three compounds were effective aneuploidy and polyploidy-inducing agents *in vitro*. While the Aurora kinase inhibitors also resulted in increases in chromosome breakage, treatment with fisetin at low-cytotoxic concentrations resulted almost exclusively in chromosome loss, highlighting a key difference between these agents. Topo II inhibitors, aclarubicin, merbarone, etoposide, mitoxantrone, ICRF-154, and ICRF-87, all induced concentration-dependent increases in micronuclei, primarily through chromosome breakage. These results indicated that stabilization of the cleavage complex might not be necessary for chromosome breakage. Because of this, we characterized and quantified stabilized topo II cleavage complexes (SCCs) in intact cells. While topo II poisons are known to cause chromosome breakage by persistent stabilization of the enzyme-DNA cleavage complex, treatment of cells with post-religation catalytic inhibitors ICRF-154 and ICRF-187 also led to increases in cells with SCCs. In contrast, treatment with either aclarubicin or merbarone led to no increases in cells with SCCs. With regards to flavonoids of possible concern, cells treated with genistein, but not fisetin, led to increases in cells with SCCs.

Table of Contents

List of Figures

List of Tables

Chapter 1

Introduction

Topoisomerase II

DNA topoisomerase II (topo II) is a critical nuclear enzyme that plays a role in catalyzing topological changes of DNA during key cellular events to relieve torsional strain within double stranded DNA[1–4]. These include DNA replication and transcription, decatanation of sister chromatids during mitosis, as well as some DNA repair pathways. There are two isoforms of topo II encoded by different genes in mammalian genomes, topo IIa and topo IIb. Topo IIb is expressed at relatively low levels throughout the cell cycle and is expressed in both proliferating and differentiated cells, whereas topo IIa is predominantly in proliferating cells with increasing expression levels found during the G2/M phase of the cell cycle. The differential expression of the two isoforms suggests that both topo IIa and topo IIb may have different roles in the indentified cellular processes.

Mechanistically, the catalytic cycle of topo II can be separated in to six steps: 1) binding of topo II to a DNA duplex; 2) establishing pre-strand passage cleavage/religation equilibrium which involves formation of a transient double strand break (DSB) and formation of a stabilized cleavage complex (SCC); 3) DNA strand passage upon ATP binding; 4) establishing post-strand passage cleavage/religation equilibrium; 5) hydrolysis of ATP which results in 6) the dissociation of the enzyme from the DNA [5,6]. (figure 1-1)

Because topo II plays an important role in several processes related to cell proliferation, these enzymes make good targets for cancer chemotherapeutic drugs. Topo II inhibitors fall into two major categories: topo II poisons and catalytic

inhibitors (figures 1-1 and 1-2) [2,7]. Commonly used drugs such as etoposide

which fall in the category of topo II poisons act at a specific stage of the catalytic

cycle by preventing religation of the transient double strand break. Catalytic

inhibitors, on the other hand, can act at any of the other stages of the catalytic cycle.

Inhibitors that we used in our studies are Aclarubicin, which prevents binding of the

enzyme to the DNA by intercalation; merbarone, which is believed to inhibit the step

prior to formation of the DSB; and ICRF-154 and ICRF-187, which act at a step

following religation trapping the enzyme in a closed-clamp formation when it is not

longer covalently bound to DNA but unable to release from the strand. Most of these

topo ii inhibitors have been shown to have clastogenic effects. Each of the tested

inhibitors are briefly described below.

Aclarubicin

Aclarubicin is an anthracycline compound used in the in the treatment of acute

myelocytic leukemia [8]. It is believed that aclarubicin acts by intercalating in DNA

and preventing the binding of topo II to the DNA strand [9]. This mechanism of

catalytic inhibition by aclarubicin is actually in contrast to other commonly used

anthracycline compounds such as doxorubicin, which are believed to act by

poisoning the enzyme. It has also been demonstrated that aclarubicin can act as a

dual topoisomerase inhibitor with several investigators (Nitiss et al [10], Sorenson

et al [11], and Bridewell et al [12]) showing that aclarubicin can inhibit

topoisomerase I (topo I) with stabilization of covalent topo I complexes at high

concentrations and inhibition of topo I binding at lower more biologically relevant

concentrations. As for its genotoxic effects, aclarubicin has been shown to induce DNA strand breaks in both human myeloid cell lines and cultured Chinese hamster V79 cells using the *in vitro* comet assay as well as induced formation of micronuclei [13,14].

Merbarone

Merbarone is a conjugate of thiobarbituric acid and aniline. It inhibits the catalytic activity of topoisomerase II with some selectivity toward the topo IIa isoform [15,16]. A detailed study of the different steps in the catalytic cycle shows that merbarone has no effect on either DNA binding or ATP hydrolysis but is a potent inhibitor of enzyme-mediated DNA cleavage [17]. Furthermore, merbarone is able to compete with etoposide, suggesting that the two agents might be competing for similar binding sites on topoisomerase II. Inhibition of topo II by merbarone has been shown to induce double stranded DNA breaks *in vitro* using both the Comet assay as well as visualization of gamma-H2AX foci in treated cells [18]. In addition, merbarone has been shown to induce micronuclei *in vitro* and *in vivo [19]*.

Etoposide and Mitoxantrone

Etoposide and mitoxantrone are both commonly prescribed topo II poisons used to treat several types of cancers as well as other diseases such as multiple sclerosis. These compounds act to disrupt the DNA cleavage/religation equilibrium established in the catalytic cycle as previously described. In the absence of these drugs, this equilibrium heavily favors religation, meaning that most of the enzyme found in the cell is free and not covalently bound to DNA. By inhibiting the religation

step, topo II poisons act to stabilize the topo II-DNA cleavage complex leading to persistence of the otherwise transient double stranded break that occurs during the enzyme's catalytic cycle [20]. Subsequent removal of the covalently bound topo II found in the cleavage complex can occur by either endonucleolytic cleavage [21], enzyme-mediated hydrolysis, [22,23], or proteasomal degradation [24] exposing an unprotected DNA double strand break that can result in chromosomal breaks and translocations. Both mitoxantrone and etoposide have been shown *in vitro* and *in vivo* to cause DNA strand breaks as well as micronuclei [20,25,26]

ICRF-154, ICRF-187, and other bisdioxopiperazines.

This class of topo II catalytic inhbitors was originally synthesized as membrane permeable analogs of the metal chelator EDTA [27]. Bisdioxopiperazines have been shown to block topo II in the catalytic cycle after strand passage and religation but before the hydrolysis of the second ATP and release of the enzyme[8]. This mechanism of inhibition results in an enzyme that encircles the strand that had previously been cleaved resulting in a closed-clamp formation. While bisdioxopiperazines are generally not used as primary anti-cancer drugs, a structurally related compound, bimolane, has been used in China for treatment of psoriasis and cancer [28,29]. In addition, the chelating properties of ICR-187, also known as dexrazoxane, make it useful in helping prevent cardiac toxicity caused by generation of reactive oxygen species and associated with chemotherapeutic drugs like doxorubicin. Several bisdioxopiperazines, including ICRF-154, ICRF-187, and

ICRF-193, have been shown to be genotoxic with increases DNA strand breaks, micronuclei, and polyploidy seen in various cell types treated with these compounds [19,30–32].

Topoisomerase II inhibitors and acute leukemia

While several drugs targeting topo II are front line therapies for the treatment of several types of cancer, one limitation of their use is increased risk for development of treatment-related acute leukemia [1–4,6]. These leukemias are secondary to the original cancers for which the topo II inhibitors were originally prescribed and have characteristically short median latency periods of <2-3 years [33–36]. Topo II poisons etoposide and doxorubicin have been associated with treatment-related acute myelogenous leukemia (t-AML) caused by balanced translocations involving the *MLL* gene on chromosome band 11q23 [33,34]. Similarly, mitoxantrone, has been associated with development of a form of acute promyelocytic leukemia (t-APL) as a result of a reciprocal translocation fusing the retinoic acid receptor alpha gene (*RARA*) from chromosome 17 to the promyelocytic leukemia gene (*PML*) on chromosome 15 resulting in the stable expression of a PML-RARa fusion protein [35,36]. In addition, there is some concern that exposure to naturally occurring topo II poisons such as genistein (found in soy products) and other bioflavonoids *in utero* may play a role in development of infant AML which exhibit the same translocations [37,38].

The role of topo II inhibition in the development of leukemia is best understood in the case of development of t-AML following treatment with etoposide.

Studies have indicated that etoposide and its metabolite etoposide quinone can intercalate into the double helix at the cleavage site preventing topo II from rejoining the DNA strands [39–41]. In addition, another metabolite, etoposide catechol, has been shown to poison topo II through covalently binding the enzyme and altering its conformation [42,43]. Double stranded breaks in the *MLL* gene following treatment of etoposide and other topo II poisons appear to preferentially occur within a 1KB breakpoint cluster region (BCR) compared to the much larger 8.3 KB BCR associated with *de novo* AML [44–46]. In addition, in patient studies, most of the breakpoints that have been mapped in the *MLL* gene as well the translocation partner genes fall within a few base pairs of drug-induced enzyme-mediated DNA cleavage sites [39,47,48]. Once both requisite DNA double-stranded breaks have been formed, translocations result from DNA repair processes, in particular non-homologous end joining (NHEJ). More specifically, the alternative NHEJ (aNHEJ) pathway has been implicated in translocations involved with t-AML [49].

The association between mitoxantrone and t-APL has been limited so far to studies in patients who have developed leukemia after treatment with the drug. Interestingly, mitoxantrone is also commonly used in the treatment of multiple sclerosis and t-APL has been reported amongst these patients as well [50]. Similar to other t-AML, the breakpoints mapped in patients appear to occur within hotspot regions more restricted than in *de novo* cases of APL. For instance, approximately half of the t-APL breakpoints involving chromosome 15 map to an 8 bp hotspot in

intron 6 of the *PML* gene in patients treated with mitoxantrone [1,35,50,51]. Further studies are needed to elucidate the mechanisms by which these t-APL specific translocations occur.

There is also some evidence that catalytic inhibitors may induce similar leukemogenic effects as seen with topo II poisons etoposide and mitoxantrone. For instance, patients treated with bimolane and ICRF-154 have been reported to develop t-AML. These patients were typically diagnosed with acute myeloblastic leukemia characterized by the 8;21 (q22;q22) translocation or with t-APL with the 15;17 translocation (q22;q12). The mechanisms by which these and other catalytic inhibitors induce double stranded breaks and subsequent translocations are not well understood.

Aurora Kinases

Aurora kinases are a family of Ser/Thr kinases and are critical for the proper passage of cells through several stages of the cell cycle (Table 1-1). Aurora A kinase localizes to the centrosomes and spindle poles, and plays an important role in the development of the centrosomes and in bipolar spindle formation [52]. Aurora B kinase localizes along the chromosome arms and at centromeres in prophase, at the inner centromeric region during metaphase, at the central spindle and cortex during anaphase, and in the midbody in telophase [53]. It has been shown to play an important role in chromosome biorientation, destabilization of improper microtubule attachments, phosphorylation of histone H3, and cytokinesis. A third

kinase in this family, Aurora C, is thought to have overlapping functions with Aurora

B kinase and acts primarily in germ-line cells functioning during meiosis.

Overexpression of both Aurora A and B kinases has been associated with several

types of cancer including breast, colorectal, ovarian, and pancreatic cancer among

others [54–56]. Overexpression of Aurora A kinase leads to an early entry into

mitosis due to hyperactive centrosomes and multipolar spindle formation, and can

lead to chromosome instability [57]. Similarly, overexpression of Aurora B kinase is

thought play a role in chromosomal instability by interfering with chromosome

biorientation and the spindle assembly checkpoint [52,57]. In addition to

deregulated cell cycle progression, overexpression of Aurora kinases can contribute

to tumorigenesis due to the complex networks formed by their targets [58]. For

instance, both Aurora A and Aurora B have been shown to phosphorylate p53

directly as well as inhibit the protein through activation of upstream regulators of

p53, leading to both decreased p53 transcriptional activity and increased Mdm2-

mediated degradation of the protein and loss of tumor suppressor function.

Similarly, Aurora kinases have been shown to be involved in networks related to

BRCA1 and BRCA2 tumor suppressor proteins and well as myc signaling pathways.

As a result, both Aurora A and B kinases are thought to be promising targets for

chemotherapeutic agents (Table 1) [58].

Flavonoids and Cancer

Flavonoids comprise a large group of secondary metabolites in plants and are common constituents of fruits, vegetables and dietary supplements. Estimated dietary intake of flavonoids through diet range from 100-500 mg/day but can reach levels of 1 g or higher if taken in the form of supplements [59]. Flavonoids are typically associated with anti-carcinogenic, cardioprotective, and anti-oxidant properties with these effects shown *in vitro* and in animal models. Several studies have shown, however, that certain flavonoids may also possess genotoxic and carcinogenic properties. Compounds such as quercetin have been shown to be mutagenic in the Ames assay, induce chromosomal aberrations, lead to increases in micronuclei, and damage DNA through generation of reactive oxygen species [60–64]. There is also evidence to suggest that flavonoids, such as quercetin, genistein, and fisetin inhibit DNA topoisomerases, which might play a role in the genotoxicity associated with these compounds. As described previously, there is some concern that exposure to genistein and other flavanoids may play a role in development of infant AML as many of these cancers are associated with the same or similar translocations involving the chromosome band 11q23 as do the t-AMLs associated with etoposide described earlier.

In addition to topo II, flavonoids have been reported to affect several targets within the cell [65–67]. Among these are cyclin dependent kinases as well as the Aurora family of Ser/Thr kinases, which may play a role in certain types of cancers. The broad range of targets that flavonoids are reported to affect and their roles in

10

cancer formation and treatment make this an interesting and important class of compounds.

Specific aims of this research

1. **Characterize the genotoxic effects of two small molecule Aurora kinase inhibitors and compare effects seen to flavonoid fisetin**. The goals of this project are to further characterize the genotoxic effects of fisetin, particularly the aneugenic effects which are not well understood. In addition, since inhibition of Aurora kinases and disruption of the spindle assembly checkpoint can lead to segregation errors and aneuploidy, we decided to follow up on a recent report showing that fisetin may inhibit Aurora B, to see if this might provide a possible explanation as to how fisetin induces aneuploidy. To do this we compared effects seen with fisetin to two known small molecule aurora kinase inhibitors, VX-680 and ZM-447439. Lastly, as part of an ongoing effort in the lab, we wanted to validate a flow cytometry based assay to detect numerical chromosomal aberrations by testing these kinase inhibitors which act to induce aneuploidy and polyploidy through a unique mechanism.

2. **Examine dose-response relationships for induction of micronuclei *in vitro* in cells treated with topoisomerase II inhibitors.** Compounds such as fisetin and other flavonoids have previously been reported to inhibit topoisomerase II in cell-free enzyme activity assays, however the aneugenic

responses we observed in cells treated with fisetin were not consistent with clastogenic effects normally associated with topo II poisons. Because of this we wanted to further investigate the examine the genotoxic effects of known topo II inhibitors by looking at dose-response relationships in vitro using a broad range inhibitors to determine the types of chromosomal alterations induced by different classes of inhibitors and see how different mechanisms may influence the shape of the dose-response curve. In doing so, we also wanted to compare the use of traditional microscopy based techniques to measure chromosome damage using the MN assay with a more recently developed flow-cytometry based version of the assay. Last, and largely based on our previous experiences in the lab working with data from some of these flow based assays, we wanted to address some potential statistical limitations associated with *in vitro* dose-response data for genotoxicants.

3. **Characterize ability of various topo II inhibitors and flavonoids to stabilize topo II cleavage complexes in human lymphoblastoid cells**. Here we further investigated dose-response relationships of several topoisomerase II inhibitors by looking the ability of these compounds to stabilize the cleavage complex, an important step that occurs prior to the formation of double stranded breaks and micronuclei. We used a recently published flow cytometry based assay to detect topo II covalently bound to DNA to see if this method could be used to not only characterize dose-

response relationships SCC formation, but also identify where in the catalytic cycle a proposed topo II inhibitor might act. Our studies included the topo II poisons etoposide and mitoxantrone, as well as catalytic inhibitors aclarubicin, merbarone, the bisdioxopiperazines, ICRF-154 and ICRF-187, which all act through different mechanisms. We also examined two flavonoid compounds fisetin and genistein, which have both been reported to affect topoisomerase II using isolated enzymes in cell free assays to see if similar effects on topo II can be observed in cells.

Table 1-1 Summary of Aurora kinase functions and their roles in cancer
(adapted from Tang *et al [58]*)

Kinase	Localization	Function	Cancers associated with overexpression	Inhibitors in clinical studies
Aurora A	Centrosomes, Spindles, midbody	Centrosomes maturation, bipolar spindle assembly, mitotic entry/exit	Breast cancer Ovarian cancer Colorectal cancer Lung cancer Prostate cancer Acute Myeloid Leukemia	MLN8054; phase I ENMD-2076; phase II MLN8237; phase III VX-680; phase III AMG-900; phase I
Aurora B	Chromosome arms, kinetochores, midbody	Chromosome condensation, kinetochore-microtubule attachments, chromosome segregation, regulation of cytokinesis	Breast cancer Ovarian cancer Colorectal cancer Prostate cancer Cervical cancer Acute Myeloid Leukemia	AZD1152; phase II/III VX-680; phase III, PHA68032; preclinical PHA-739358, phase II
Aurora C	Chromosomes, midbody	Meiotic chromosome segregation, cytokinesis	Breast cancer Cervical cancer Prostate cancer Glioma	VX-680; phase III, PHA68032; preclinical PHA-739358, phase II

Figure 1-1 Topoisomerase II Catalytic Cycle
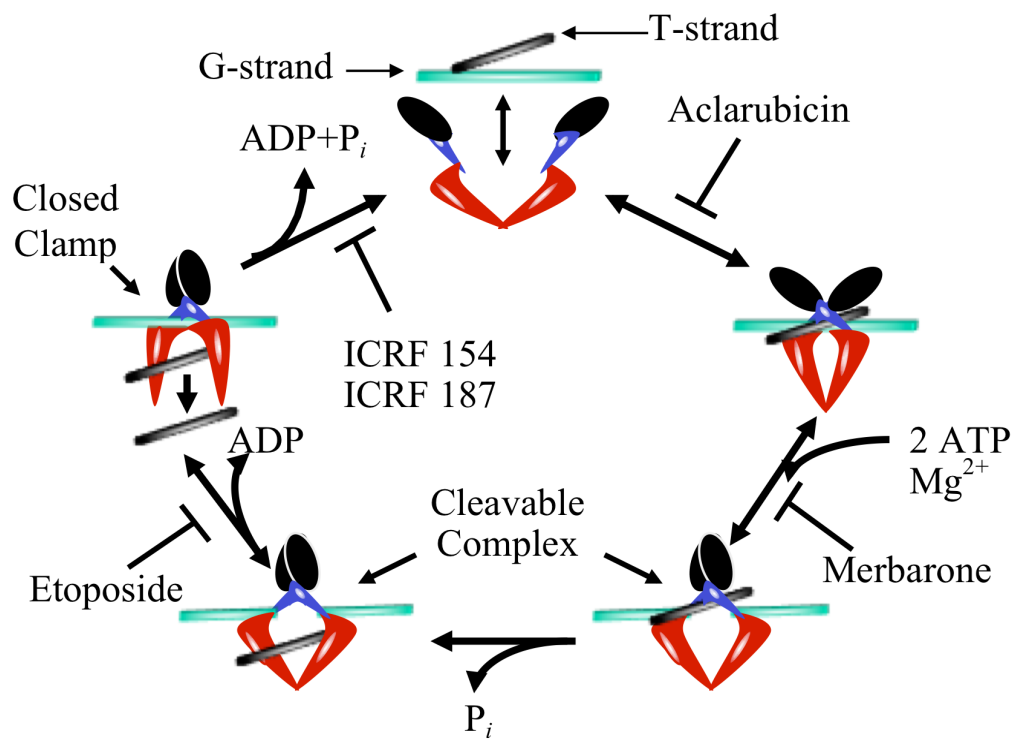
Figure 1-1 Topo II catalytic cycle. The sides of action of known topo II inhibitors used in the current study are shown. Adapted from Mondrala S and Eastmond DA, 2010 [5]

Figure 1-2 Chemical Structures of Select Topoisomerase II Inhibitors

Aclarubicin   Merbarone

Etoposide

ICRF-154   ICRF-187

Mitoxantrone
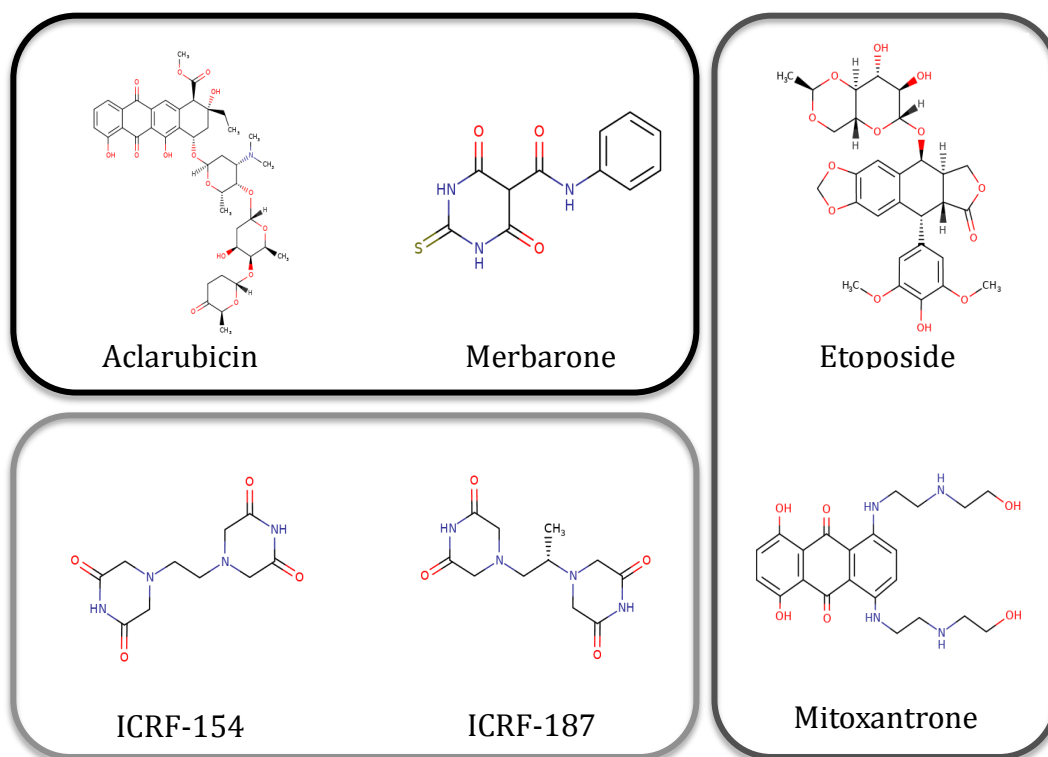
Figure 1-2 Chemical structures of the topoisomerase II inhibitors studied. The top left box depicts two catalytic inhibitors, aclarubicin and merbarone, that act prior to formation of the cleavage complex. The vertically oriented box on the right show chemical structures of topo II poisons etoposide and mitoxantrone. Last, boxed on the bottom left are the bisdioxopiperazines, ICRF-154 and ICRF-187, which act following religation of the double stranded break.

References

1. Pendleton M, Hunter Lindsey R, Felix CA, Grimwade D, Osheroff N. Topoisomerase II and leukemia. Ann N Y Acad Sci. 2014;1310: 98–110.

2. McClendon AK, Kathleen McClendon A, Osheroff N. DNA topoisomerase II, genotoxicity, and cancer. Mutat Res/Fundam Mol Mech Mutag. 2007;623: 83–97.

3. Deweese JE, Osheroff N. The DNA cleavage reaction of topoisomerase II: wolf in sheep's clothing. Nucleic Acids Res. 2009;37: 738–748.

4. Vos SM, Tretter EM, Schmidt BH, Berger JM. All tangled up: how cells direct, manage and exploit topoisomerase function. Nat Rev Mol Cell Biol. 2011;12: 827–841.

5. Mondrala S, Eastmond DA. Topoisomerase II inhibition by the bioactivated benzene metabolite hydroquinone involves multiple mechanisms. Chem Biol Interact. 2010;184: 259–268.

6. Nitiss JL. DNA topoisomerase II and its growing repertoire of biological functions. Nat Rev Cancer. 2009;9: 327–337.

7. Nitiss JL. Targeting DNA topoisomerase II in cancer chemotherapy. Nat Rev Cancer. 2009;9: 338–350.

8. Larsen AK, Escargueil AE, Skladanowski A. Catalytic topoisomerase II inhibitors in cancer therapy. Pharmacol Ther. 2003;99: 167–181.

9. Sørensen BS, Sinding J, Andersen AH, Alsner J, Jensen PB, Westergaard O. Mode of action of topoisomerase II-targeting agents at a specific DNA sequence. Uncoupling the DNA binding, cleavage and religation events. J Mol Biol. 1992;228: 778–786.

10. Nitiss JL, Pourquier P, Pommier Y. Aclacinomycin A stabilizes topoisomerase I covalent complexes. Cancer Res. 1997;57: 4564–4569.

11. Sørensen BS, Jensen PB, Sehested M, Jensen PS, Kjeldsen E, Nielsen OF, et al. Antagonistic effect of aclarubicin on camptothecin induced cytotoxicity: role of topoisomerase I. Biochem Pharmacol. 1994;47: 2105–2110.

12. Bridewell DJ, Finlay GJ, Baguley BC. Differential actions of aclarubicin and doxorubicin: the role of topoisomerase I. Oncol Res. 1997;9: 535–542.

13. Hajji N, Mateos S, Pastor N, Domínguez I, Cortés F. Induction of genotoxic and cytotoxic damage by aclarubicin, a dual topoisomerase inhibitor. Mutat Res. 2005;583: 26–35.

14. Gieseler F, Bauer E, Nuessler V, Clark M, Valsamas S. Molecular effects of topoisomerase II inhibitors in AML cell lines: correlation of apoptosis with topoisomerase II activity but not with DNA damage. Leukemia. 1999;13: 1859–1863.

15. Drake FH, Hofmann GA, Mong SM, Bartus JO, Hertzberg RP, Johnson RK, et al. In vitro and intracellular inhibition of topoisomerase II by the antitumor agent merbarone. Cancer Res. 1989;49: 2578–2583.

16. Drake FH, Hofmann GA, Bartus HF, Mattern MR, Crooke ST, Mirabelli CK. Biochemical and pharmacological properties of p170 and p180 forms of topoisomerase II. Biochemistry. 1989;28: 8154–8160.

17. Fortune JM, Osheroff N. Merbarone inhibits the catalytic activity of human topoisomerase IIalpha by blocking DNA cleavage. J Biol Chem. 1998;273: 17643–17650.

18. Pastor N, Domínguez I, Orta ML, Campanella C, Mateos S, Cortés F. The DNA topoisomerase II catalytic inhibitor merbarone is genotoxic and induces endoreduplication. Mutat Res. 2012;738-739: 45–51.

19. Wang L, Eastmond DA. Catalytic inhibitors of topoisomerase II are DNA-damaging agents: induction of chromosomal damage by merbarone and ICRF-187. Environ Mol Mutagen. 2002;39: 348–356.

20. Lynch A, Harvey J, Aylott M, Nicholas E, Burman M, Siddiqui A, et al. Investigations into the concept of a threshold for topoisomerase inhibitor-induced clastogenicity. Mutagenesis. 2003;18: 345–353.

21. Hartsuiker E, Neale MJ, Carr AM. Distinct requirements for the Rad32(Mre11) nuclease and Ctp1(CtIP) in the removal of covalently bound topoisomerase I and II from DNA. Mol Cell. 2009;33: 117–123.

22. Cortes Ledesma F, El Khamisy SF, Zuma MC, Osborn K, Caldecott KW. A human 5'-tyrosyl DNA phosphodiesterase that repairs topoisomerase-mediated DNA damage. Nature. 2009;461: 674–678.

23. Borda MA, Palmitelli M, Verón G, González-Cid M, de Campos Nebel M. Tyrosyl-DNA-phosphodiesterase I (TDP1) participates in the removal and repair of stabilized-Top2α cleavage complexes in human cells. Mutat Res. 2015;781: 37–48.

24. Mao Y, Desai SD, Ting CY, Hwang J, Liu LF. 26 S proteasome-mediated degradation of topoisomerase II cleavable complexes. J Biol Chem. 2001;276: 40652–40658.

25. Wang L, Roy SK, Eastmond DA. Differential cell cycle-specificity for chromosomal damage induced by merbarone and etoposide in V79 cells. Mutat Res/Fundam Mol Mech Mutag. 2007;616: 70–82.

26. Boos G, Stopper H. Genotoxicity of several clinically used topoisomerase II inhibitors. Toxicol Lett. 2000;116: 7–16.

27. Creighton AM, Birnie GD. Biochemical studies on growth-inhibitory bisdioxopiperazines. I. Effect on dna, rna and protein synthesis in mouse-embryo fibroblasts. International Journal of Cancer. 1970;5: 47–54.

28. Li YS, Zhao YL, Jiang QP, Yang CL. Specific chromosome changes and nonoccupational exposure to potentially carcinogenic agents in acute leukemia in China. Leuk Res. 1989;13: 367–376.

29. Xue Y, Lu D, Guo Y, Lin B. Specific chromosomal translocations and therapy-related leukemia induced by bimolane therapy for psoriasis. Leuk Res. 1992;16: 1113–1123.

30. Vuong MC, Hasegawa LS, Eastmond DA. A comparative study of the cytotoxic and genotoxic effects of ICRF-154 and bimolane, two catalytic inhibitors of topoisomerase II. Mutat Res. 2013;750: 63–71.

31. Hajji N, Pastor N, Mateos S, Domínguez I, Cortés F. DNA strand breaks induced by the anti-topoisomerase II bis-dioxopiperazine ICRF-193. Mutat Res. 2003;530: 35–46.

32. Pastor N, Domínguez I, Mateos S, Cortés F. A comparative study of genotoxic effects of anti-topoisomerase II drugs ICRF-193 and bufalin in Chinese hamster ovary cells. Mutation Research/Genetic Toxicology and Environmental Mutagenesis. 2002;515: 171–180.

33. Park SH, Chi H-S, Cho Y-U, Jang S, Park C-J. Evaluation of prognostic factors in patients with therapy-related acute myeloid leukemia. Blood Res. 2013;48: 185–192.

34. Mauritzson N, Albin M, Rylander L, Billström R, Ahlgren T, Mikoczy Z, et al. Pooled analysis of clinical and cytogenetic features in treatment-related and de novo adult acute myeloid leukemia and myelodysplastic syndromes based on a consecutive series of 761 patients analyzed 1976-1993 and on 5098 unselected cases reported in the literature 1974-2001. Leukemia. 2002;16: 2366–2378.

35. Joannides M, Mays AN, Mistry AR, Hasan SK, Reiter A, Wiemels JL, et al. Molecular pathogenesis of secondary acute promyelocytic leukemia. Mediterr J Hematol Infect Dis. 2011;3: e2011045.

36. Rashidi A, Fisher SI. Therapy-related acute promyelocytic leukemia: a systematic review. Med Oncol. 2013;30: 625.

37. Strick R, Strissel PL, Borgers S, Smith SL, Rowley JD. Dietary bioflavonoids induce cleavage in the MLL gene and may contribute to infant leukemia. Proc Natl Acad Sci U S A. 2000;97: 4790–4795.

38. Spector LG, Xie Y, Robison LL, Heerema NA, Hilden JM, Lange B, et al. Maternal diet and infant leukemia: the DNA topoisomerase II inhibitor hypothesis: a report from the children's oncology group. Cancer Epidemiol Biomarkers Prev. 2005;14: 651–655.

39. Lovett BD, Strumberg D, Blair IA, Pang S, Burden DA, Megonigal MD, et al. Etoposide metabolites enhance DNA topoisomerase II cleavage near leukemia-associated MLL translocation breakpoints. Biochemistry. 2001;40: 1159–1170.

40. Gantchev TG, Hunting DJ. Inhibition of the topoisomerase II-DNA cleavable complex by the ortho-quinone derivative of the antitumor drug etoposide (VP-16). Biochem Biophys Res Commun. 1997;237: 24–27.

41. Gantchev TG, Hunting DJ. The ortho-quinone metabolite of the anticancer drug etoposide (VP-16) is a potent inhibitor of the topoisomerase II/DNA cleavable complex. Mol Pharmacol. 1998;53: 422–428.

42. Bender RP, Ham A-JL, Osheroff N. Quinone-Induced Enhancement of DNA Cleavage by Human Topoisomerase IIα: Adduction of Cysteine Residues 392 and 405†. Biochemistry. 2007;46: 2856–2864.

43. Bender RP, Osheroff N. Mutation of Cysteine Residue 455 to Alanine in Human Topoisomerase IIα Confers Hypersensitivity to Quinones: Enhancing DNA Scission by Closing the N-Terminal Protein Gate†. Chem Res Toxicol. 2007;20: 975–981.

44. Felix CA, Kolaris CP, Osheroff N. Topoisomerase II and the etiology of chromosomal translocations. DNA Repair . 2006;5: 1093–1108.

45. Cowell IG, Austin CA. Mechanism of generation of therapy related leukemia in response to anti-topoisomerase II agents. Int J Environ Res Public Health. 2012;9: 2075–2091.

46. Ezoe S. Secondary leukemia associated with the anti-cancer agent, etoposide, a topoisomerase II inhibitor. Int J Environ Res Public Health. 2012;9: 2444–2453.

47. Cowell IG, Sondka Z, Smith K, Lee KC, Manville CM, Sidorczuk-Lesthuruge M, et al. Model for MLL translocations in therapy-related leukemia involving topoisomerase II -mediated DNA strand breaks and gene proximity. Proceedings of the National Academy of Sciences. 2012;109: 8989–8994.

48. Lovett BD, Lo Nigro L, Rappaport EF, Blair IA, Osheroff N, Zheng N, et al. Near-precise interchromosomal recombination and functional DNA topoisomerase II cleavage sites at MLL and AF-4 genomic breakpoints in treatment-related acute lymphoblastic leukemia with t(4;11) translocation. Proc Natl Acad Sci U S A. 2001;98: 9802–9807.

49. Wray J, Williamson EA, Singh SB, Wu Y, Cogle CR, Weinstock DM, et al. PARP1 is required for chromosomal translocations. Blood. 2013;121: 4359–4365.

50. Hasan SK, Mays AN, Ottone T, Ledda A, La Nasa G, Cattaneo C, et al. Molecular analysis of t(15;17) genomic breakpoints in secondary acute promyelocytic leukemia arising after treatment of multiple sclerosis. Blood. American Society of Hematology; 2008;112: 3383–3390.

51. Joannides M, Grimwade D. Molecular biology of therapy-related leukaemias. Clin Transl Oncol. 2010;12: 8–14.

52. Lens SMA, Voest EE, Medema RH. Shared and separate functions of polo-like kinases and aurora kinases in cancer. Nat Rev Cancer. 2010;10: 825–841.

53. Katayama H, Sen S. Aurora kinase inhibitors as anticancer molecules. Biochimica et Biophysica Acta (BBA) - Gene Regulatory Mechanisms. 2010;1799: 829–839.

54. Sakakura C, Hagiwara A, Yasuoka R, Fujita Y, Nakanishi M, Masuda K, et al. Tumour-amplified kinase BTAK is amplified and overexpressed in gastric cancers with possible involvement in aneuploid formation. Br J Cancer. 2001;84: 824–831.

55. Takahashi T, Futamura M, Yoshimi N, Sano J, Katada M, Takagi Y, et al. Centrosomal Kinases, HsAIRK1 and HsAIRK3, are Overexpressed in Primary Colorectal Cancers. Jpn J Cancer Res. 2000;91: 1007–1014.

56. Gritsko TM, Coppola D, Paciga JE, Yang L, Sun M, Shelley SA, et al. Activation and overexpression of centrosome kinase BTAK/Aurora-A in human ovarian cancer. Clin Cancer Res. 2003;9: 1420–1426.

57. Baba Y, Nosho K, Shima K, Irahara N, Kure S, Toyoda S, et al. Aurora-A expression is independently associated with chromosomal instability in colorectal cancer. Neoplasia. 2009;11: 418–425.

58. Tang A, Gao K, Chu L, Zhang R, Yang J, Zheng J. Aurora kinases: novel therapy targets in cancers. Oncotarget. 2017;8: 23937–23954.

59. Skibola CF, Smith MT. Potential health impacts of excessive flavonoid intake. Free Radic Biol Med. 2000;29: 375–383.

60. Bjeldanes LF, Chang GW. Mutagenic activity of quercetin and related compounds. Science. 1977;197: 577–578.

61. Carver JH, Carrano AV, MacGregor JT. Genetic effects of the flavonols quercetin, kaempferol, and galangin on Chinese hamster ovary cells in vitro. Mutat Res. 1983;113: 45–60.

62. Caria H, Chaveca T, Laires A, Rueff J. Genotoxicity of quercetin in the micronucleus assay in mouse bone marrow erythrocytes, human lymphocytes, V79 cell line and identification of kinetochore-containing (CREST staining) micronuclei in human lymphocytes. Mutat Res. 1995;343: 85–94.

63. Rueff J, Laires A, Borba H, Chaveca T, Gomes MI, Halpern M. Genetic toxicology of flavonoids: the role of metabolic conditions in the induction of reverse mutation, SOS functions and sister-chromatid exchanges. Mutagenesis. 1986;1: 179–183.

64. Hodnick WF, Kung FS, Roettger WJ, Bohmont CW, Pardini RS. Inhibition of mitochondrial respiration and production of toxic oxygen radicals by flavonoids. A structure-activity study. Biochem Pharmacol. 1986;35: 2345–2357.

65. Lu X, Jung J in, Cho HJ, Lim DY, Lee HS, Chun HS, et al. Fisetin inhibits the activities of cyclin-dependent kinases leading to cell cycle arrest in HT-29 human colon cancer cells. J Nutr. 2005;135: 2884–2890.

66. Sung B, Pandey MK, Aggarwal BB. Fisetin, an inhibitor of cyclin-dependent kinase 6, down-regulates nuclear factor-kappaB-regulated cell proliferation, antiapoptotic and metastatic gene products through the suppression of TAK-1 and receptor-interacting protein-regulated IkappaBalpha kinase activation. Mol Pharmacol. 2007;71: 1703–1714.

67. Salmela A-L, Pouwels J, Varis A, Kukkonen AM, Toivonen P, Halonen PK, et al. Dietary flavonoid fisetin induces a forced exit from mitosis by targeting the mitotic spindle checkpoint. Carcinogenesis. 2009;30: 1032–1040.

Chapter 2

A Comparative Study of the Aneugenic and Polyploidy-inducing Effects of Fisetin and Two Model Aurora Kinase Inhibitors

Abstract

Fisetin, a plant flavonol commonly found in fruits, nuts and vegetables, is frequently added to nutritional supplements due to its reported cardioprotective, anti-carcinogenic and antioxidant properties. Earlier reports from our laboratory and others have indicated that fisetin has both aneugenic and clastogenic properties in cultured cells. More recently, fisetin has also been reported to target Aurora B kinase, a Ser/Thr kinase involved in ensuring proper microtubule attachment at the spindle assembly checkpoint, and an enzyme that is overexpressed in several types of cancer. Here we have further characterized the chromosome damage caused by fisetin and compared it with that induced by two known Aurora kinase inhibitors, VX-680 and ZM-447439, in cultured TK6 cells using the micronucleus assay with CREST staining as well as a flow cytometry-based assay that measures multiple types of numerical chromosomal aberrations. The three compounds were highly effective in inducing aneuploidy and polyploidy as evidenced by increases in kinetochore-positive micronuclei, hyperdiploidy, and polyploidy. With fisetin, however, the latter two effects were most significantly observed only after cells were allowed to overcome a cell cycle delay, and occurred at higher concentrations than those induced by the other Aurora kinase inhibitors. Modest increases in kinetochore-negative micronuclei were also seen with the model Aurora kinase inhibitors. These results indicate that fisetin induces multiple types of chromosome abnormalities in human cells, and indicate a need for a thorough investigation of fisetin-augmented dietary supplements.

Introduction

Fisetin is a plant flavonol commonly found in fruits, vegetables, nuts, and wine [1]. It is also frequently used as an additive in nutritional supplements due to its reported cardiprotective, anti-carcinogenic and antioxidant properties [2, 3]. In addition, fisetin has been reported to have a number of potentially adverse cellular and biochemical effects including prevention of cell proliferation and angiogenesis *in vitro* as well as inhibition of critical enzymes such as cyclin-dependent kinases and topoisomerase II [4-10]. Earlier reports from our laboratory and others have indicated that fisetin has both aneugenic and, to a lessor degree, clastogenic properties in cultured cells [9, 11, 12]. Recently, fisetin has also been reported to target Aurora B kinase, a Ser/Thr kinase involved in ensuring proper microtubule attachment at the spindle assembly checkpoint [13].

Aurora kinases are critical for the proper passage of cells through several stages of the cell cycle. Aurora A kinase localizes to the centrosomes and spindle poles, and plays an important role in the development of the centrosomes and in bipolar spindle formation [14]. Aurora B kinase localizes along the chromosome arms and at centromeres in prophase, at the inner centromeric region during metaphase, at the central spindle and cortex during anaphase, and in the midbody in telophase [15]. It has been shown to play an important role in chromosome biorientation, destabilization of improper microtubule attachments, phosphorylation of histone H3, and cytokinesis [15]. A third kinase in this family,

Aurora C, is thought to have overlapping functions with Aurora B kinase and acts primarily in germ-line cells.

Overexpression of Aurora A kinase leads to an early entry into mitosis due to hyperactive centrosomes and multipolar spindle formation, and can lead to chromosome instability [16]. Similarly, overexpression of Aurora B kinase is thought play a role in chromosomal instability by interfering with chromosome biorientation and the spindle checkpoint [14]. Overexpression of both Aurora A and B kinases has been associated with several types of cancer including breast, colorectal, ovarian, and pancreatic cancer among others [17-19]. As a result, both Aurora A and B kinases are thought to be promising targets for chemotherapeutic agents.

As a follow-up to the recent report on its Aurora B kinase inhibiting properties, we decided to more fully characterize the aneugenic and polyploidy-inducing effects of fisetin and compare them with those seen with two known small molecule model Aurora kinase inhibitors, VX-680 and ZM-447439, which act preferentially on Aurora A and Aurora B kinases, respectively. Disruption of the spindle assembly and inhibition of Aurora kinases could lead to segregation errors and aneuploidy, providing insights into the mechanisms by which these agents could induce aneuploidy and polyploidy. While some information is known about the ability of fisetin to induce micronuclei and aneuploidy *in vitro*, very little is known about the chromosome-altering effects of other Aurora kinase inhibitors such as VX-680 and ZM-447439.

Methods

Cell culture and treatments

The human lymphoblastoid cell line TK6 was maintained in RPMI 1640 medium (GIBCO; Carlsbad, CA) containing 10% iron-supplemented calf serum (Hyclone; Logan, UT) with 2 mM l-glutamine, 100 U/ml penicillin, and 100 µg/ml streptomycin (Fisher Scientific; Pittsburg, PA) at 37 °C in an atmosphere of 5% CO_2/95% air. Exponentially growing cells at a starting density of $2.5x10^5$ cells/ml were treated with various concentrations of either fisetin (Sigma Aldrich; St Louis, MO), or the Aurora kinase inhbitors VX-680 or ZM-447439 (Cayman Chemical; Ann Arbor, MI) in a final dimethylsulfoxide (DMSO) concentration of 0.1%. Cells were harvested at 24 hours after treatment. For time course experiments, the test media was removed at 24 hours and cells were resuspended in fresh media for an additional 6 to 24 hours.

In vitro Micronucleus assay with CREST staining

The procedure for the in vitro micronucleus assay was performed as previously described with minor modifications [20]. Cytochalasin B was added 24 hours prior to harvest to the treatment flasks designated for manual scoring of micronuclei. Aliquots of the cell suspension were centrifuged directly onto slides and then briefly air-dried and fixed in 100% methanol. Prepared slides were then stained with CREST primary antibody, followed by a FITC-conjugated secondary antibody (both obtained from Antibodies Inc.; Davis, CA), with DAPI used as a DNA counterstain. Slides were then coded and 1000 binucleated cells per test

concentration were scored for the presence of kinetochore-positive (K+) and kinetochore-negative (K-) micronuclei. Means and standard error of the means were calculated with data from 2-4 separate experiments.

Numerical Chromosomal Aberration Assay by Flow Cytometry.

For the detection of chromosomal abnormalities by flow cytometry, the staining, data acquisition and analytical methods previously described by Meuhlbauer and Schuler [21] were employed with one notable modification; A trapezoid-shaped gate was used to more efficiently exclude doublets and apoptotic cells in the hyperdiploid and polyploidy region. Colcemid was added to cell cultures 2-3 hours prior to harvesting, which occurred at 24 hr (or later for the time-course experiments), and the cells were fixed in 70% ethanol. Fixed cells were then stained with phospho-histone H3 (Ser10) 6G3 monoclonal mouse antibody (Cell Signaling Technologies; Beverly, MA) followed by an Alexa-Fluor 488 conjugated goat anti-mouse IgG secondary antibody (Molecular Probes; Eugene, OR) in order to identify mitotic cells. The DNA was then stained with propidium iodide (PI) and ploidy of the mitotic cells was measured. Hypodiploid cells were defined as mitotic cells with >2C but <4C DNA content. Cells with >4C but <8C DNA content were considered hyperdiploid, and cells with >8C DNA content were classified as polyploid. Data from 2000 mitotic cells per test concentration were acquired and analyzed using a Becton Dickinson FACSort flow cytometer and CellQuest software. Means and standard error of the means were calculated with data from 2-6 separate experiments.

Statistical Analysis

Dose-related increases in micronucleated and aneuploid/polyploid cells were determined using the Cochran–Armitage test for trend in binomial proportions [22]. Following a positive response in the trend test, a one-tailed Fisher's exact test was used to compare individual treatments against the respective DMSO-treated controls [23]. In the flow experiments with fisetin, unusually high variability was seen, particularly at the higher test concentrations. As a result, linear regression was used to determine if there was a dose-related increase in ploidy, and positive results were followed by a Mann-Whitney U test to compare individual treatments with DMSO treated controls. For all studies, critical values were determined using a 0.05 probability of type I error.

Results

<u>Fisetin</u>

As reported previously, treatment with fisetin resulted dose-related increase in the formation micronuclei in TK6 cells (Fig 2-1a). Strong and significant increases in K+ micronuclei, indicating chromosome loss were seen, confirming our previous report that fisetin acts as an aneugen [9]. To further investigate its aneugenic and polyploidy-inducing properties, numerical chromosomal aberrations induced by fisetin were also assessed using flow cytometry. At the same 24 hr time point at which the strong increase in K+ MN was observed following treatment with fisetin, only a modest, albeit statistically significant, increase in hypodiploidy was seen by flow cytometry (r^2=0.2381, p=0.0002) (Fig 2-1b). Similarly, a small increase

in hyperdiploidy was also observed (r^2=0.2183, p=0.0003). There also appeared to be a modest increase in polyploidy at some of the concentrations tested. Because the dose-response curve was non-monotonic with a reduced increase in polyploidy at the highest concentrations, the trend was not statistically significant using linear regression (p=0.05). However, pair-wise comparisons using the Mann-Whitney U test indicated that modest, but significant, increases in polyploidy were induced at concentrations between 13.6-20 μM.

The unusual pattern and variability of the results raised the possibility that treatment with fisetin may have triggered a cell cycle delay, hindering cells from progressing to a second metaphase and therefore preventing chromosome loss from being detected in the flow-based assay. To explore this possibility, a time course experiment was performed with washout of the fisetin after 24 hours. Cells were then harvested at 12 and 24 hours after the washout to allow the treated cells to overcome a cell cycle delay. In this extended time course study (fig. 2-2), fisetin at the 20 μM and higher concentrations induced large increases in hyperdiploidy and polyploidy at time points 36 and 48 hours after initial treatment, consistent with a cell cycle delay. At the 36 hr. harvest time, there was an ∼6-fold increase in hyperdiploidy and a very large ∼50-fold increase in polyploid cells observed in the cultures. Interestingly, additional increases in hypodiploidy were not observed.

Model Aurora kinase inhibitors

For comparison, similar studies were performed with the model Aurora kinase inhibitors VX-680 and ZM-447439. Similar to fisetin, both VX-680 and ZM-447439

induced significant dose-related increases in micronuclei with significant

approximately four-fold increases seen at concentrations as low as 25 nM for VX-

680 and 100nM for ZM-447439 (Fig 2-3a and Fig 2-3b). Whereas fisetin induced

primarily K+ micronuclei, both model kinase inhibitors led to a significant increase

in K- as well as K+ micronuclei, indicating that they induced both chromosome

breakage and loss at concentrations that did not cause appreciable cytostatic effects.

As before, the flow-cytometry based assay was used to look at numerical

chromosomal aberrations after treatment with the two Aurora kinase inhibitors (Fig

2-3c and Fig 2-3d). Somewhat surprisingly, no increase in hypodiploidy was

detected after 24 hours with the Aurora kinase inhibitors despite the observed

increase in K+ micronuclei. Treatment with VX-680 caused a very large increase in

polyploidy at 24 hr. with ~70% of the cells exhibiting polyploidy at the 25 nM

concentration. Significant increases in hyperdiploidy were also seen. In contrast,

ZM-447439 induced polyploidy, but no increase in hyperdiploidy was seen.

As a follow-up, extended time course studies were performed and consistent

differences in numerical chromosomal aberrations were not seen between the 24,

36 and 48 hr time points (data not shown).

Discussion

The goal of the present study was to characterize the chromosome altering

effects of fisetin, a natural compound found in plants that has recently been

reported to inhibit Aurora B kinase, and compare the results to those of two model

Aurora kinase inhibitors, VX-680 and ZM-447439. Our results showed that all three

compounds were effective at inducing numerical chromosomal alterations although different patterns were seen with the different agents. At micromolar concentrations fisetin induced strong increases in K+ MN indicative of chromosome loss, hyperdiploidy and polyploidy; The latter two effects were maximally detected at a later 36 hr harvest (12 hr after fisetin had been removed from the cultures) which allowed the cells to overcome a cell cycle delay. VX-680 caused a modest increase in K+ MN as well as very large increases in polyploid and hyperdiploid cells. Similarly, ZM-447439 induced a modest increase in K+ MN as well as a strong increase in polyploidy although no increase in hyperdiploidy being seen. Both model Aurora kinase inhibitors induced K- MN indicating that they could also cause chromosome breakage.

The results of these experiments confirm previous reports that fisetin acts as an aneugen [9, 11], with strong increases in K+ micronuclei observed across the concentration range tested. We did not, however, observe any noticeable increases in micronuclei due to breakage after treatment with fisetin. While at first glance this appears to differ from our earlier results in which fisetin was reported to induce K-MN, it should be noted that the major clastogenic effect seen in the previous study occurred at a 45 μM concentration which is above our highest test concentration of 30 μM, and where considerable cytotoxicity would be expected (Figure 2-1a and b) [9]. In comparison, VX-680 and ZM-447439 induced approximately even amounts of both K+ and K- micronuclei at concentrations where appreciable cytotoxicity was not seen. The similarity in the types of micronuclei formed after treatment with the

two kinase inhibitors is of note and suggests that similar targets are being affected by these agents, even at the sub-micro molar concentrations used in our experiments. Previous studies have reported that both VX-680 and ZM-447439 are able to inhibit both Aurora A and Aurora B kinases [24-26].

The observation that VX-680 and ZM-447439 have both aneugenic and clastogenic effects is also interesting. Inhibition of Aurora kinases is thought to interfere mostly with spindle formation and separation of sister chromatids. As a result, one would expect that treatment with Aurora Kinase inhibitors would lead to increases in segregation errors and thus increases in of K+ micronuclei. The observed increase in chromosome breakage and K- micronuclei at non-cytotoxic concentrations, however, was unexpected and the mechanisms underlying this effect are not as well understood. One possibility is that Aurora B kinase inhibition could result in lagging chromosomes that are broken by the cleavage furrow due to premature abscission and deregulated cytokinesis. In yeast, the Aurora B homolog, Ipl-1, has been shown to play a key role in the regulation of cytokinesis as part of the NoCut pathway [27]. Mutations that result in inactivation of Ipl-1 have been reported to cause premature cytokinesis in yeast cells, resulting in breakage of lagging chromosomes. While Aurora B in mammalian cells has also been shown to play an important role in controlling the timing of cytokinesis, to our knowledge, it has yet to be shown that a similar clastogenic effect occurs in human cells.

It is also unclear whether the clastogenic effects of the model Aurora kinase inhibitors are related to those that have been associated with fisetin. It has

previously been reported that fisetin can directly inhibit topoisomerase II-alpha, providing a possible mechanism by which fisetin can induce chromosome breakage [9, 10, 28]. The breakage also occurred under cytotoxic conditions, which may have played a role in the breakage observed in the earlier fisetin study [29, 30]. Since both kinase inhibitors we tested are considered to be highly specific to the Aurora kinases and act at relatively non-toxic, nanomolar concentrations, it seems unlikely that treatment with either VX-680 or ZM-447439 would also lead to inhibition of topoisomerase II or that the breaks would be a consequence of cytotoxicity. As another possible explanation, it has previously been reported that sustained mitotic delay caused by compounds such as spindle disrupting agents can lead to chromosome breakage, likely as an early apoptotic stress response [31]. Since inhibition of Aurora kinases is known to disrupt the spindle assembly checkpoint, it is possible that the breakage observed here might be due to a similar type of stress response.

One unexpected finding was that much smaller increases in hypodiploidy were detected using the flow cytometry-based assay to detect numerical chromosomal aberrations despite the appearance of significant increases in K+ micronuclei following treatment with either fisetin or the Aurora kinase inhibitors. This was unexpected since previous studies in our laboratory using a variety of aneugenic agents have generally seen qualitatively similar results using the micronucleus and flow-based assays (data not shown). There are a number of possible explanations for the differences observed in this study. For instance, in

their previous study detailing the use of this assay, Muehlbauer and Schuler [21] suggested that one potential limitation of the flow assay might be a limited capacity for detecting single chromosome loss events due to gating requirements. Manual scoring of binucleated cells treated with either fisetin or the two Aurora kinase inhibitors with the *in vitro* micronucleus assay with CREST staining showed that most cells exhibiting chromosome loss had only a single K+ micronucleus even at the higher concentrations, indicating that an inability to establish discriminating gating parameters could provide a possible explanation for the differences seen. Consistent with this explanation, when performing the flow assay with the fisetin-treated cultures, occasionally a separate cluster of cells was seen that was close to the hypodiploid gate but still within the normal gate settings for diploid cells (data not shown).

Other possible explanations for the somewhat disparate results include re-incorporation of the micronuclei or sub-optimal timing of the cell harvest. For example, while previous studies have generally assumed that micronuclei are either extruded or degraded, Crasta and associates provided data to indicate that chromosomes contained in the micronuclei can be reincorporated into daughter cells during mitosis [32]. It is therefore possible that if cells treated with either fisetin or the Aurora kinase inhibitors lose a chromosome during the first mitosis and if reincorporation of that chromosome occurs early during the second mitosis, then the cell could appear to be normal in the flow assay which measures ploidy during the second mitosis.

Another possible explanation for the differing results is that fisetin as well as the Aurora Kinase inhibitors may cause a cell cycle delay. The main difference between the MN assay and the flow-based aneuploidy assay is the stage of the cell cycle in which the cells are evaluated. With the *in vitro* micronucleus assay, cells have completed mitosis and are back in interphase, while the flow-based aneuploidy assay generally detects cells during their second metaphase. If there is an effect that causes a cell cycle delay that prevents cells from progressing to metaphase, then it is possible that the chromosome loss will not be detected. As indicated above, to examine this possibility, initial follow-up time course experiments were performed with chemical washout at 24hrs, looking at aneuploidy at time points of 24, 36, and 48 hours after initial treatment. With Aurora kinase inhibitors, there was no difference when the later time points were compared to the initial 24 hr treatment. With fisetin, large increases in hyperdiploidy and polyploidy were observed 36 and 48 hr (12 and 24 hours after chemical washout), with a profile resembling more closely those of cells treated with VX-680 and ZM-447439. A related possibility is that we may have missed a transient wave of hypodiploid cells because the 12 hr sample collection window between 24 and 36 hr was too wide. To further investigate this possibility, we conducted an additional time course experiment using a smaller dose range and an intermediate harvest time of 30 hr (6 hours after chemical washout). While a small increase in hypodiploidy was seen at the 13.4 μM concentration, it was not seen at the 20 μM concentration (data not shown)

36

suggesting that an inadequate sampling time was unlikely to explain the differences seen.

In addition to the similarities seen between fisetin and the model Aurora kinase inhibitors such as the induction of K+ MN, hyperdiploidy, and polyploidy, there was one particularly notable difference. Our time course experiments indicate that treatment of cells with fisetin caused a substantial cell cycle delay whereas there was no evidence of a cell cycle delay seen with the model Aurora kinase inhibitors. While both VX-680 and ZM-447439 have previously been shown to be fairly selective inhibitors of the Aurora kinases, fisetin has been reported to have a broader range of targets within the cell. Among the known targets of fisetin are cyclin-dependent kinases, which when inhibited can cause cell cycle arrest [7, 8]. Inhibition of these cyclin-dependent kinases could be the mechanism underlying the cell cycle delay seen with fisetin.

These results also underscore the challenges in trying to identify multiple types of numerical chromosomal alterations at a single harvest time. For the Aurora kinase inhibitors, a single harvest at 24 hrs was sufficient to detect significant increases in micronuclei, hyperdiploidy (for VX-680) and polyploidy. In contrast, while a substantial increase in micronuclei was seen with fisetin, only modest increases in the other ploidy measures were seen at the 24 hr harvest time. Following removal of the test agent and with a 12 hr recovery, a much largeer increase in hyperdiploidy and a very large increase in polyploidy were seen. These numerical changes would likely have been regarded as only minor effects if only the

37

24 hr harvest period had been used. By evaluating the later time points, fisetin was shown to be a potent inducer of hyperdiploidy and polyploidy. One of the advantages of the flow cytometry method is that the cell cultures can be rapidly and simultaneously evaluated for hypodiploidy, hyperdiploidy and polyploidy, thereby allowing multiple time points to be evaluated if there is a concern about cell cycle delay. Previous studies from our laboratory have shown a generally good qualitative concordance between the K+ MN frequency and hypodiploidy as measured by the flow assay. However, in a number of circumstances, such as in this case with fisetin, manual scoring of MN appears to be more sensitive at detecting chromosome loss than the detection of hypodiploidy as measured by flow cytometry.

In conclusion, our results clearly demonstrate that fisetin, VX-680 and ZM-447439 are effective aneuploidy and polyploidy-inducing agents *in vitro*, and indicate that numerical chromosomal alterations result from the inhibition of Aurora kinases in human cells. Given that these effects were seen at nanomolar concentrations with VX-680 and ZM-447939, these types of chromosomal changes would likely to contribute to potential anti-neoplastic effects of these Aurora kinase inhibitors. With fisetin, the induced chromosomal alterations were seen at much higher micromolar concentrations. If similar effects occur *in vivo*, this would be a concern as fisetin is currently being used at high concentrations in dietary supplements [13], which typically receive little or no testing prior to marketing.

Acknowledgments

Figure 2-1a

Figure 2-1b

Figure 2-1. a) Frequencies of micronucleated cells (MNC), CREST-negative micronucleated cells (K-MNC), and CREST-positive micronucleated cells (K+ MNC) in TK6 cells treated with fisetin. 1000 binucleated cells were scored per test concentration and the means and SEM from 2-4 separate experiments are shown. The relative cytochalasin B proliferation index (RCBI), a measure of cytotoxicity, for each test concentration is also shown. *Statistically significant *vs.* the DMSO controls (Fisher's exact test; $P \leq 0.05$). b) Numerical chromosomal aberrations measured by flow cytometry. Aberrations were computed as a percentage of 2000 gated mitotic events in TK6 cultures treated with fisetin for 24 h. The means and SEM from 5-6 separate experiments are shown. The relative mitotic index (RMI) is also shown. *Statistically significant *vs.* the DMSO controls (Mann-Whitney U test; $P \leq 0.05$).

Figure 2-2
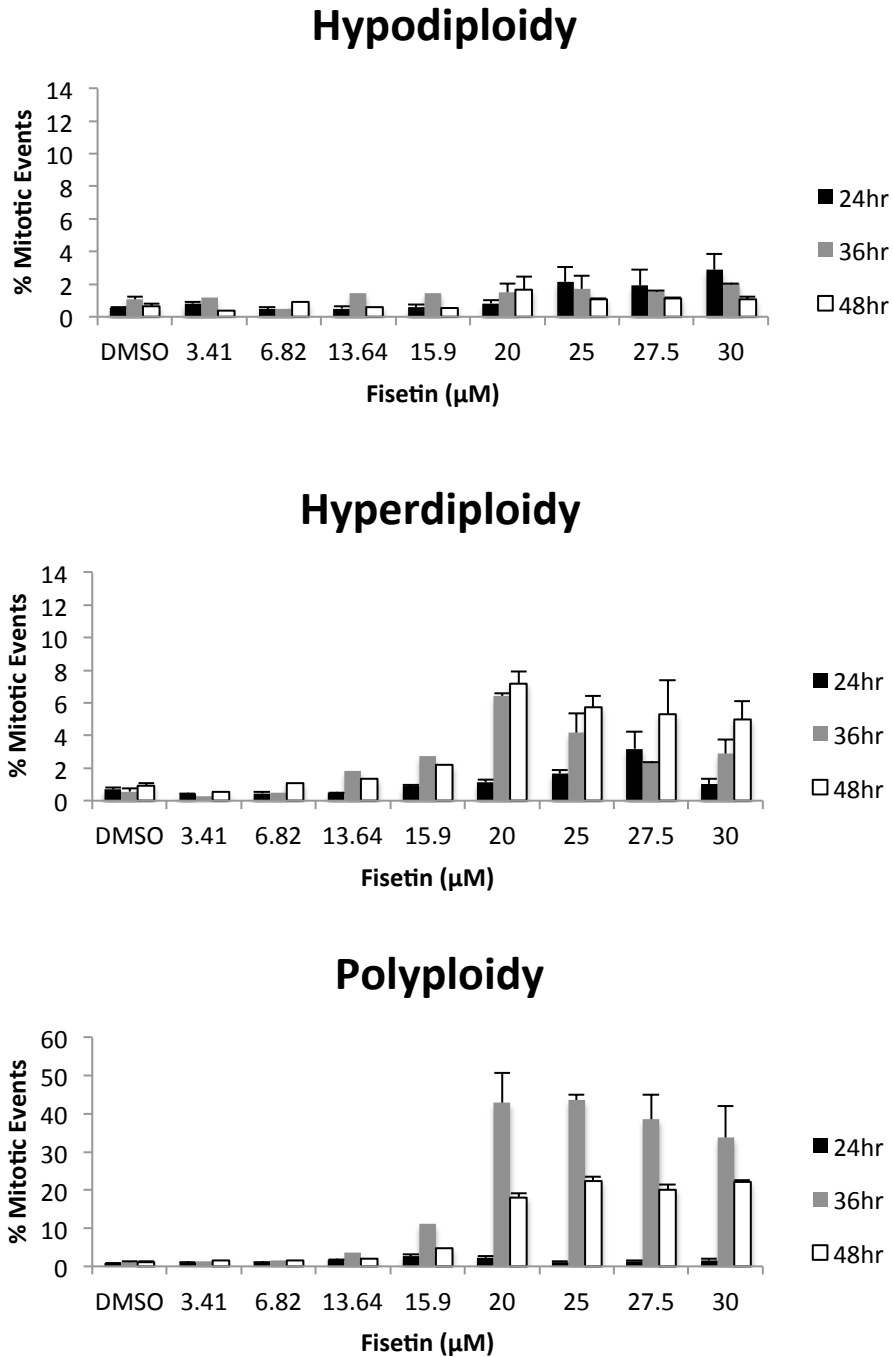
Figure 2-2 Time-course evaluation of hypodiploidy, hyperdiploidy, and polyploidy in TK6 cells treated with fisetin for 24 h. Cells were re-suspended in fresh media and numerical chromosomal aberrations were monitored at 0, 12 and 24 hours after the end of treatment. The results from the 24 hr treatment with immediate harvest are the same as those presented in Fig. 1b.

Figure 2-3a
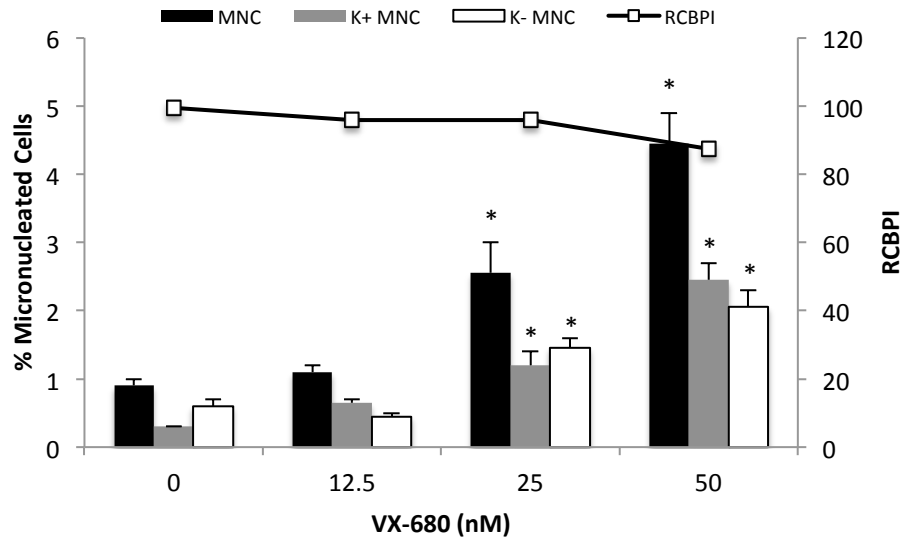
Figure 2-3b
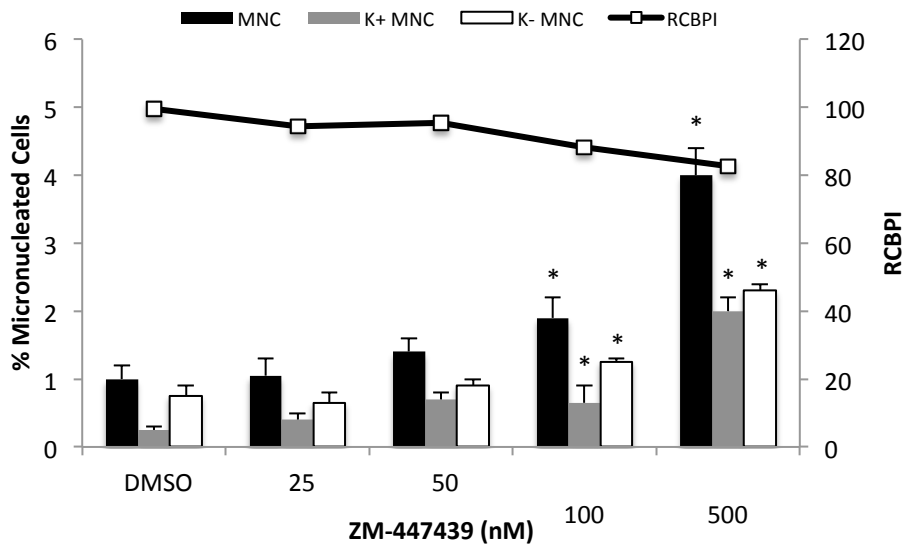
Figure 2-3c
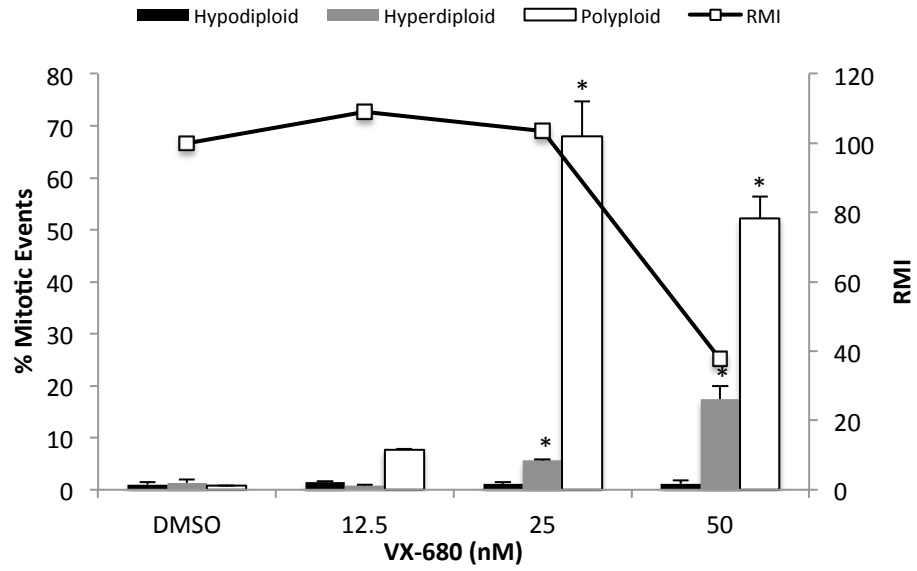
Figure 2-3d
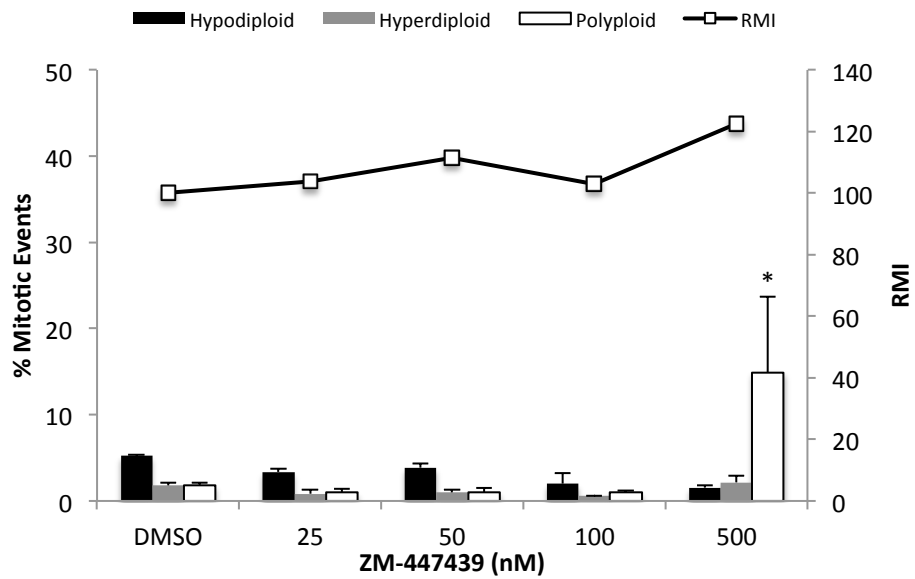
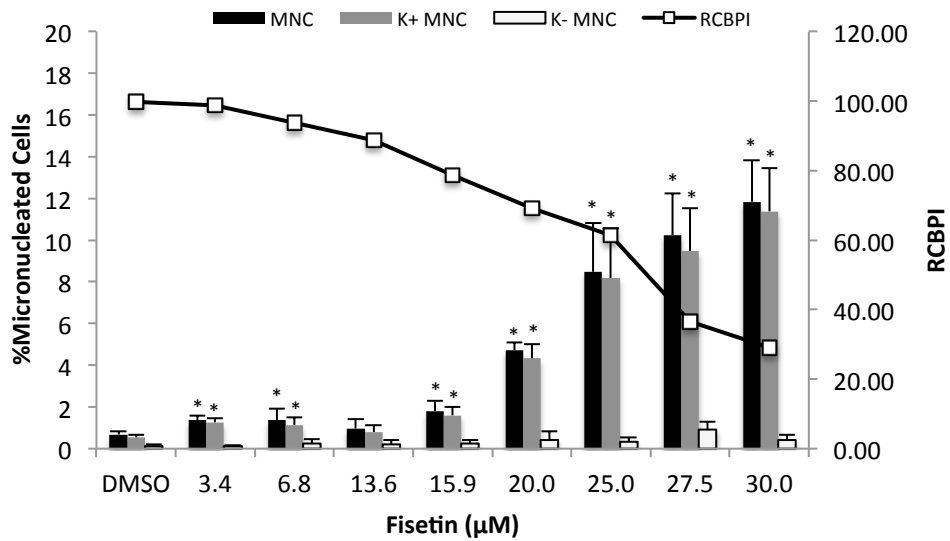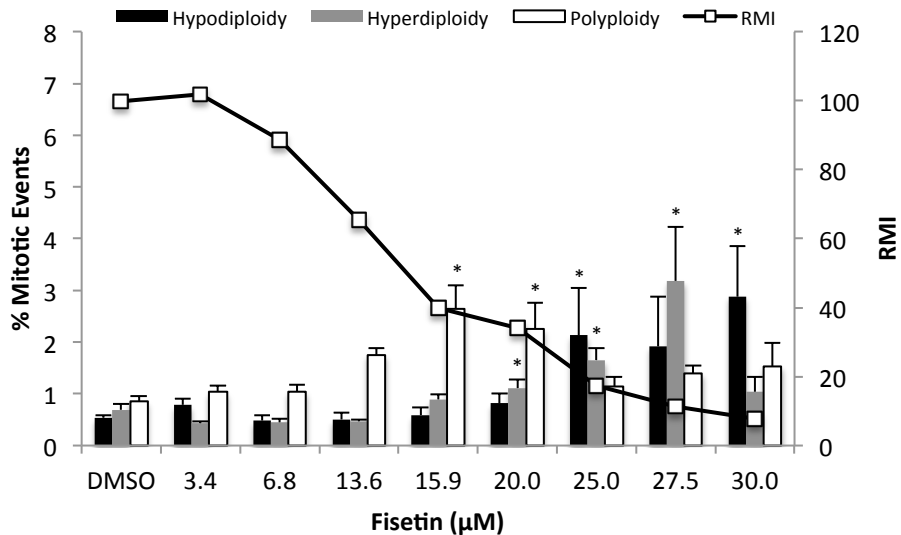**Figure 2-3.** a-b) Frequencies of micronucleated cells (MNC), CREST-negative micronucleated cells (K-MNC), and CREST-positive micronucleated cells (K + MNC) in TK6 cells treated with the Aurora kinase inhibitors (a) VX-680 or (b) ZM-447439 for 24 h. 1000 binucleated cells were scored for micronuclei per test concentration and the means and SEM from 2 separate experiments are shown. The relative cytochalasin B proliferation index (RCBI) for each test concentration is also shown. c-d) Numerical chromosomal aberrations measured by flow cytometry. Aberrations were computed as a percentage of 2000 gated mitotic events in TK6 cultures treated with (c) VX-680 or (d) ZM-447439 for 24 h. The means and SEM from 2-3 separate experiments are shown. The relative mitotic index (RMI) is also shown. *Statistically significant *vs.* the DMSO controls (Fisher's exact test; $P \leq 0.05$).

References

[1] M. Kimira, Y. Arai, K. Shimoi, S. Watanabe, Japanese intake of flavonoids and isoflavonoids from foods, Journal of epidemiology / Japan Epidemiological Association, 8 (1998) 168-175.

[2] F.A. van Acker, O. Schouten, G.R. Haenen, W.J. van der Vijgh, A. Bast, Flavonoids can replace alpha-tocopherol as an antioxidant, FEBS letters, 473 (2000) 145-148.

[3] P.G. Pietta, Flavonoids as antioxidants, Journal of natural products, 63 (2000) 1035-1042.

[4] O.L. Woodman, E. Chan, Vascular and anti-oxidant actions of flavonols and flavones, Clinical and experimental pharmacology & physiology, 31 (2004) 786-790.

[5] T. Fotsis, M.S. Pepper, E. Aktas, S. Breit, S. Rasku, H. Adlercreutz, K. Wahala, R. Montesano, L. Schweigerer, Flavonoids, dietary-derived inhibitors of cell proliferation and in vitro angiogenesis, Cancer research, 57 (1997) 2916-2921.

[6] S. Kuntz, U. Wenzel, H. Daniel, Comparative analysis of the effects of flavonoids on proliferation, cytotoxicity, and apoptosis in human colon cancer cell lines, European journal of nutrition, 38 (1999) 133-142.

[7] X. Lu, J. Jung, H.J. Cho, D.Y. Lim, H.S. Lee, H.S. Chun, D.Y. Kwon, J.H. Park, Fisetin inhibits the activities of cyclin-dependent kinases leading to cell cycle arrest in HT-29 human colon cancer cells, The Journal of nutrition, 135 (2005) 2884-2890.

[8] B. Sung, M.K. Pandey, B.B. Aggarwal, Fisetin, an inhibitor of cyclin-dependent kinase 6, down-regulates nuclear factor-kappaB-regulated cell proliferation, antiapoptotic and metastatic gene products through the suppression of TAK-1 and receptor-interacting protein-regulated IkappaBalpha kinase activation, Molecular pharmacology, 71 (2007) 1703-1714.

[9] A.J. Olaharski, S.T. Mondrala, D.A. Eastmond, Chromosomal malsegregation and micronucleus induction in vitro by the DNA topoisomerase II inhibitor fisetin, Mutation research, 582 (2005) 79-86.

[10] R. Strick, P.L. Strissel, S. Borgers, S.L. Smith, J.D. Rowley, Dietary bioflavonoids induce cleavage in the MLL gene and may contribute to infant leukemia, Proceedings of the National Academy of Sciences of the United States of America, 97 (2000) 4790-4795.

[11] K. Hashimoto, Y. Nakajima, S. Matsumura, F. Chatani, An in vitro micronucleus assay with size-classified micronucleus counting to discriminate aneugens from clastogens, Toxicology in vitro : an international journal published in association with BIBRA, 24 (2010) 208-216.

[12] R.D. Snyder, P.J. Gillies, Evaluation of the clastogenic, DNA intercalative, and topoisomerase II-interactive properties of bioflavonoids in Chinese hamster V79 cells, Environmental and molecular mutagenesis, 40 (2002) 266-276.

[13] A.L. Salmela, J. Pouwels, A. Varis, A.M. Kukkonen, P. Toivonen, P.K. Halonen, M. Perala, O. Kallioniemi, G.J. Gorbsky, M.J. Kallio, Dietary flavonoid fisetin induces a forced exit from mitosis by targeting the mitotic spindle checkpoint, Carcinogenesis, 30 (2009) 1032-1040.

[14] S.M. Lens, E.E. Voest, R.H. Medema, Shared and separate functions of polo-like kinases and aurora kinases in cancer, Nature reviews. Cancer, 10 (2010) 825-841.

[15] H. Katayama, S. Sen, Aurora kinase inhibitors as anticancer molecules, Biochimica et biophysica acta, 1799 (2010) 829-839.

[16] Y. Baba, K. Nosho, K. Shima, N. Irahara, S. Kure, S. Toyoda, G.J. Kirkner, A. Goel, C.S. Fuchs, S. Ogino, Aurora-A expression is independently associated with chromosomal instability in colorectal cancer, Neoplasia, 11 (2009) 418-425.

[17] C. Sakakura, A. Hagiwara, R. Yasuoka, Y. Fujita, M. Nakanishi, K. Masuda, K. Shimomura, Y. Nakamura, J. Inazawa, T. Abe, H. Yamagishi, Tumour-amplified kinase BTAK is amplified and overexpressed in gastric cancers with possible involvement in aneuploid formation, British journal of cancer, 84 (2001) 824-831.

[18] T. Takahashi, M. Futamura, N. Yoshimi, J. Sano, M. Katada, Y. Takagi, M. Kimura, T. Yoshioka, Y. Okano, S. Saji, Centrosomal kinases, HsAIRK1 and HsAIRK3, are overexpressed in primary colorectal cancers, Japanese journal of cancer research : Gann, 91 (2000) 1007-1014.

[19] T.M. Gritsko, D. Coppola, J.E. Paciga, L. Yang, M. Sun, S.A. Shelley, J.V. Fiorica, S.V. Nicosia, J.Q. Cheng, Activation and overexpression of centrosome kinase BTAK/Aurora-A in human ovarian cancer, Clinical cancer research : an official journal of the American Association for Cancer Research, 9 (2003) 1420-1426.

[20] D.A. Eastmond, J.D. Tucker, Identification of aneuploidy-inducing agents using cytokinesis-blocked human lymphocytes and an antikinetochore antibody, Environmental and molecular mutagenesis, 13 (1989) 34-43.

[21] P.A. Muehlbauer, M.J. Schuler, Detection of numerical chromosomal aberrations by flow cytometry: a novel process for identifying aneugenic agents, Mutation research, 585 (2005) 156-169.

[22] B.H. Margolin, M.A. Resnick, J.Y. Rimpo, P. Archer, S.M. Galloway, A.D. Bloom, E. Zeiger, Statistical analyses for in vitro cytogenetic assays using Chinese hamster ovary cells, Environ Mutagen, 8 (1986) 183-204.

[23] S.C. Gad, Statistics and Experimental Design for Toxicologists and Pharmacologists, 4th ed., CRC Taylor and Francis, Boca Raton, FL, 2006.

[24] R.K. Tyler, N. Shpiro, R. Marquez, P.A. Eyers, VX-680 inhibits Aurora A and Aurora B kinase activity in human cells, Cell Cycle, 6 (2007) 2846-2854.

[25] C. Ditchfield, N. Keen, S.S. Taylor, The Ipl1/Aurora kinase family: methods of inhibition and functional analysis in mammalian cells, Methods Mol Biol, 296 (2005) 371-381.

[26] F. Girdler, K.E. Gascoigne, P.A. Eyers, S. Hartmuth, C. Crafter, K.M. Foote, N.J. Keen, S.S. Taylor, Validating Aurora B as an anti-cancer drug target, Journal of cell science, 119 (2006) 3664-3675.

[27] C. Norden, M. Mendoza, J. Dobbelaere, C.V. Kotwaliwale, S. Biggins, Y. Barral, The NoCut pathway links completion of cytokinesis to spindle midzone function to prevent chromosome breakage, Cell, 125 (2006) 85-98.

[28] M. Lopez-Lazaro, E. Willmore, C.A. Austin, The dietary flavonoids myricetin and fisetin act as dual inhibitors of DNA topoisomerases I and II in cells, Mutation research, 696 (2010) 41-47.

[29] S.M. Galloway, D.A. Deasy, C.L. Bean, A.R. Kraynak, M.J. Armstrong, M.O. Bradley, Effects of high osmotic strength on chromosome aberrations, sister-chromatid exchanges and DNA strand breaks, and the relation to toxicity, Mutation research, 189 (1987) 15-25.

[30] ICH, Guidance of Genotoxicity Testing and Data Interpretation for Pharmaceuticals Intended for Human Use, International Conference on Harmonisation of Technical Requirements of Registration of Pharmaceuticals for Human Use2011, pp. 29.

[31] F. Quignon, L. Rozier, A.M. Lachages, A. Bieth, M. Simili, M. Debatisse, Sustained mitotic block elicits DNA breaks: one-step alteration of ploidy and chromosome integrity in mammalian cells, Oncogene, 26 (2007) 165-172.

[32] K. Crasta, N.J. Ganem, R. Dagher, A.B. Lantermann, E.V. Ivanova, Y. Pan, L. Nezi, A. Protopopov, D. Chowdhury, D. Pellman, DNA breaks and chromosome pulverization from errors in mitosis, Nature, 482 (2012) 53-58.

Chapter 3

Dose Response Studies of the Chromosome-Damaging Effects of Topoisomerase II Inhibitors Determined *in vitro* Using Human TK6 Cells

Abstract

Topoisomerase II (topo II) inhibitors are commonly used as chemotherapy to treat multiple types of cancer, though their use is also associated with the development of therapy related acute leukemias. While the chromosome-damaging effects of etoposide, a topo II poison, have been proposed to act through a threshold mechanism, little is known about the chromosome damaging effects and dose responses for the catalytic inhibitors of the enzyme. The current study was designed to further investigate the potencies and dose-response relationships of several topoisomerase II inhibitors, including the topoisomerase II poison etoposide, as well as catalytic inhibitors aclarubicin, merbarone, ICRF-154 and ICRF-187 using both a traditional *in vitro* micronucleus assay as well as a flow-cytometry based version of the assay. Benchmark dose (BMD) analysis was used to identify models that best fit the data and estimate a BMD, in this case the concentration at which a one standard deviation increase above the control frequency would be expected. All of the agents tested were potent in inducing micronuclei in human lymphoblastoid TK6 cells, with significant increases seen at low micromolar, and in the cases of aclarubicin and etoposide, at low nanomolar concentrations. Use of the anti-kinetochore CREST antibody with the microscopy-based assay demonstrated that the vast majority of the micronuclei originated from chromosome breakage. In comparing the two versions of the micronucleus assay, significant increases in micronucleated cells were generally observed at lower concentrations using the traditional microscopy-based assay. BMD modeling of the data exhibited several

50

advantages and proved to be a valuable alternative for dose-response analysis

producing points of departure comparable to those derived using traditional no-

observed or lowest-observed genotoxic effect level (NOGEL or LOGEL) approaches.

Introduction

Type II DNA topoisomerases are important nuclear enzymes that relieve

topological stress during DNA replication, transcription, repair, and mitosis (1-4).

The enzyme's catalytic cycle involves covalent binding of the enzyme to DNA,

forming a double stranded break and a cleavage complex through which another

DNA duplex can pass. Following strand passage, the double stranded break is

religated and the enzyme is released from the DNA (Fig 3-1) (4-5). Due to the

formation of the protected double-stranded break, disruptions in the enzyme's

catalytic cycle have the ability to lead to multiple types of chromosomal alterations

including cancer-related translocations (1-4).

A number of compounds are known to disrupt or inhibit topoisomerase II

(topo II) including some important classes of chemotherapeutic agents. These can

act at various stages of the catalytic cycle (Fig 3-1) (1,6). Topo II poisons, such as

etoposide, act to stabilize the cleavage complex and inhibit the religation step, an

important step leading to the formation of unprotected double stranded breaks.

Catalytic inhibitors, on the other hand, affect other parts of the topo II catalytic cycle

and do not directly stabilize the cleavage complex, though have been shown to have

clastogenic effects *in vitro* and *in vivo* (6-8).

While several drugs targeting topo II are front line therapies for the treatment of various types of cancer, one limitation of their use is increased risk for development of treatment-related acute leukemia (1-4, 6). These leukemias are secondary to the original cancers for which the topo II inhibitors were originally prescribed and have characteristically short median latency periods of approximately 2-3 years (9-12). Topo II poisons etoposide and doxorubicin have been associated with treatment-related acute myelogenous leukemia (t-AML), typically of monocytic or myelomonocytic origin, caused by balanced translocations involving the *MLL* gene on chromosome band 11q23 (9,12). Similarly, mitoxantrone, has been associated with development of a different subtype of t-AML, acute promyelocytic leukemia, as a result of a reciprocal translocation fusing the retinoic acid receptor alpha gene (*RARA*) from chromosome 17 to the promyelocytic leukemia gene (*PML*) on chromosome 15 resulting in the stable expression of a PML-RARa fusion protein (10,11). In addition, there is some concern that exposure to naturally occurring topo II poisons such as genistein and other bioflavonoids *in utero* may play a role in development of infant AML (13,14). While most topo II inhibitors associated with leukemia fall under the category of topo II poisons, there is also evidence of similar leukemogenic effects in patients treated with the catalytic inhibitors ICRF-154 and bimolane (12,15)

Detailed studies on the relationship between dose and response for aneugenic and clastogenic chemicals have been limited by the use of conventional cytogenetic techniques, which have depended upon labor-intensive manual scoring

using microscopy. This has limited the number of cells and test concentrations that could feasibly be evaluated. Recent developments in flow cytometry allow cytogenetic information on both aneuploidy and chromosome breakage (micronuclei) to be rapidly obtained. The use of these new flow techniques should permit much larger number of cells and test concentrations to be evaluated and allow detailed dose response information to be obtained for many types of aneugenic and clastogenic chemicals (16-17).

The goal of the current study is to more thoroughly investigate dose-response relationships of a variety of topoisomerase II inhibitors to better understand the concentrations at which damage occurs and how different mechanisms of inhibition of topo II may affect the dose-response curves. To do so, we examined the dose-responses of the topo II poison, etoposide, as well as two catalytic inhibitors that act prior to the formation of the cleavable complex (alcarubicin and merbarone) and two that act after the religation step (ICRF-154 and ICRF-187). In addition, these studies compared the results of a traditional *in vitro* micronucleus assay technique with those from a more recently developed flow cytometry-based micronucleus assay, and used benchmark dose modeling to evaluate the results.

Methods

Cell culture and treatments

The human lymphoblastoid cell line TK6 was maintained in RPMI 1640 medium (GIBCO; Carlsbad, CA) containing 10% iron-supplemented calf serum (Hyclone; Logan, UT) with 2 mM l-glutamine, 100 U/ml penicillin, and 100 µg/ml

streptomycin (Fisher Scientific; Pittsburg, PA) at 37 °C in an atmosphere of 5% CO_2/95% air. Exponentially growing cells were treated with various concentrations of each of the following topo II inhibitors: alcarubicin (Sigma; St. Louis, MO), merbarone (NCI; Bethesda, MD), ICRF-154 (NCI; Bethesda, MD), ICRF-187 (NCI; Bethesda, MD), and etoposide (Sigma; St. Louis, MO). All compounds were dissolved in dimethylsulfoxide (DMSO) with a final DMSO concentration of 0.1% in the culture flasks. Cells were harvested at 24 hours after treatment.

In vitro micronucleus assay with CREST staining

The procedure for the in vitro micronucleus assay was performed as previously described (18) with minor modifications. Cells were treated with varying concentrations of each topo II inhibitor as well as 4.5 μg/mL cytochalasin B for 24 hours before the cells were harvested for slide preparation. Aliquots of the cell suspension were centrifuged directly onto slides and then briefly air-dried and fixed in 100% methanol. Prepared slides were then stained with CREST primary antibody, followed by a FITC-conjugated secondary antibody (both obtained from Antibodies Inc.; Davis, CA), with DAPI used as a DNA counterstain. Slides were then coded and 1000 binucleated cells per test concentration were scored in a blind fashion for the presence of kinetochore-positive (K+) and kinetochore-negative (K-) micronuclei representing micronuclei formed from chromosome loss and chromosome breakage, respectively. Means and standard deviations were calculated with data from 2-3 replicate experiments.

Micronucleus assay by flow-cytometry

Staining, instrumentation, and gating for the MN assay by flow-cytometry was performed as previously described by Avelsevich *et al* (19)*.* Briefly, at time of harvest, cells previously treated in the absence of cytochalasin B were stained with ethidium monoazide (EMA). A photoactivation step resulted in covalent binding of EMA with DNA from necrotic and late-stage apoptotic cells. Following this, the cells were lysed and stained with SYTOX-Green, which binds to all DNA, resulting in a suspension of nuclei and micronuclei with differentially stained DNA to distinguish between dead or dying cells (EMA+) and live cells (EMA-/SYTOX+). Data from 20,000 EMA-/SYTOX+ cells per sample were acquired and analyzed using a Becton Dickinson FACSort flow cytometer and Cell Quest software. Micronuclei were enumerated based on size (Forward Scatter) and DNA content.

Statistical analysis and benchmark dose modeling

For MN data using the *in vitro* micronucleus assay with CREST staining, dose-related increases in micronucleated cells were determined using the Cochran–Armitage test for trend in binomial proportions. Following a positive response in the trend test, a one-tailed Fisher's exact test was used to compare individual treatments against the respective DMSO-treated controls. For data obtained from the flow-cytometry based assay, an ANOVA test was performed and Dunnett's T-test was used to compare individual treatments to the control.

BMD modeling of the micronucleus frequency was conducted using U.S. EPA BMD software (version 2.4.0, 2013). The benchmark response was defined as one

control standard deviation (BMD$_{1SD}$) and its lower 95th percentile confidence limit (BMDL$_{1SD}$) according to U.S. EPA (2012) guidance for continuous data (20). Data were fit to Exponential (3, 4, and 5), Hill, Linear, Polynomial, and Power models assuming constant variance. The factors collectively taken into consideration for selecting the best-fit model included the global goodness-of-fit p value (must be ≥ .1); lowest AIC value, Chi-square residual values of less than 2 at each dose level, visual fit, and the margin between the BMD$_{1SD}$ and BMDL$_{1SD}$ (20).

Results

Micronucleus induction by topo II inhibitors

Strong concentration-dependent increases in the induction of micronuclei were seen with all of the topo II inhibitors tested. The results for each of the chemicals is briefly described below.

A strong monotonic increase in MN was seen with the pre-cleavage complex catalytic inhibitor aclarubicin. Statistically significant increases were observed beginning at the 12.5 nM test concentration, where an approximate 2-fold increase in MN was observed compared to controls when measured using the flow-based assay. The maximum amount of MN observed at the highest test concentration was 5%, representing a 7-fold increase (Figure 3-2A). These values and the fold increase were mirrored quite closely when MN were scored manually with microscopy (Figure 3-3A). The CREST data showed that most (approximately 83-90%) of the MN induced were kinetochore-negative and formed due to chromosome breakage. The effects seen in TK6 cells treated with aclarubicin occurred at nanomolar

56

concentrations with approximately 55% cytotoxicity as measured by relative population doubling or relative increases in cell count occurring at 12.5 nM (Table 1).

Compared to aclarubicin, effects seen with merbarone, the other pre-cleavage complex catalytic inhibitor, occurred at much higher concentrations and the compound induced considerably more MN (Figure 3-2B). A statistically significant 3.5-fold increase (8.5% total MN) was seen at 5 μM where <20% cytotoxicity was observed. Doubling of the test concentration to 10 μM led to an average 11-fold increase in MN. While continued increases in MN were observed at concentrations above 10 μM, cytotoxicity greatly exceeded 60% (Table 3-1). Using the microscopy-based method, a statistically significant increase was seen at the lowest test concentration of 2.5μM, but overall increases measured on a fold basis were roughly comparable to those seen in the flow-based assay across the range (Figure 3-3B).

The topo II poison etoposide induced significant increases in micronuclei across the entire concentration range tested using both the flow cytometry and microscopy based micronucleus assays (Figures 3-2C and 3-3C). While test concentrations of 100 nM or greater were associated with cytotoxicity exceeding 60%, increases in MN were seen at lower concentrations including an approximate 8-fold increase seen at 50 nM.

Lastly, increases in MN were also seen in TK6 cells treated with both ICRF-154 and ICRF-187, which act as post-cleavage complex catalytic inhibitors at test

concentrations as low as 6.25 µM for ICRF-154 and 1.25 µM for ICRF-187 when measured by flow-cytometry (Figures 3-2D and 3-2E). With the exception of the highest concentrations tested for both compounds, the statistically significant increases in MN were observed at concentrations that were associated with approximately 60% cytotoxicity or lower (Table 3-1). Again, the majority of micronuclei induced were due to chromosome breakage as shown with large increases in K- MN using CREST staining (Figures 3-3D and 3-3E).

Comparison of flow-cytometry and manual scoring IVMN assays

Since one of the goals of this study was to assess if a flow-cytometry based micronucleus assay would help better understand dose-response relationships *in vitro*, we compared both assays using the same test compounds and concentrations (Figures 3-2 and 3-3). While the overall dose responses for each of the test compounds were similar when comparing the two assays, there were some notable differences. First, the actual MN frequency in both the controls and treated cells tended to be higher when measured by flow-cytometry than compared to microscopy. When compared on a fold-change basis, however, roughly similar increases in MN were observed when using the two different types of assay. Another significant difference between the methods was that for all of the compounds tested, significant increases in MN frequency were observed at lower concentrations using the microscopy based assay compared to the flow-cytometry assay. These results seem to indicate that the microscopy-based assay is more sensitive than the flow-based assay.

To rule out that the differences observed were not simply due to differences in statistical approaches used to analyze the datasets from the flow and manual scoring techniques, we used BMD modeling to estimate points of departure (PoD) within the concentration ranges tested for each compound (for modeling results, see supplemental data online). Using this approach, the differences between the flow-cytometry and microscopy based assays were much less pronounced than when simply comparing no observed- or lowest observed genotoxic effect levels (NOGEL and LOGEL, respectively) (Table 3-2). For instance, merbarone, ICRF-187, and aclarubicin all had comparably similar (2-fold or less) BMD and BMDL estimates when comparing results of the two different types of assay; however, for ICRF-154 and etoposide, it appears that manual scoring was considerably more sensitive than the flow-based assay with BMD/BMDL estimates one-third to one-fifth of those seen with the flow assay.

Discussion

Overall, all of the topo II inhibitors induced dose-dependent increases in micronuclei in the TK6 cells. In examining the results from the two methods of MN scoring, the increases appear to be linear or curvilinear at the test concentrations included in our studies. It should be noted that in most cases, cytotoxicity at the highest test concentrations for the five compounds often exceeded values generally considered in an acceptable range (<55% cytotoxicity; OECD, 2016) (21), but with the exception of aclarubicin, statistically-significant increases in MN were seen at

59

concentrations where relative population doubling (RPD) or relative increases in cell counts (RICC) were 75% or higher (Table 3-1).

CREST staining in manually scored cells revealed that a large majority of MN were kinetochore-negative in cells treated with all five inhibitors, indicating that most micronuclei were formed from chromosome breakage (Figure 3-3). It should be noted that increases in chromosome loss were also seen with all of the compounds tested, but the increases occurred at the higher test concentrations and at much lower magnitude than the increases in chromosome breakage.

In terms of potency, bisdioxopiperazines ICRF-154 and ICRF-187 as well as merbarone induced significant increases in MN at low micromolar concentrations (3.125 μM, 0.6125 μM, and 2.5 μM respectively). These concentrations were roughly 500-fold greater than those at which the other catalytic inhibitor tested, aclarubicin, induced significant increases in micronuclei. In fact, the 6.25 nM aclarubicin concentration was similar to the 12.5 nM concentration of the topo II poison etoposide in terms of cytotoxicity and magnitude of micronucleus induction.

The mechanism underlying the clastogenic effects induced by topo II poisons such as etoposide is fairly well understood, as stabilization of the cleavage complex and interference with religation would also lead to persistence of the otherwise transient double stranded break that occurs during the enzyme's catalytic cycle (22). Subsequent removal of the covalently bound topo II found in the cleavage complexcan occur by either endonucleolytic cleavage (23), enzyme-mediated

hydrolysis (24-25), or proteasomal degradation (26) exposing an unprotected DNA double strand break that can result in chromosomal breaks and translocations.

While the clastogenic effects induced by the catalytic inhibitors seen here are in agreement with previously reported findings, the mechanism by which chromosome breaks occur for the catalytic inhibitors is not as well understood (7-8, 27-31). Compounds such as ICRF-154 and ICRF-187 are believed to trap topo II in a "closed-clamp" formation where the double strand break has been properly ligated and the enzyme is no longer covalently bound to the DNA. The inhibited enzyme is unable to be converted back to a catalytically active form, and the enzyme continues to encircle the DNA duplex (28-29). The resulting depletion of active topo II caused by these compounds could then lead to the observed clastogenic responses as the enzyme is no longer available to relieve the torsional strain associated with DNA replication and transcription, or allow for the decatenation of sister chromatids during mitosis.

In our study, aclarubicin was the one catalytic inhibitor tested that behaved considerably differently than the others. It is believed that aclarubicn acts through intercalation, thereby preventing topo II from binding to DNA (30). The low nanomolar concentrations at which effects are seen, however, seem inconsistent with the results seen with other compounds believed to act through similar mechanisms (31). It seems likely, as has been reported by others (30, 33, 34), that aclarubicin has additional targets in the cell and topo II is not be the only enzyme or process affected.

As shown in Table 3-1, substantial differences were seen using the different measures of cytotoxicity/cell proliferation. For manual scoring by microscopy using cytochalasin B, the OECD TG 487 recommends using the CBPI as the measurement of cytotoxicity (21). Compared to the two other measures, RPD and RICC, the CBPI showed substantially less cytotoxicity, particularly at higher concentrations. The reason for the observed differences is not known. However, previous studies have shown that treatment with ICRF 154 and bimolane, both topo II catalytic inhibitors, can produce binucleated cells in the absence of cytochalasin B (7, 35). These earlier results indicate that the CPBI may not be the most accurate measure of cytotoxicity for this class of compounds.

A common and accepted approach to describe dose-response data is by identifying no-observed or lowest-observed genotoxic effect levels (NOGELs or LOGELs). These are in effect similar to the more traditionally used PoD values of NOAELs or LOAELs commonly used in toxicology to describe "apical" effects occurring at the organ or whole-animal level. For dose-response data from the flow-cytometry based assay, NOGEL values were identified for 4 of the 5 inhibitors studied (Table 2). In contrast using the microscopy-based assay, the MN frequency at the lowest concentrations tested for all of the inhibitors, except for aclarubicin, were significantly increased compared to the control, and as a result, NOGEL values could not be identified. While assay sensitivity may contribute to some of the differences seen, it should be noted that different statistical approaches were used to analyze data from the two different types of assay. The data from the microscopy-

based assay was analyzed by conducting a binomial trend test followed by a Fisher's exact test to compare individual treatment to DMSO treated controls. This statistical analysis approach has been largely derived from earlier work evaluating chromosomal aberration frequencies where the numbers of cells scored were quite low. Using the microscopy-based assay with 1000 cells scored and two to three replicates at each concentration, this approach for analysis of data begins to become quite sensitive though statistically significant increases still occur at what intuitively seem to be biologically relevant ranges of 70-80% above the control frequencies, depending on the number of cells scored and whether replicates were combined. When using this approach with the flow-cytometry data, however, increases in micronuclei as low as 8-10% above the control frequency would be concluded to be significantly elevated with low associated p-values due to the large numbers of cells scored. These small increases above the control frequency also lie well within the inter-replicate range of controls. For this reason, a different type of analysis was used; in this case, following a positive ANOVA result, a Dunnett's T-test was used to analyze the flow data, a common statistical approach and consistent with the one recommended by Johnson *et al* (36). This resulted in statistically significant increases at responses deemed to be more biologically relevant. The use of different approaches probably contributed to the different NOGEL values that were obtained using the microscopy and flow-cytometry based assays in our parallel experiments, making it more difficult to make direct comparisons between the two assays.

Because of this, an alternative approach of BMD modeling was explored to describe the dose-response data for the five topo II inhibitors tested.

As mentioned previously, BMD modeling has been used in other fields of toxicology and risk assessment to overcome some pitfalls when estimating PoDs, and more recently in dose-response modeling of genotoxicity data (36-37). BMD modeling is advantageous since it considers the entire range of the experimental data as opposed to only specific tested doses from which NOGEL or LOGEL values are identified, which can be highly influenced by sample size and dose-spacing, and do not take into consideration the slope or shape of the dose-response curve or describe variability or uncertainty (20,38). The estimated PoD, in this case, a BMD, indicates the dose or concentration at which a specified benchmark response (BMR) above the control response would be expected and includes a lower bound confidence limit. The BMR specified here was one standard deviation from controls as specified by the US EPA guidance for BMD modeling of continuous data (20). It should be noted that selection of specific response rates is currently an area of active discussion. Recent reports from working groups utilizing the BMD approach with genotoxicity data such as micronucleus induction have used response rates of 5% or 10%. Based on our experience, a 5-10% increase above the control frequency falls well within normal assay variability and would yield a highly conservative PoD estimate (37, 39). Table 3-2 compares NOGEL or LOGEL values for each of the compounds tested to BMD_{1SD} estimates and their associated lower confidence bounds ($BMDL_{1SD}$). BMD_{1SD} estimates were in a range where minimal but significant

increases are expected to be observed. In most cases, the BMD_{1SD} estimates fell

between the NOGEL and the LOGEL values or, when a NOGEL was not available,

between the control and the LOGEL, thus within the range of observation and

consistent with the goal of having BMDLs agree, on average, with NOAELs (or in this

case NOGELs) thus contributing to the weight of evidence (40). Also, while using the

NOGEL/LOGEL approach was problematic when comparing POD estimates between

manual and flow-cytometric studies, BMD_{1SD} and $BMDL_{1SD}$ values were often quite

comparable between the two assays, as seen with merbarone, ICRF-187, and

aclarubicin.

The mode of action by which a genotoxic agent acts plays an important role

in determining whether or not a threshold exists in the low dose region. Agents that

act through non-DNA reactive mechanisms are generally believed to exhibit

thresholds in their dose responses whereas the risks associated with clastogens and

DNA-reactive mechanisms are often believed to decrease linearly with dose into the

very low dose region (16-17, 41). Recently, increasing evidence has suggested that

at least some clastogens and DNA-reactive genotoxicants may exhibit threshold

dose-responses. For example, alkylating agents such as ethyl methanesulfonate and

methyl methanesulfonate have been predicted to follow a non-linear dose response

due to natural cellular defense pathways such as DNA repair that allows cells to

overcome low levels of DNA damage (42). The existence of thresholds for these

classes of genotoxic agents continues to be made on a case-by-case basis requiring

extensive mechanistic work following positive results in genotoxicity assays.

While some topo II inhibitors have previously been reported to exhibit thresholds *in vitro*, studies have largely focused on topo II poisons such as etoposide (22). Lynch *et al.* compared micronucleus induction using microscopy and stabilization of the cleavage complex, an important step in the formation of double stranded breaks caused by topo II poisons. They concluded that "pragmatic" thresholds could be derived utilizing a modeling approach for the micronucleus dose response data and the mechanistic argument that clastogenicity caused by topo II poisons occurs indirectly due to improper repair following removal of the cleavage complex. Further studies on the mode of action of etoposide by Li Z *et al.* (43) suggest that changes and activation of DNA repair machinery play a role in the clearance of accumulated DSBs caused by topo II-DNA stabilized cleavage complexes. In the current study, we examined whether the flow-cytometric analysis of MN induction in a large number of cells could help identify apparent thresholds and if similar dose-responses could be observed with different classes of topo II inhibitors. It is interesting to note that none the inhibitors tested exhibited a clear threshold type of dose response with linear to curvilinear increases generally being seen at the lower doses tested when using a robust flow-cytometry based assay, highlighting one difficulty of using *in vitro* genotoxicity endpoints to identify threshold type dose-response. While it is certain that further studies with additional lower test concentrations would show NOGEL values for all of these inhibitors tested, it would also be difficult, if not impossible, to determine whether those concentrations were actually true thresholds or would merely appear to be such due

66

to a combination of dose selection, variability and sensitivity limitations of the

assay. Because the error bars at the lowest concentrations overlapped or came close

to overlapping those of the control, it was concluded that there would be little value

in repeating each study where a NOGEL was not obtained to add additional lower

doses. As apparent from the above, decisions about whether genotoxic or other

types of toxic effects exhibit thresholds, need to be largely based on mechanistic and

theoretical considerations, as it is often not possible to empirically distinguish

linear, curvilinear or threshold (hockey stick) types of responses in the low dose

region of many bioassays (44-45). Indeed, many types of biological and

toxicological responses exhibit curvilinear sigmoidal shapes in their low dose

responses, highlighting the need for additional mechanistic information to inform

risk assessment decisions.

These results presented above, also indicate that BMD modeling is an

appropriate and useful method for quantitatively describing dose-response data for

micronucleus induction, which combined with appropriate *in vitro* and *in vivo*

mechanistic information, could help identify biologically relevant PoD estimates.

This is in agreement with several recently published reports highlighting the use of

BMD modeling for genotoxicity data with model compounds utilizing large curated

datasets (36-37,46). Our results indicate that BMD modeling can provide reliable

PoD estimates for dose response studies even when relatively few doses are

available. Further studies will be useful to refine study design to identify an optimal

number of doses, dose spacing, and confirming one standard deviation or another value as the appropriate benchmark response.

Acknowledgements

Table 3-1 Measures of Cytotoxicity for TK6 cells treated with Topo II inhibitors

Concentration	Relative Population Doubling (RPD)	Relative Increase in Cell Counts (RICC)	Relative Cytokinesis-Blocked Proliferation Index (RCBPI)
Aclarubicin (nM)			
0	100.00	100.00	100
3.125	98.74	98.07	92.47
6.25	82.84	73.56	80.54
12.5	50.11	36.09	67.67
25	26.25	16.92	51.37
50	19.89	11.77	31.97
Merbarone (µM)			
0	100.00	100.00	100
2.5	97.52	96.07	92.67
5	87.97	82.01	73.69
10	40.24	27.07	63.61
20	7.93	4.42	52.96
Etoposide (nM)			
0	100.00	100.00	100
12.5	86.76	79.12	89.42
25	76.18	64.82	76.00
50	59.56	45.45	66.03
100	9.23	5.23	57.06
200	0*	0*	33.76
ICRF-154 (µM)			
0	100.00	100.00	100
3.125	103.13	104.78	95.41
6.25	101.60	102.38	94.40
12.5	98.29	97.95	80.88
25	49.32	37.00	73.42
50	0*	0*	57.36
ICRF-187 (µM)			
0	100.00	100.00	100
0.6125	84.48	76.23	97.64
1.25	88.09	81.96	94.75
2.5	57.50	43.69	81.39
5	23.59	14.64	63.06
10	0*	0*	50.21

* A minimum value of 0 used in cases where the cell counts after treatments became lower than initial pre-treatment counts.

Table 3-2 Comparison of NOGEL/LOGEL values with BMD$_{1SD}$ and BMDL$_{1SD}$ for topo II inhibitors using microscopy and flow-cytometry based micronucleus assays

	Microscopy				Flow-cytometry			
	NOGEL	LOGEL	BMD$_{1SD}$	BMDL$_{1SD}$	NOGEL	LOGEL	BMD$_{1SD}$	BMDL$_{1SD}$
Aclarubicin	6.25 nM	12.5 nM	4.9 nM	2.6 nM	6.25 nM	12.5 nM	4.1 nM	3.1 nM
Merbarone	N/A	2.5 µM	1.8 µM	1.2 µM	2.5 µM	5 µM	3.2 µM	2.5 µM
Etoposide	N/A	12.5 nM	6.2 nM	3 nM	N/A	12.5 nM	29 nM	13 nM
ICRF-154	N/A	3.13 µM	2.4 µM	1.6 µM	3.13 µM	6.25 µM	8 µM	6 µM
ICRF-187	N/A	0.63 µM	0.7 µM	0.4 µM	0.63 µM	1.25 µM	0.7 µM	0.3 µM

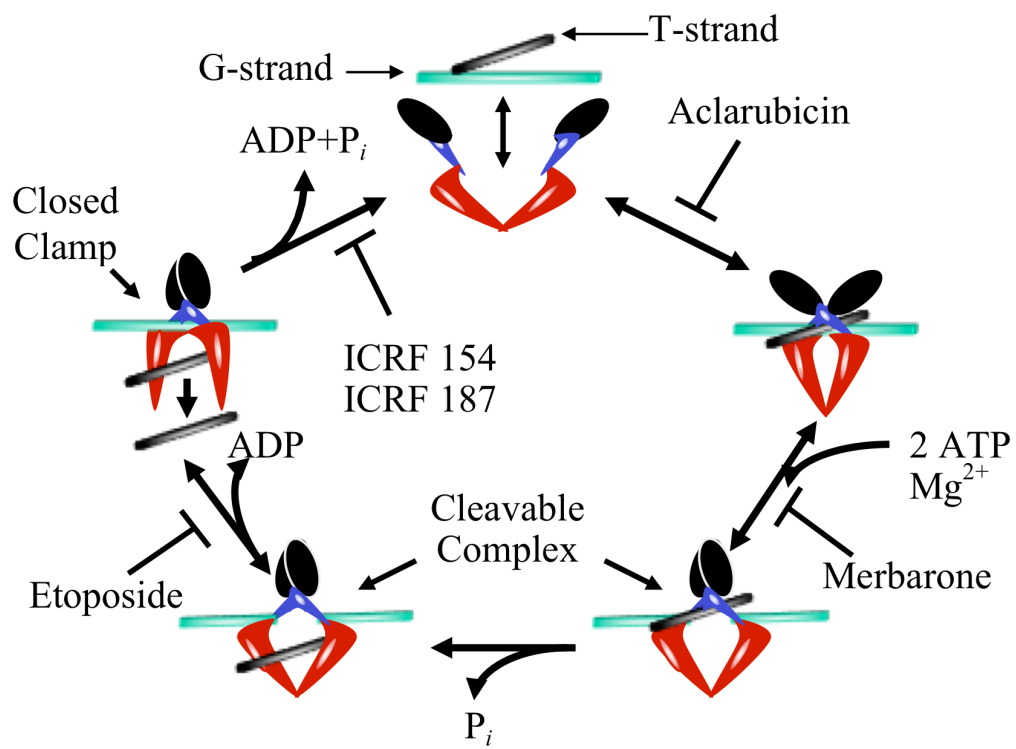**Figure 3-1 Topoisomerase II Catalytic Cycle**

Figure 3-1. Topo II catalytic cycle. The sites of action of the topo II inhibitors used in current study are shown. Adapted from Mondrala S and Eastmond DA. (5)

Figure 3-2 Topoisomerase II Inhibitor Induced Micronuclei Formation Measured by Flow-cytometry
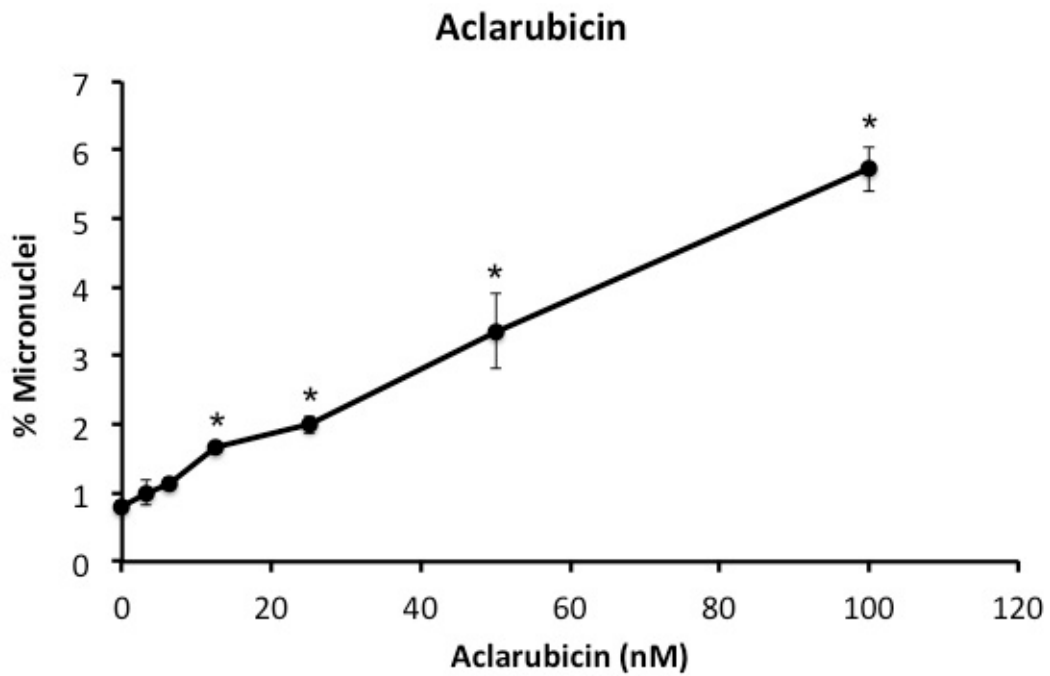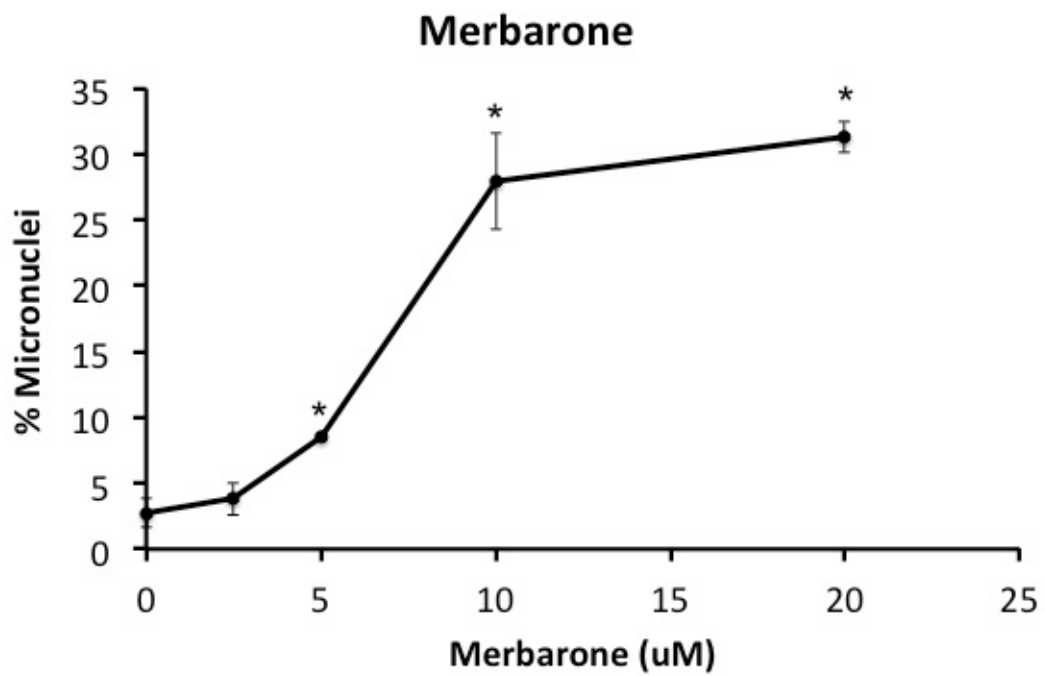
Figure 3-2a

Aclarubicin

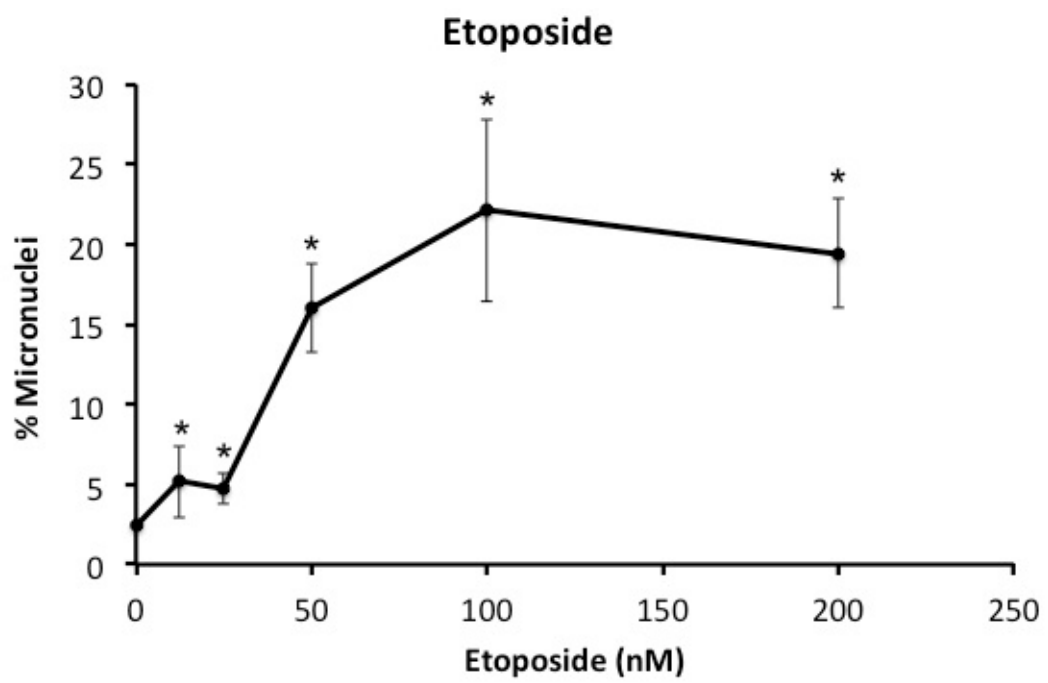**Figure 3-2b**

Figure 3-2c

Figure 3-2d

ICRF-154
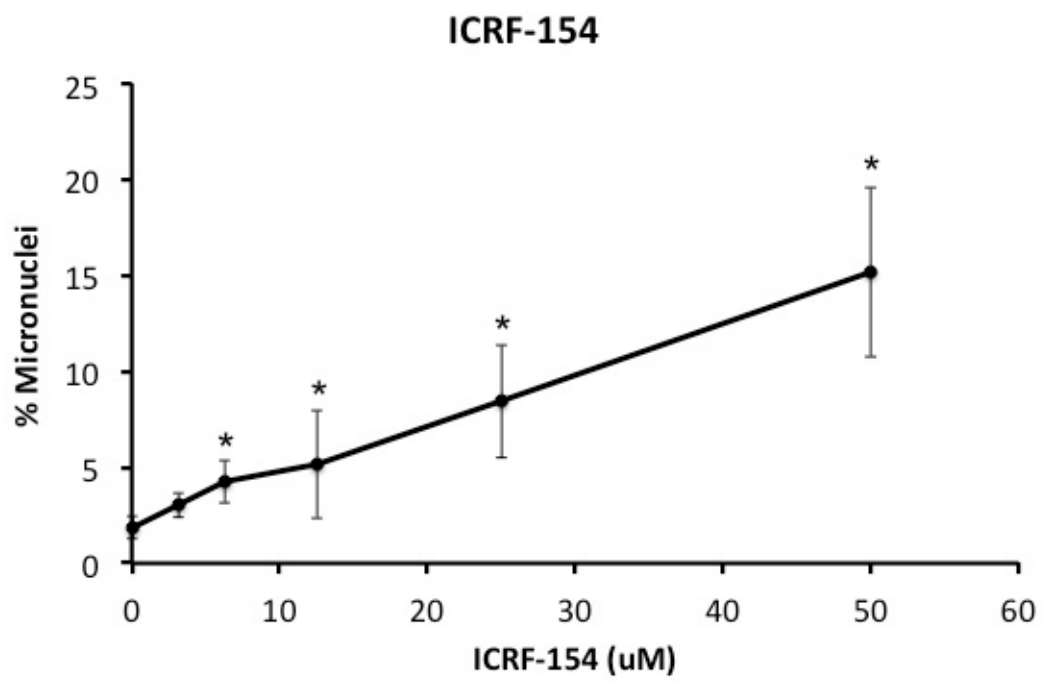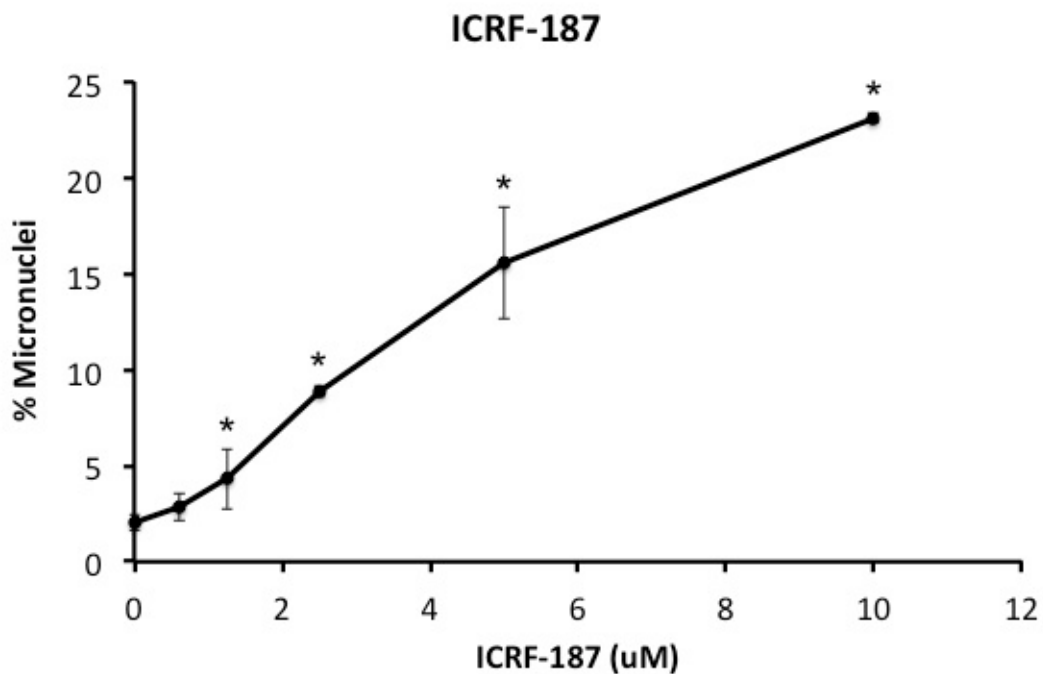
Figure 3-2e

Figure 3-2 a-e. Percentages of micronuclei in TK6 cells treated with the five tested topo II inhibitors measured using a flow cytometry-based *in vitro* micronucleus assay. Data represents means and standard deviation. *Statistically significant *vs.* the DMSO controls (Dunnet's T-test; $P \leq 0.05$)

**Figure 3-3 Topoisomerase II Inhibitor Induced Micronuclei Formation
Measured by Microscopy**

Figure 3-3a
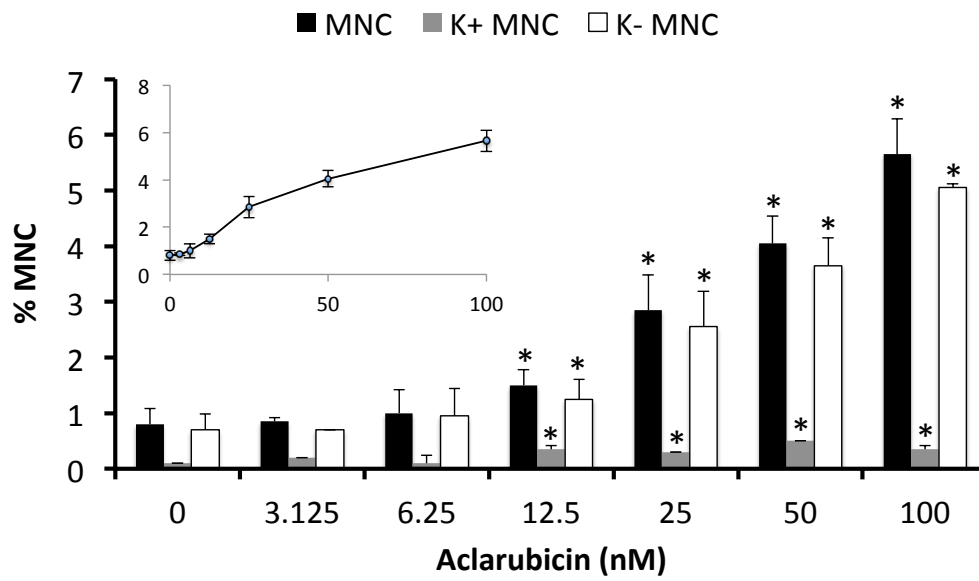
Figure 3-3b
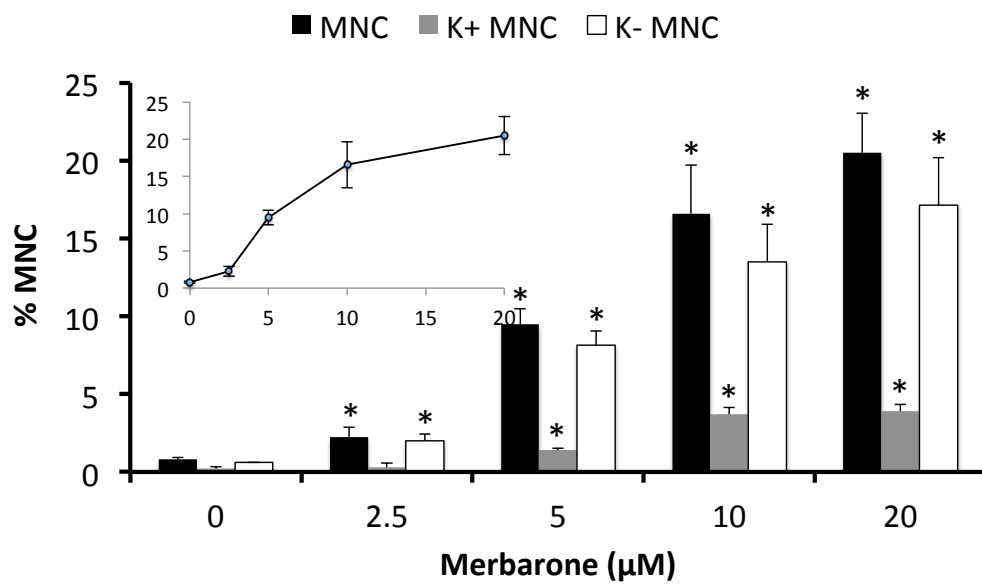
Figure 3-3c
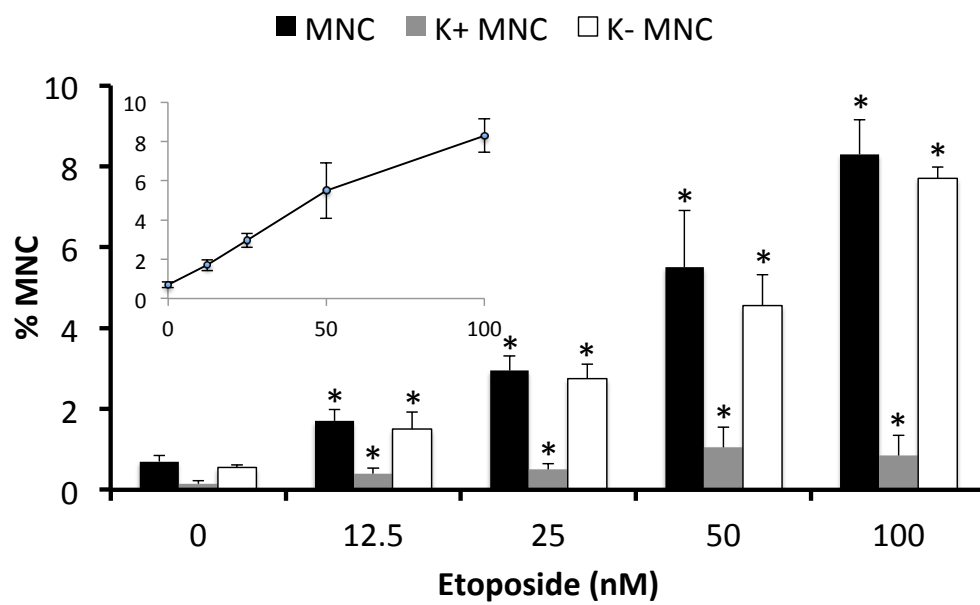
Figure 3-3d
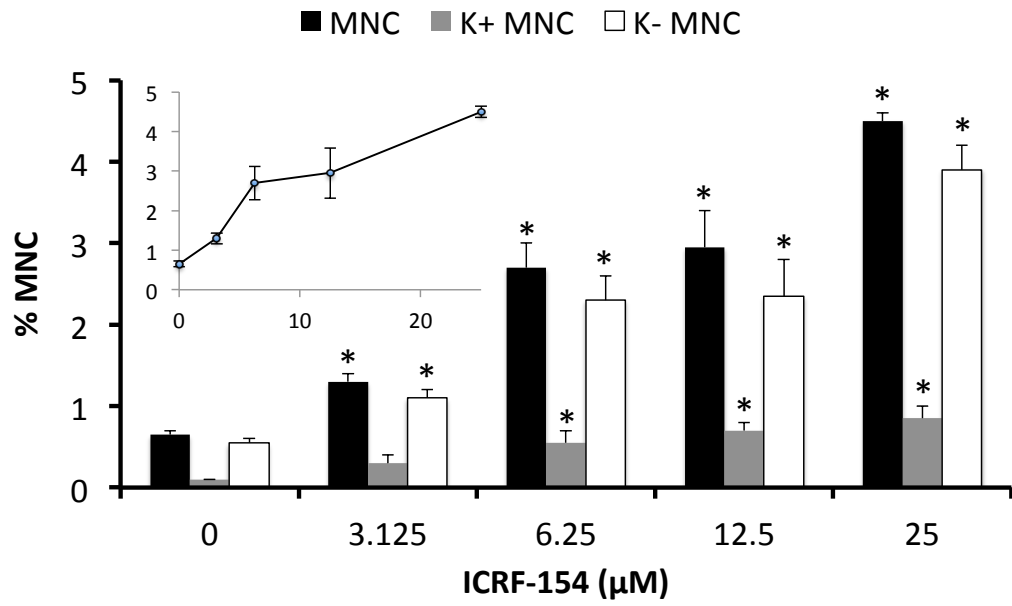
Figure 3-3e
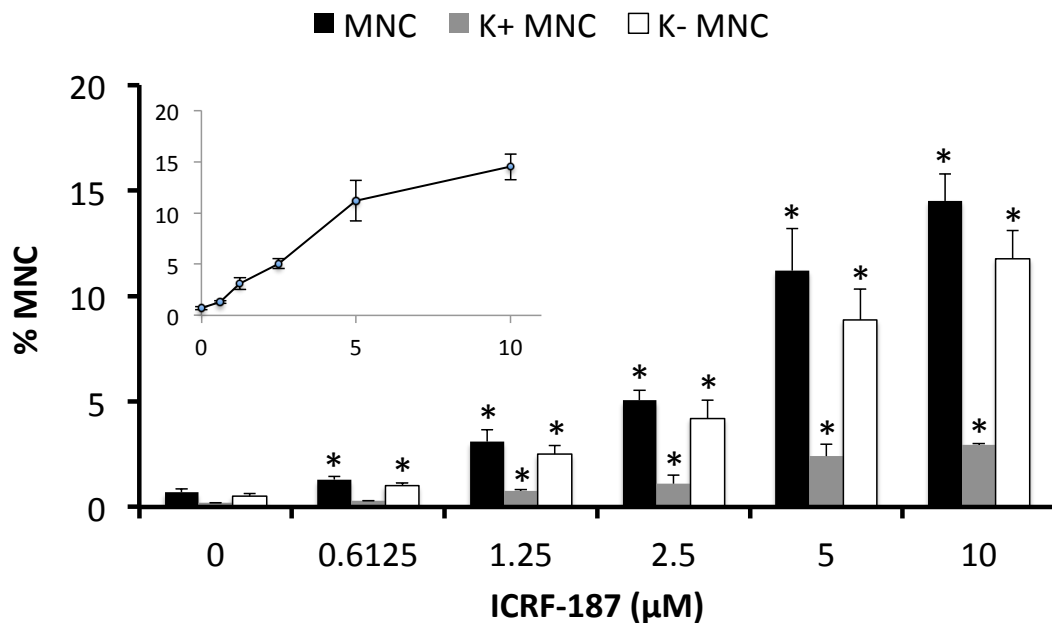
Figure 3-3 a-e. Frequency of micronucleated cells in TK6 cells treated with the tested topo II inhibitors measured using a microscopy-based *in vitro* micronucleus assay are represented in the bar graph as percent micronucleated cells (# per hundred) as well as percentages of kinetochore-positive (K+) and kinetochore-negative (K-) micronucleated cells. The insert represents the micronucleus frequencies from the same experiments plotted on a linear x-axis scale to facilitate comparison of dose-response relationships with the flow cytometry results shown in Figure 2. The means and standard deviations are shown. *Statistically significant *vs.* the DMSO controls (Fisher's exact test; $P \leq 0.05$).

References

1. Pendleton M, Lindsey RH Jr, Felix CA, Grimwade D, Osheroff N. Topoisomerase II and leukemia. Ann N Y Acad Sci. 2014;1310: 98–110.

2. McClendon AK, Osheroff N. DNA topoisomerase II, genotoxicity, and cancer. Mutat Res. 2007;623: 83–97.

3. Deweese JE, Osheroff N. The DNA cleavage reaction of topoisomerase II: wolf in sheep's clothing. Nucleic Acids Res. 2009;37: 738–748.

4. Vos SM, Tretter EM, Schmidt BH, Berger JM. All tangled up: how cells direct, manage and exploit topoisomerase function. Nat Rev Mol Cell Biol. 2011;12: 827–841.

5. Mondrala S, Eastmond DA. Topoisomerase II inhibition by the bioactivated benzene metabolite hydroquinone involves multiple mechanisms. Chem Biol Interact. 2010;184: 259–268.

6. Nitiss JL. DNA topoisomerase II and its growing repertoire of biological functions. Nat Rev Cancer. 2009;9: 327–337.

7. Vuong MC, Hasegawa LS, Eastmond DA. A comparative study of the cytotoxic and genotoxic effects of ICRF-154 and bimolane, two catalytic inhibitors of topoisomerase II. Mutat Res. 2013;750: 63–71.

8. Wang L, Eastmond DA. Catalytic inhibitors of topoisomerase II are DNA-damaging agents: induction of chromosomal damage by merbarone and ICRF-187. Environ Mol Mutagen. 2002;39: 348–356.

9. Mauritzson N, Albin M, Rylander L, Billström R, Ahlgren T, Mikoczy Z, et al. Pooled analysis of clinical and cytogenetic features in treatment-related and de novo adult acute myeloid leukemia and myelodysplastic syndromes based on a consecutive series of 761 patients analyzed 1976-1993 and on 5098 unselected cases reported in the literature 1974-2001. Leukemia. 2002;16: 2366–2378.

10. Joannides M, Mays AN, Mistry AR, Hasan SK, Reiter A, Wiemels JL, et al. Molecular pathogenesis of secondary acute promyelocytic leukemia. Mediterr J Hematol Infect Dis. 2011;3: e2011045.

11. Rashidi A, Fisher SI. Therapy-related acute promyelocytic leukemia: a systematic review. Med Oncol. 2013;30: 625.

12. Li Y-S, Zhao Y-L, Jiang Q-P, Yang C-L. Specific chromosome changes and non-occupational exposure to potentially carcinogenic agents in acute leukemia in china. Leuk Res. 1989;13: 367–376.

13. Strick R, Strissel PL, Borgers S, Smith SL, Rowley JD. Dietary bioflavonoids induce cleavage in the MLL gene and may contribute to infant leukemia. Proc Natl Acad Sci U S A. 2000;97: 4790–4795.

14. Spector LG, Xie Y, Robison LL, Heerema NA, Hilden JM, Lange B, et al. Maternal diet and infant leukemia: the DNA topoisomerase II inhibitor hypothesis: a report from the children's oncology group. Cancer Epidemiol Biomarkers Prev. 2005;14: 651–655.

15. Xue Y, Lu D, Guo Y, Lin B. Specific chromosomal translocations and therapy-related leukemia induced by bimolane therapy for psoriasis. Leuk Res. 1992;16: 1113–1123.

16. Bryce SM, Avlasevich SL, Bemis JC, Phonethepswath S, Dertinger SD. Miniaturized flow cytometric in vitro micronucleus assay represents an efficient tool for comprehensively characterizing genotoxicity dose-response relationships. Mutat Res. 2010;703: 191–199.

17. Elhajouji A, Lukamowicz M, Cammerer Z, Kirsch-Volders M. Potential thresholds for genotoxic effects by micronucleus scoring. Mutagenesis. 2011;26: 199–204.

18. Eastmond DA, Tucker JD. Identification of aneuploidy-inducing agents using cytokinesis-blocked human lymphocytes and an antikinetochore antibody. Environ Mol Mutagen. 1989;13: 34–43.

19. Avlasevich SL, Bryce SM, Cairns SE, Dertinger SD. In vitro micronucleus scoring by flow cytometry: differential staining of micronuclei versus apoptotic and necrotic chromatin enhances assay reliability. Environ Mol Mutagen. 2006;47: 56–66.

20. Epa US, ORD, NCEA. Benchmark Dose Technical Guidance. 2014; Available: https://www.epa.gov/risk/benchmark-dose-technical-guidance

21. OECD (2010), *Test No. 487: In Vitro Mammalian Cell Micronucleus Test*, OECD Publishing, Paris, https://doi.org/10.1787/9789264091016-en.

22. Lynch A, Harvey J, Aylott M, Nicholas E, Burman M, Siddiqui A, et al. Investigations into the concept of a threshold for topoisomerase inhibitor-induced clastogenicity. Mutagenesis. 2003;18: 345–353.

23. Hartsuiker E, Neale MJ, Carr AM. Distinct requirements for the Rad32(Mre11) nuclease and Ctp1(CtIP) in the removal of covalently bound topoisomerase I and II from DNA. Mol Cell. 2009;33: 117–123.

24. Cortes Ledesma F, El Khamisy SF, Zuma MC, Osborn K, Caldecott KW. A human 5'-tyrosyl DNA phosphodiesterase that repairs topoisomerase-mediated DNA damage. Nature. 2009;461: 674–678.

25. Borda MA, Palmitelli M, Verón G, González-Cid M, de Campos Nebel M. Tyrosyl-DNA-phosphodiesterase I (TDP1) participates in the removal and repair of stabilized-Top2α cleavage complexes in human cells. Mutat Res. 2015;781: 37–48.

26. Mao Y, Desai SD, Ting CY, Hwang J, Liu LF. 26 S proteasome-mediated degradation of topoisomerase II cleavable complexes. J Biol Chem. 2001;276: 40652–40658.

27. Larsen AK, Escargueil AE, Skladanowski A. Catalytic topoisomerase II inhibitors in cancer therapy. Pharmacol Ther. 2003;99: 167–181.

28. Tanabe K, Ikegami Y, Ishida R, Andoh T. Inhibition of topoisomerase II by antitumor agents bis(2,6-dioxopiperazine) derivatives. Cancer Res. 1991;51: 4903–4908.

29. Andoh T, Ishida R. Catalytic inhibitors of DNA topoisomerase II. Biochim Biophys Acta. 1998;1400: 155–171.

30. Sørensen BS, Sinding J, Andersen AH, Alsner J, Jensen PB, Westergaard O. Mode of action of topoisomerase II-targeting agents at a specific DNA sequence. Uncoupling the DNA binding, cleavage and religation events. J Mol Biol. 1992;228: 778–786.

31. Monnot M, Mauffret O, Simon V, Lescot E, Psaume B, Saucier JM, et al. DNA-drug recognition and effects on topoisomerase II-mediated cytotoxicity. A three-mode binding model for ellipticine derivatives. J Biol Chem. 1991;266: 1820–1829.

32. Snyder RD, Arnone MR. Putative identification of functional interactions between DNA intercalating agents and topoisomerase II using the V79 in vitro micronucleus assay. Mutat Res. 2002;503: 21–35.

33. Pang B, Qiao X, Janssen L, Velds A, Groothuis T, Kerkhoven R, et al. Drug-induced histone eviction from open chromatin contributes to the chemotherapeutic effects of doxorubicin. Nat Commun. 2013;4: 1908.

34. Pang B, de Jong J, Qiao X, Wessels LFA, Neefjes J. Chemical profiling of the genome with anti-cancer drugs defines target specificities. Nat Chem Biol. 2015;11: 472–480.

35. Roy SK, Eastmond DA. Bimolane induces multiple types of chromosomal aberrations in human lymphocytes in vitro. Mutat Res. 2011;726: 181–187.

36. Johnson GE, Soeteman-Hernández LG, Gollapudi BB, Bodger OG, Dearfield KL, Heflich RH, et al. Derivation of point of departure (PoD) estimates in genetic toxicology studies and their potential applications in risk assessment. Environ Mol Mutagen. 2014;55: 609–623.

37. Gollapudi BB, Johnson GE, Hernandez LG, Pottenger LH, Dearfield KL, Jeffrey AM, et al. Quantitative approaches for assessing dose-response relationships in genetic toxicology studies. Environ Mol Mutagen. 2013;54: 8–18.

38. Davis JA, Gift JS, Zhao QJ. Introduction to benchmark dose methods and U.S. EPA's benchmark dose software (BMDS) version 2.1.1. Toxicol Appl Pharmacol. 2011;254: 181–191.

39. Bemis JC, Wills JW, Bryce SM, Torous DK, Dertinger SD, Slob W. Comparison of in vitro and in vivo clastogenic potency based on benchmark dose analysis of flow cytometric micronucleus data. Mutagenesis. 2016;31: 277–285.

40. Haber LT, Dourson ML, Allen BC, Hertzberg RC, Parker A, Vincent MJ, et al. Benchmark dose (BMD) modeling: current practice, issues, and challenges. Crit Rev Toxicol. 2018;48: 387–415.

41. Pottenger LH, Gollapudi BB. Genotoxicity testing: moving beyond qualitative "screen and bin" approach towards characterization of dose-response and thresholds. Environ Mol Mutagen. 2010;51: 792–799.

42. Doak SH, Jenkins GJS, Johnson GE, Quick E, Parry EM, Parry JM. Mechanistic influences for mutation induction curves after exposure to DNA-reactive carcinogens. Cancer Res. 2007;67: 3904–3911.

43. Li Z, Sun B, Clewell RA, Adeleye Y, Andersen ME, Zhang Q. Dose-response modeling of etoposide-induced DNA damage response. Toxicol Sci. 2014;137: 371–384.

44. Bailey GS, Reddy AP, Pereira CB, Harttig U, Baird W, Spitsbergen JM, et al. Nonlinear cancer response at ultralow dose: a 40800-animal ED(001) tumor and biomarker study. Chem Res Toxicol. 2009;22: 1264–1276.

45. Spassova MA, Miller DJ, Eastmond DA, Nikolova NS, Vulimiri SV, Caldwell J, et al. Dose-response analysis of bromate-induced DNA damage and mutagenicity is consistent with low-dose linear, nonthreshold processes. Environ Mol Mutagen. 2013;54: 19–35.43.

46. MacGregor JT, Frötschl R, White PA, Crump KS, Eastmond DA, Fukushima S, et al. IWGT report on quantitative approaches to genotoxicity risk assessment II. Use of point-of-departure (PoD) metrics in defining acceptable exposure limits and assessing human risk. Mutat Res Genet Toxicol Environ Mutagen. 2015;783: 66–78.

Chapter 3: Supplemental Data

Model inclusion and selection for benchmark dose analysis of micronucleus data

For each of the topoisomerase II inhibitors, micronucleus frequencies were fit to Exponential (2, 3, 4, and 5), Hill, power (restricted), linear (1°), and polynomial (2°) dose-response models. Each model was run assuming constant variance, and the benchmark response factor was set to 1.00 of the control group standard deviation (SD). According to benchmark dose guidelines (U.S. EPA, 2012), models with a global goodness-of-fit p value < 0.1 were excluded; p values of 1 indicate a perfect fit, meaning the predicted response of model is identical to the observed response. To select the best globally fitting model with the least complexity, the model with the lowest Akaike Information Criterion (AIC is −2L + 2p, where L is the log-likelihood at the maximum likelihood estimates for p estimated parameters) (Akaike, 1973) was selected as the final model. In unusual instances, such as etoposide assessed by flow cytometry and ICRF-154 assessed by microscopy, inclusion of the entire concentration range tested resulted in no models with an acceptable fit based on the global goodness-of-fit p value. In those cases, the highest concentration was then omitted and the models were re-run which resulted in acceptable fits. Conversely, with etoposide assessed by microscopy and merbarone assessed by flow cytometry, where multiple models fit the above criteria equally well, a visual comparison of the appropriate models was used to select the best fitting model. In the case of aclarubicin assessed by flow cytometry, two different

models actually yielded the same exact output, indicating both equally fit the data. The tables in this appendix show the BMD outputs for the various models run and information for the model selected is shaded in gray. The corresponding plots for the best fitting model selected for each chemical are also presented with data representing means and their 95% confidence limits calculated using a student t-distribution as described in (EPA ORD, NCEA. Benchmark Dose Technical Guidance. 2014; Available: https://www.epa.gov/risk/benchmark-dose-technical-guidance)

Table & Figure 3-S1: BMD modeling for Aclarubicin (microscopy)

Model Name	p-value (Global Fit)	AIC	BMD	BMDL	BMD/ BMDL
Exponential 2	< 0.0001	10.4905	28.3	22.1	1.3
Exponential 3	< 0.0001	10.4905	28.3	22.1	1.3
Exponential 4	0.2452	-14.502	2.8	2.0	1.4
Exponential 5	0.2888	-14.1823	4.2	2.3	1.9
Hill	0.4109	-15.06268	4.9	2.6	1.9
Linear	0.001816	-2.80779	8.7	6.5	1.3
Polynomial	0.001816	-2.80779	8.7	6.5	1.3
Polynomial	0.001816	-2.80779	8.7	6.5	1.3
Power	0.001816	-2.80779	8.7	6.5	1.3

Hill Model, with BMR of 1 Std. Dev. for the BMD and 0.95 Lower Confidence Limit for the BMDL
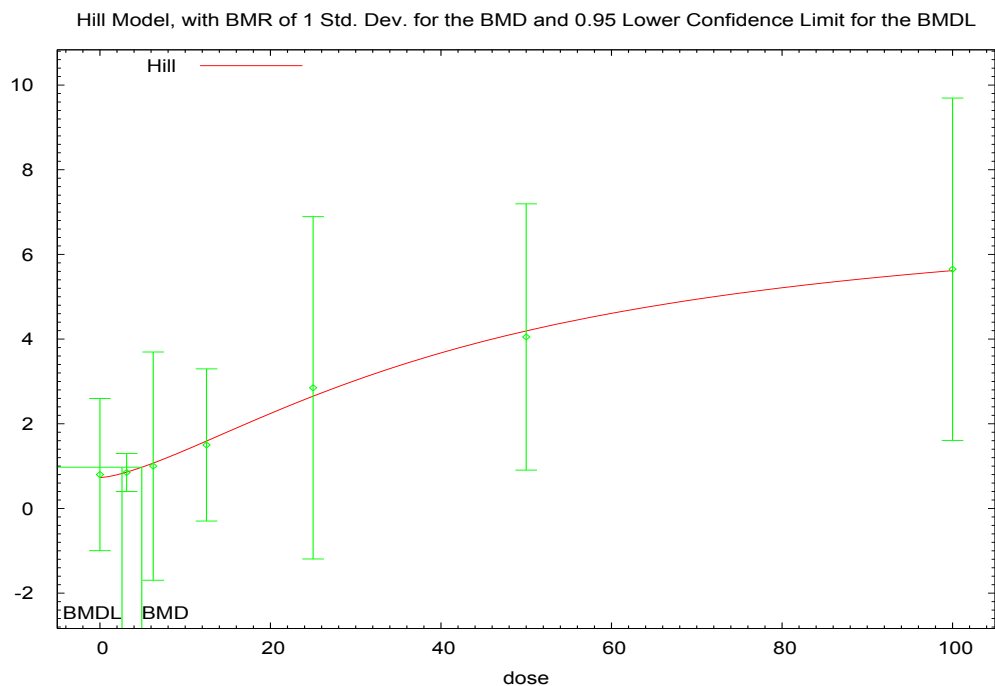
Table & Figure 3-S2: BMD modeling for Merbarone (microscopy)

Model Name	p-value (Global Fit)	AIC	BMD	BMDL	BMD/ BMDL
Exponential 2	< 0.0001	43.7841	7.9	6.0	1.3
Exponential 3	< 0.0001	43.7841	7.9	6.0	1.3
Exponential 4	0.001656	29.56222	0.8	0.6	1.5
Exponential 5	0.04586	22.74228	1.4	0.9	1.5
Hill	0.2079	20.341825	1.8	1.2	1.4
Linear	<.0001	36.596979	2.7	1.9	1.4
Polynomial	<.0001	36.596979	2.7	1.9	1.4
Polynomial	<.0001	36.596979	2.7	1.9	1.4
Power	<.0001	36.596979	2.7	1.9	1.4

Hill Model, with BMR of 1 Std. Dev. for the BMD and 0.95 Lower Confidence Limit for the BMDL
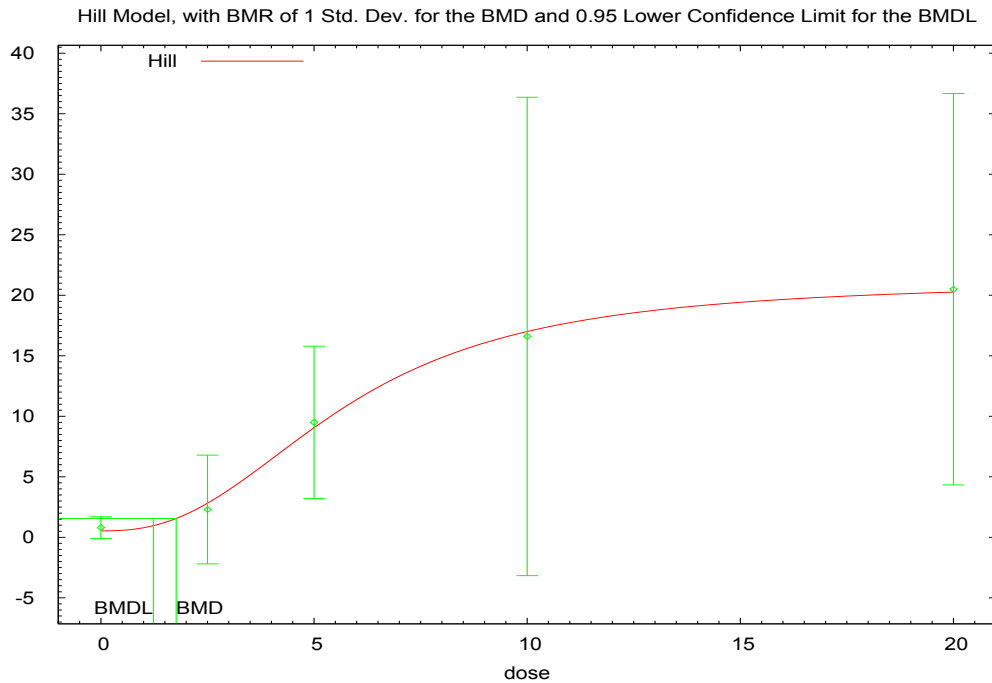
Table & Figure 3-S3: BMD modeling for Etoposide (microscopy)

Model Name	p-value (Global Fit)	AIC	BMD	BMDL	BMD/ BMDL
Exponential 2	0.0003336	15.61053	27.5	20.7	1.3
Exponential 3	0.0003336	15.61053	27.5	20.7	1.3
Exponential 4	0.3948	0.8873607	3.7	2.5	1.5
Exponential 5	0.9271	1.037166	6.2	3.0	2.1
Hill	0.8326	1.073483	6.6	3.0	2.2
Linear	0.07731	3.864818	7.1	5.1	1.4
Polynomial	0.07731	3.864818	7.1	5.1	1.4
Polynomial	0.07731	3.864818	7.1	5.1	1.4
Power	0.07731	3.864818	7.1	5.1	1.4

Exponential Model 5, with BMR of 1 Std. Dev. for the BMD and 0.95 Lower Confidence Level for BMDL
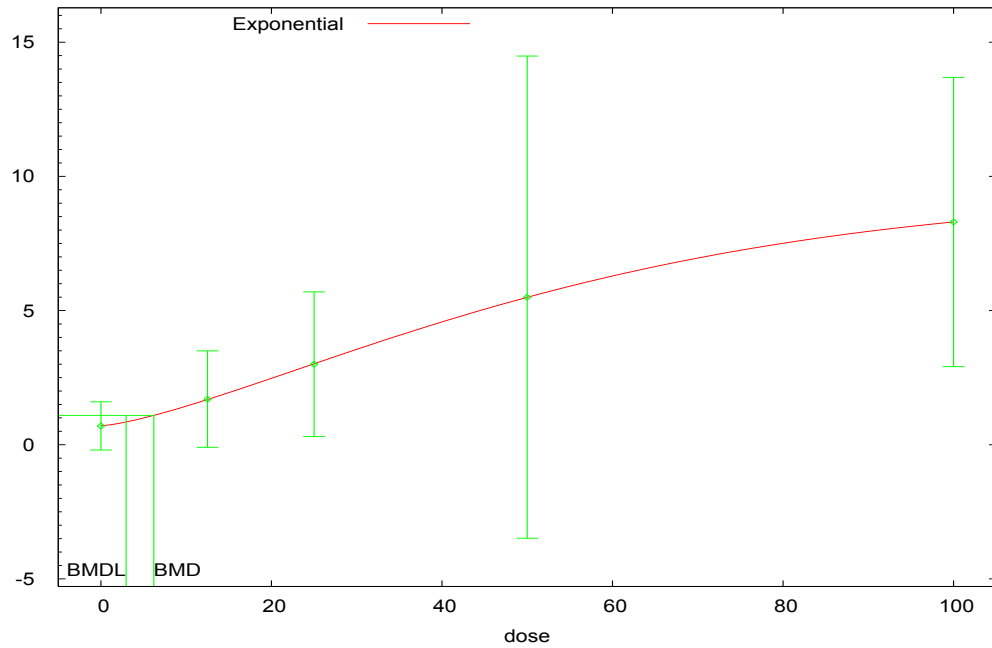

92

Table & Figure 3-S4: BMD modeling for ICRF-154 (microscopy)

Model Name	p-value (Global Fit)	AIC	BMD	BMDL	BMD/ BMDL
Exponential 2	0.0008082	3.432635	4.5	3.2	1.4
Exponential 3	0.0008082	3.432635	4.5	3.2	1.4
Exponential 4	0.006756	-1.472134	0.9	0.5	1.7
Exponential 5	N/A	-6.808742	2.1	1.3	1.6
Hill	N/A	-6.808742	2.3	1.6	1.4
Linear	0.004191	0.140696	2.2	1.5	1.5
Polynomial	0.004191	0.140696	2.2	1.5	1.5
Polynomial	0.004191	0.140696	2.2	1.5	1.5
Power	0.004191	0.140696	2.2	1.5	1.5

Hill Model, with BMR of 1 Std. Dev. for the BMD and 0.95 Lower Confidence Limit for the BMDL
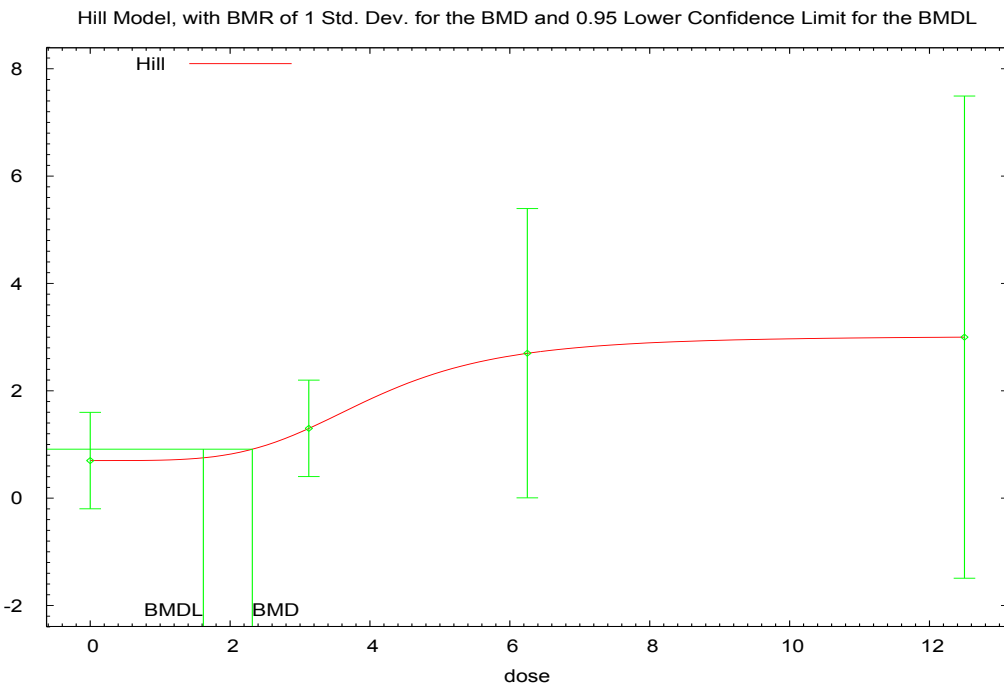
Table & Figure 3-S5: BMD modeling for ICRF-187 (microscopy)

Model Name	p-value (Global Fit)	AIC	BMD	BMDL	BMD/ BMDL
Exponential 2	< 0.0001	37.98269	3.5	2.7	1.3
Exponential 3	< 0.0001	37.98269	3.5	2.7	1.3
Exponential 4	0.006314	16.13346	0.3	0.2	1.4
Exponential 5	0.1485	9.610898	0.7	0.4	1.6
Hill	<.0001	56.605202	0.0	0.0	-
Linear	<.0001	25.751528	1.0	0.7	1.4
Polynomial	<.0001	25.751528	1.0	0.7	1.4
Polynomial	<.0001	25.751528	1.0	0.7	1.4
Power	<.0001	25.751528	1.0	0.7	1.4

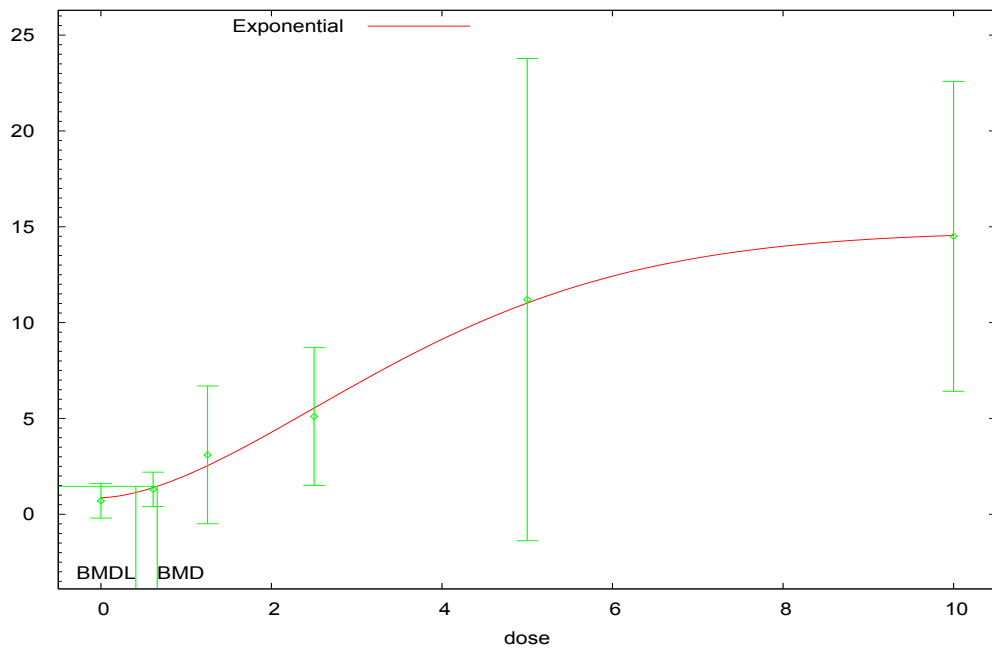Exponential Model 5, with BMR of 1 Std. Dev. for the BMD and 0.95 Lower Confidence Level for BMDL

Table & Figure 3-S6: BMD modeling for Aclarubicin (Flow-cytometry)

Model Name	p-value (Global Fit)	AIC	BMD	BMDL	BMD/ BMDL
Exponential 2	0.0005799	-6.096969	17.7	13.7	1.3
Exponential 3	0.0005799	-6.096969	17.7	13.7	1.3
Exponential 4	0.5773	-22.9785	3.9	2.8	1.4
Exponential 5	0.5773	-22.9785	3.9	2.8	1.4
Hill	0.5774	-22.979054	3.9	2.8	1.4
Linear	0.6892	-24.793438	4.1	3.1	1.3
Power	0.6892	-24.793438	4.1	3.1	1.3

Linear Model, with BMR of 1 Std. Dev. for the BMD and 0.95 Lower Confidence Limit for the BMDL
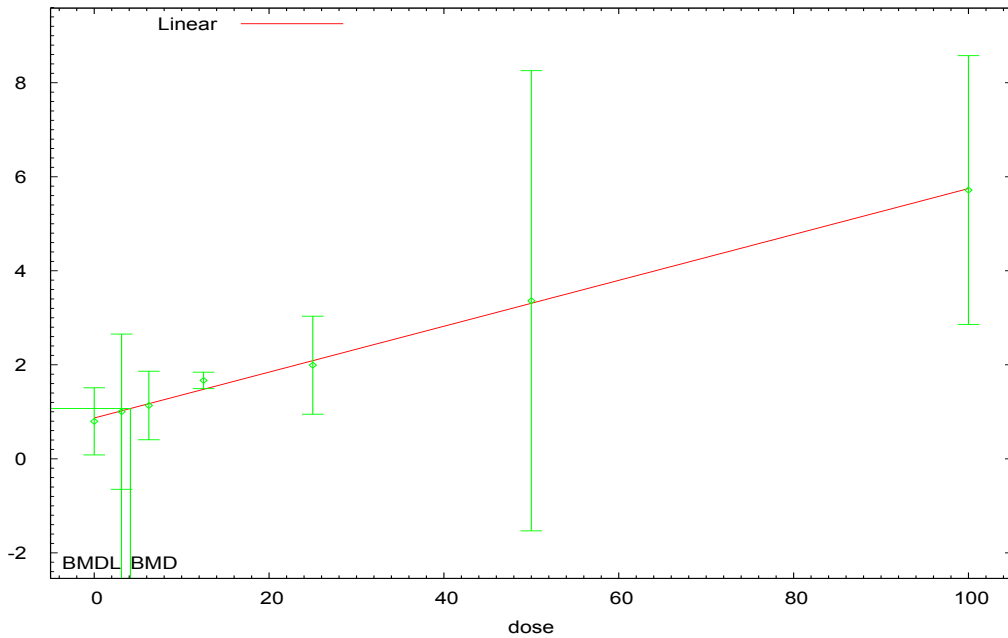
Power Model, with BMR of 1 Std. Dev. for the BMD and 0.95 Lower Confidence Limit for the BMDL
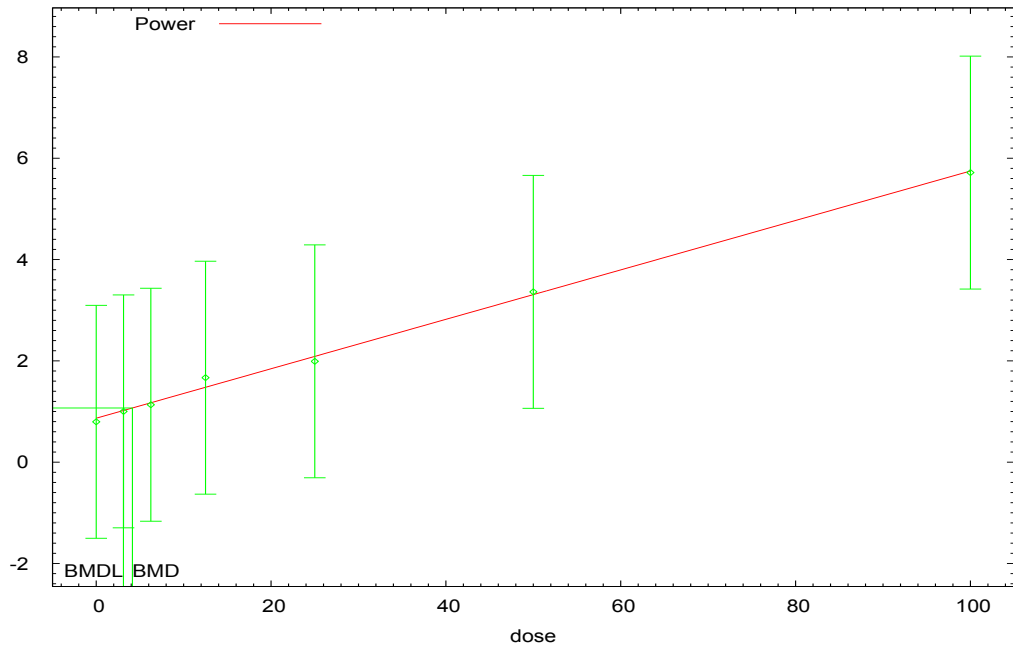
Table & Figure 3-S7: BMD modeling for Merbarone (Flow-cytometry)

Model Name	p-value (Global Fit)	AIC	BMD	BMDL	BMD/ BMDL
Exponential 2	< 0.0001	53.68182	8.4	6.4	1.3
Exponential 3	< 0.0001	53.68182	8.4	6.4	1.3
Exponential 4	< 0.0001	46.33297	1.4	0.9	1.5
Exponential 5	0.7751	25.72911	3.2	2.5	1.3
Hill	0.5556	25.994778	3.7	3.1	1.2
Linear	<.0001	47.775787	3.1	2.1	1.4
Polynomial	<.0001	47.775787	3.1	2.1	1.4
Polynomial	<.0001	47.775787	3.1	2.1	1.4
Power	<.0001	47.775787	3.1	2.1	1.4

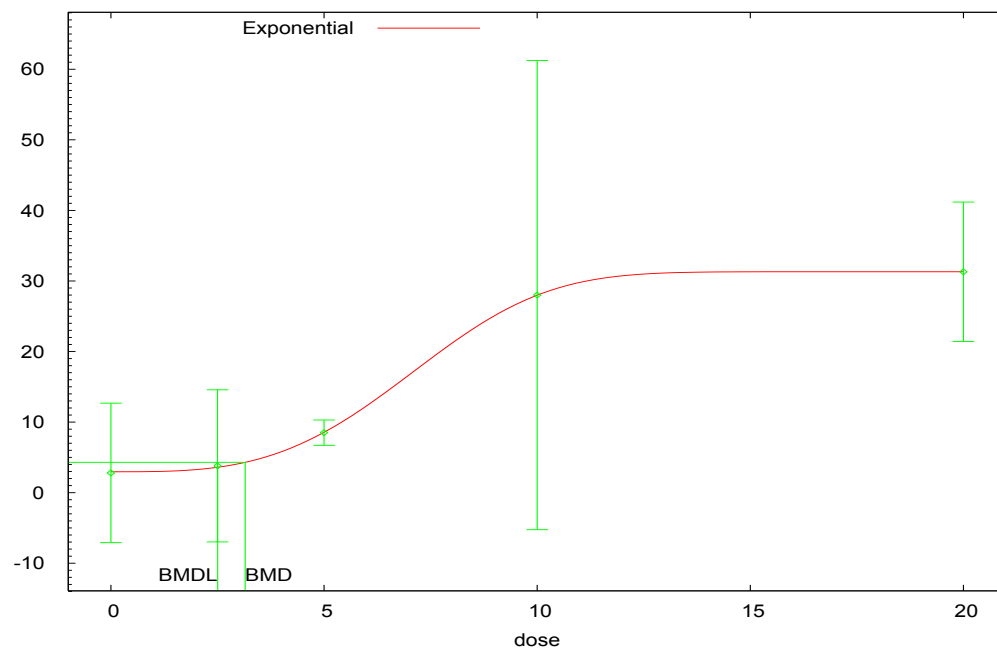Exponential Model 5, with BMR of 1 Std. Dev. for the BMD and 0.95 Lower Confidence Level for BMDL

Table & Figure 3-S8: BMD modeling for Etoposide (Flow-cytometry)

Model Name	p-value (Global Fit)	AIC	BMD	BMDL	BMD/ BMDL
Exponential 2	0.01584	41.65264	35.6	27.0	1.3
Exponential 3	0.01584	41.65264	35.6	27.0	1.3
Exponential 4	0.06098	38.9005	10.7	6.0	1.8
Exponential 5	0.2369	36.70514	29.3	13.3	2.2
Hill	0.2317	36.736388	29.4	14.4	2.0
Linear	0.1081	37.379934	14.0	9.8	1.4
Polynomial	0.1081	37.379934	14.0	9.8	1.4
Polynomial	0.1081	37.379934	14.0	9.8	1.4
Power	0.1081	37.379934	14.0	9.8	1.4

Exponential Model 5, with BMR of 1 Std. Dev. for the BMD and 0.95 Lower Confidence Level for BMDL
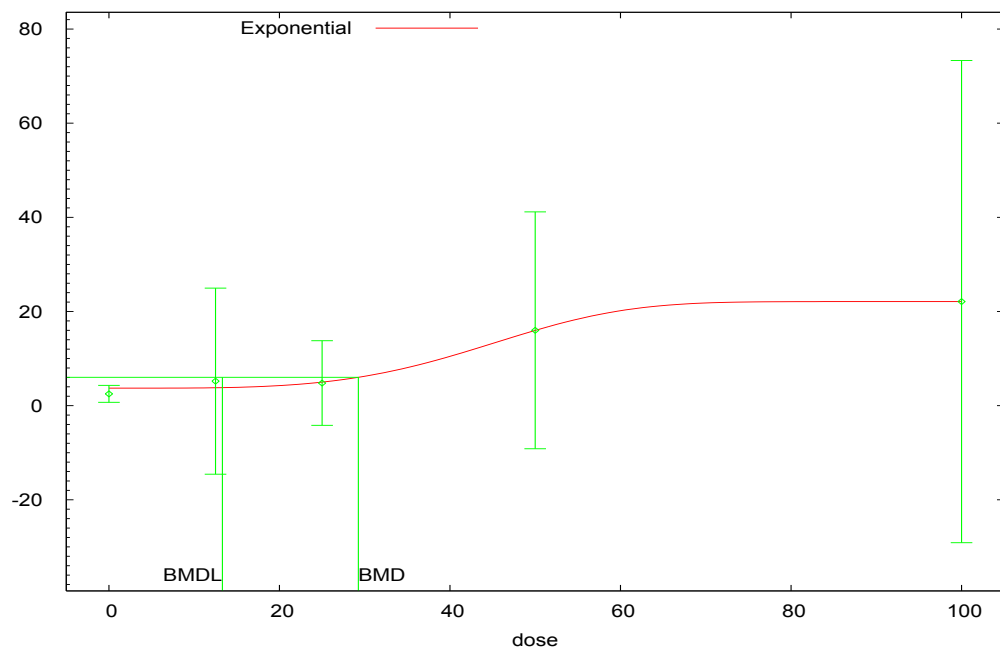

98

Table & Figure 3-S9: BMD modeling for ICRF-154 (Flow-cytometry)

Model Name	p-value (Global Fit)	AIC	BMD	BMDL	BMD/ BMDL
Exponential 2	0.5913	52.51056	16.6	13.4	1.2
Exponential 3	0.9534	52.04189	8.0	6.0	1.3
Exponential 4	0.8459	54.04191	8.0	4.6	1.7
Exponential 5	0.8446	54.045033	8.0	4.5	1.8
Hill	0.9875	50.041831	8.0	6.0	1.3
Linear	0.9559	52.028824	8.3	6.0	1.4
Polynomial	0.9576	52.020113	8.3	6.0	1.4
Polynomial	0.9534	52.04182	8.0	6.0	1.3
Power	0.5913	52.51056	16.6	13.4	1.2

Linear Model, with BMR of 1 Std. Dev. for the BMD and 0.95 Lower Confidence Limit for the BMDL
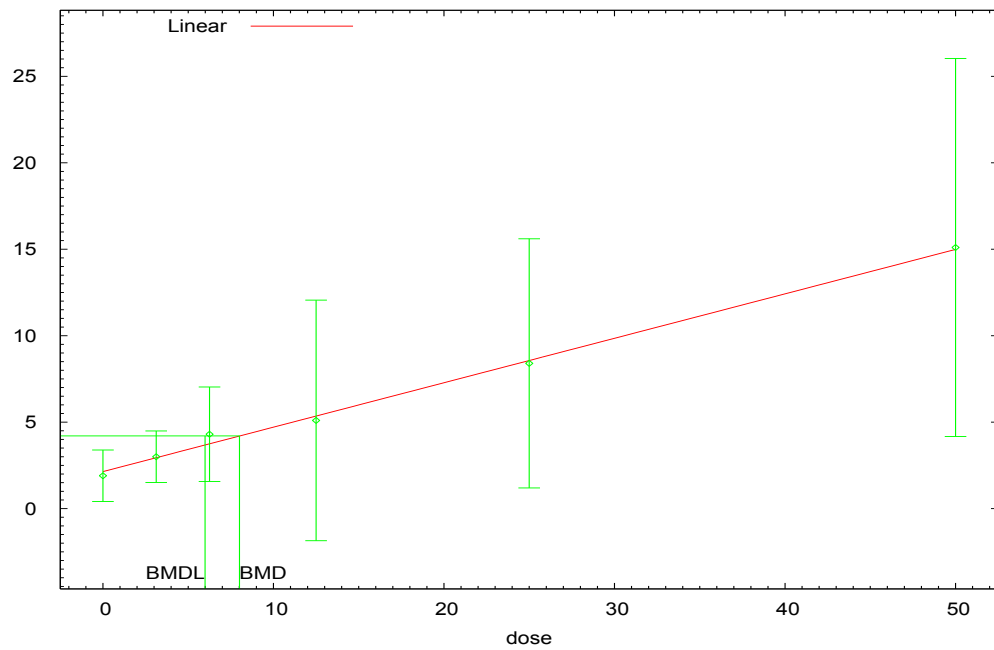
Table & Figure 3-S10: BMD modeling for ICRF-187 (Flow-cytometry)

Model Name	p-value (Global Fit)	AIC	BMD	BMDL	BMD/ BMDL
Exponential 2	< 0.0001	43.04621	2.9	2.2	1.3
Exponential 3	< 0.0001	43.04621	2.9	2.2	1.3
Exponential 4	0.296	23.44528	0.3	0.2	1.4
Exponential 5	0.7438	22.33944	0.6	0.3	1.9
Hill	0.8322	22.114627	0.7	0.3	1.9
Linear	0.02786	28.634548	0.7	0.5	1.4
Polynomial	0.02786	28.634548	0.7	0.5	1.4
Polynomial	0.02786	28.634548	0.7	0.5	1.4
Power	0.02786	28.634548	0.7	0.5	1.4

Hill Model, with BMR of 1 Std. Dev. for the BMD and 0.95 Lower Confidence Limit for the BMDL
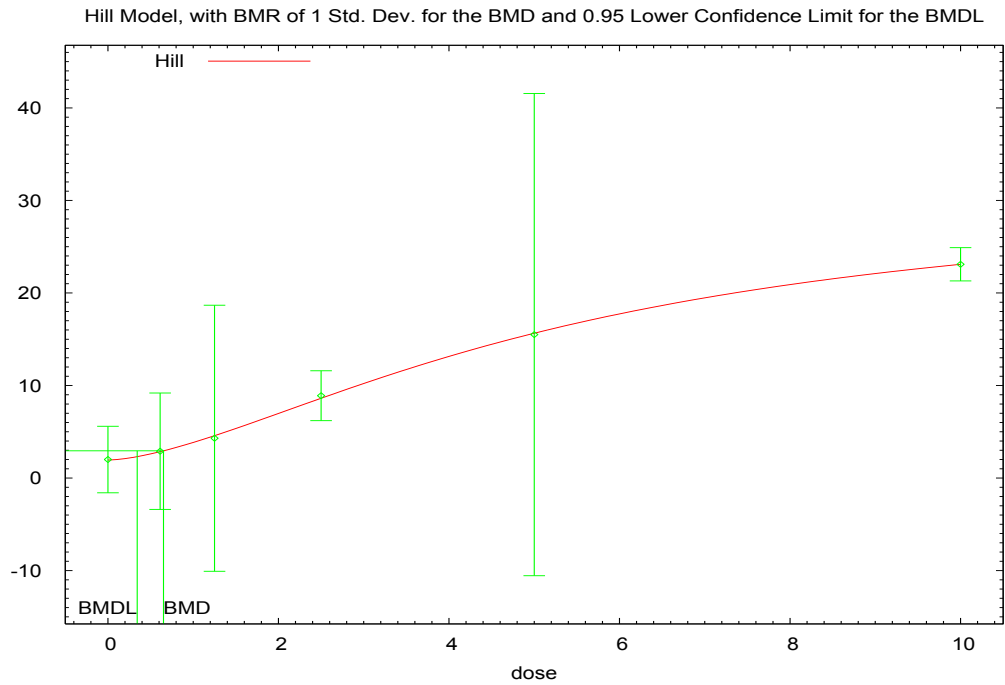
Chapter 4

A Comparison of Dose Response Relationships of Topoisomerase II Inhibitor-Induced Stabilized Cleavage Complexes and Micronucleus Formation in Human Lymphoblastoid Cells

Abstract

Topoisomerase II inhibitors are commonly used chemotherapeutic compounds that are associated with increased risk of therapy-related acute myeloid leukemias. Studies from our lab have investigated dose response relationships of micronucleus induction *in vitro* by a range of topoisomerase II inhibitors including aclarubicin and merbarone, which act prior to the formation of the cleavage complex; etoposide and mitoxantrone, which are topo II poisons and prevent religation of the double stranded break; and two bisdioxopiperazines, ICRF-154 and ICRF-187, which act after religation and trap the enzyme in a closed-clamp formation. All of the agents tested were potent in inducing micronuclei in human TK6 cells with significant increases seen at low to very low concentrations. Current studies have focused on comparing the induction of micronuclei in TK6 cells with the formation of stabilized topoisomerase II cleavage complexes using flow cytometry. The cleavage complex forms during the enzyme's catalytic cycle and its stabilization is a critical step leading to the formation of double stranded breaks by many topoisomerase II inhibitors. Both topoisomerase II poisons (etoposide and mitoxantrone) and the bisdioxopiperzines (ICRF-154 and -187) induced concentration-dependent increases in cells with stabilized cleavage complexes, though the magnitude of response varied, with a greater than 20-fold increase observed at the highest concentrations in cells treated with the topo II poisons compared to approximate 5-fold increases seen with the bisdioxopiperazines. As anticipated, agents that act prior to the cleavage step during the topoisomerase II catalytic cycle did not show

an increase in cells with stabilized cleavage complexes at concentrations that were

associated with large increases in micronuclei due to chromosome breakage. These

results show that this newly developed flow cytometry-based approach can be used

to assess dose response relationships for topoisomerase II inhibitor-induced

stabilized cleavage complex formation on a per cell basis, and when combined with

information on micronucleus formation (increases and origin), can be used in

human cells to distinguish between topoisomerase II poisons and catalytic

inhibitors that act either before cleavage or after religation of the double stranded

break.

Introduction

Type II DNA topoisomerases are critical nuclear enzymes that relieve

topological stress during cellular processes including DNA replication, transcription,

repair, and mitosis (1-4). During the catalytic cycle of the enzyme, topoisomerase II

(topo II) covalently binds to a DNA strand, leading to formation of a double stranded

break and a cleavage complex that serves as a gate through which the other DNA

duplex can pass. Following strand passage, the double stranded break is religated

and the enzyme is released from the DNA (Fig 4-1) (4). Disruptions to the enzyme's

catalytic cycle have the ability to lead to chromosomal abnormalities including

cancer initiating translocations (1-4).

Topo II inhibitors can act at various stages of catalytic cycle and fall into two

major classes: topo II poisons and catalytic inhibitors (Fig 4-1) (1,5). Topo II

poisons, such as etoposide, act to stabilize the cleavage complex and inhibit the

religation step, an important step leading to the formation of double stranded

breaks. Catalytic inhibitors, on the other hand, affect other parts of the topo II

catalytic cycle and have not been shown to significantly directly stabilize the

cleavage complex, though they have been shown to have clastogenic effects *in vitro*

and *in vivo* (5-7).

Because of its role in processes related to cell proliferation, topo II is a

common target for chemotherapeutic drugs, and several topo II inhibitors are front

line therapies for the treatment of a number of types of cancer. An early limiting

factor in the use of topo II inhibitors was an increased risk for development of

treatment-related acute leukemias (t-AML) (1-5) that develop secondary to the

original cancers for which the topo II inhibitors were originally prescribed. These

are characterized by short median latency periods of <2-3 years (8-11). Topo II

poisons etoposide and doxorubicin have been associated with t-AML caused by

balanced translocations involving the *MLL* gene on chromosome band 11q23 (8-9).

Similarly, mitoxantrone, prescribed both for treatment of certain cancers and

multiple sclerosis has been associated with a form of therapy related acute

promyelocytic leukemia (t-APL) caused by a reciprocal translocation fusing the

retinoic acid receptor alpha gene (*RARA*) from chromosome 17 to the promyelocytic

leukemia gene (*PML*) on chromosome 15 resulting in the stable expression of a

PML-RARa fusion protein (10-11). In addition to chemotherapy drugs, there is some

concern about dietary exposure to compounds, such as genistein, *in utero* leading to

increased risks of infant and childhood leukemias, as many flavonoids have been reported to inhibit isolated topo II in cell-free assays (12-13). While most research on topo II inhibitors has focused on topo II poisons, there is some evidence of similar leukemogenic effects seen in patients treated with reported catalytic inhibitors ICRF-154 and bimolane (14-15).

Topo II inhibitors have been categorized as a class of chemicals that exhibit a threshold dose response. This is largely been based on dose response data for formation of micronuclei with limited mechanistic work focusing primarily on topo II poisons (16). Meanwhile, topo II catalytic inhibitors have also been shown to have clastogenic effects *in vitro,* and have been associated with leukemogenic effects. Previous work from our lab has also shown that various types of catalytic inhibitors induce concentration dependent increases in micronuclei *in vitro*. The goal of the current study is to further investigate dose-response relationships of several topoisomerase II inhibitors by examining the ability of these compounds to stabilize the cleavage complex, an important step that occurs prior to the formation of unprotected double stranded breaks and the related formation of micronuclei. In the current study, we use a recently developed flow cytometry-based assay to detect topo II covalently bound to DNA to see if this method could be used to not only characterize dose-response relationships of SCC formation, but also identify where in the catalytic cycle a known or suspected topo II inhibitor might act. Our studies include the topo II poisons etoposide and mitoxantrone, as well as catalytic inhibitors aclarubicin, merbarone, and the bisdioxopiperazines, ICRF-154 and ICRF-

187, which act through a variety of different mechanisms. We also examined two

flavonoid compounds fisetin and genestein, which have both been reported to affect

topoisomerase II using isolated enzymes in cell free assays to see if similar effects

on topo II can be observed in cells.

Materials and Methods

Cell culture and treatments

The human lymphoblastoid cell line TK6 was maintained in RPMI 1640 medium

(GIBCO; Carlsbad, CA) containing 10% iron-supplemented calf serum (Hyclone;

Logan, UT) with 2 mM l-glutamine, 100 U/ml penicillin, and 100 μg/ml

streptomycin (Fisher Scientific; Pittsburg, PA) at 37 °C in an atmosphere of 5%

CO_2/95% air. Exponentially growing cells were treated with various concentrations

of each of the following topo II inhibitors: alcarubicin (Sigma; St. Louis, MO),

merbarone (NCI; Bethesda, MD), ICRF-154 (NCI; Bethesda, MD), ICRF-187 (NCI;

Bethesda, MD), mitoxantrone (insert company), and etoposide (Sigma; St. Louis, MO

). All compounds were dissolved in dimethylsulfoxide (DMSO) with a final DMSO

concentration of 0.1% in the culture flasks. Cells were treated continuously for 24

hours.

Sample preparation for Flow-cytometry and analysis

The procedure was performed as previously described by de Campos-Nebel *et al*

(17). Briefly, treated cells were washed twice with phosphate-buffered saline (PBS)

and allowed to recover for 60 minutes in fresh media. Cells were then centrifuged

and resuspended in 1ml of PHEM buffer (65 mM Pipes, 30 mM HEPES, 10 mM EGTA,

2 mM Mg$_2$Cl, pH 6.9) containing 1 mM PMSF, 0.5% Triton X-100 and heparin (0.01mg/ml) to extract free and weakly bound topo II from the cell. Cells were then fixed in 4% paraformaldehyde for 30 minutes. After washing with PBS, samples were resuspended in blocking buffer (3% BSA, 0.5% Triton X-100 in PBS) and incubated for 1 h. Samples were then incubated with the primary topo II antibody (Santa Cruz Biotechnology; Dallas, TX) diluted in blocking buffer to 1μg/ml for 2 h at room temperature. The cells were then washed and incubated with either an Alexa-Flour 488 or FITC conjugated secondary antibody (Jackson Immunoresearch Laboratories; West Grove PA) diluted in blocking buffer for 1 h. Finally cells were resuspended in PBS containing 200 μg/ml of RNAse A and 20 μg/ml of propidium iodide (PI) and incubated at room temperature for 30 min. Data from 20,000 cells per sample were acquired and analyzed using a Becton Dickinson FACSort flow cytometer and Cell Quest software using the same gating strategy outlined by de Campos-Nebel *et al* (17).

Statistical Analysis of Flow-Cytometry Data

For data obtained from the flow-cytometry based assay, an ANOVA test was performed and Dunnett's T-test was used to compare individual treatments to controls.

Results

Etoposide and Mitoxantrone

Topo II poisons etoposide and mitoxantrone have long been shown to interfere with the religation step of the topo II catalytic cycle through stabilization of the cleavage complex. Their inclusion in the current studies was to ensure that the flow-cytometry based assay was accurate and reliable and could be used to measure formation of stabilized cleavage complexes on a per cell basis. Our studies confirm that the previously published method by de Campos-Nebel *et al.* was reproducible in our lab, that the data acquired by the flow-cytometer could be analyzed on a per cell basis, and could consistently detect relatively small changes in the percentage of topo II+ cells, making it suitable for dose-response characterization of SCC formation.

Using the flow-cytometry based assay, both model topo II poisons etoposide and mitoxantrone induced significant concentration dependent increases in stabilized cleavage complexes with approximately 25-28% of cells containing SCCs at the highest concentrations tested (Figs 4-2A and 4-2B). The concentrations and treatment conditions for the current studies were selected to mirror those from a previous study in which dose response relationships for induction of micronuclei by topo II inhibitors were examined. Compared to the micronucleus data from these previous studies, stabilized cleavage complex formation by etoposide paralleled formation of micronuclei with significant increases seen of both across the entire concentration range tested. With mitoxantrone, every concentration tested resulted

in a higher percentage of cells with stabilized topo II compared to the percent of micronuclei formed.

Bisdioxopiperazines ICRF-154 and -187

Two representative bisdioxopiperazines, ICRF-154 and ICRF-187, have previously been shown to induce the formation of micronuclei due to both chromosome breakage and chromosome loss in concentration dependent manners with the percentages of total micronuclei formed at the highest concentrations actually being quite similar to those seen with topo II poisons etoposide and mitoxantrone. Also similar to the topo II poisons, both compounds induced concentration-dependent increases in cells with SCCs, albeit at much lower levels than the increases seen in cells treated with either etoposide or mitoxantrone, with a maximum of approximately 6% of cells treated with ICRF-154 and 11% of cells treated with ICRF-187 (figs 4-2C and 4-2D) exhibiting SCCs. At lower concentrations, the percent of cells showing stabilized cleavage complex formation for both ICRF-154 (≤12.5 μM) and ICRF-187 (≤ 2.5μM) were actually quite similar to the percent of micronuclei observed. At the higher concentrations, however, considerably more micronuclei were observed than cells with stabilized topo II.

Aclarubicin

In previous studies, aclarbucin induced concentration-dependent increases in micronuclei at low nanomolar concentrations. Parallel studies with kinetochore staining indicated that while a small portion of the increase in micronuclei was due to loss of whole chromosomes, nearly 90% of the micronuclei induced were due to

chromosome breakage. The current study showed no significant increase in stabilized cleavage complexes when tested using the same concentration range and treatment conditions used with the previously performed micronucleus assays (Fig 4-2E).

Merbarone

Merbarone, like aclarubicn, is believed to act prior to the cleavage step of the catalytic cycle of topo II. Once again, our previous studies indicated that merbarone also induced significant increases in micronuclei with the vast majority of the micronuclei were formed due to chromosome breakage. The increases in total micronuclei at the highest concentrations tested were actually the highest among all topo II inhibitors tested at nearly 11-fold higher than the control. In terms of induction of SCC, merbarone did not induce formation of stabilized cleavage complexes in cells across the concentration range tested (Fig 4-2f).

Time course comparisons of topo II poisons and bisdioxopiperazines

Another major goal of the current study was to determine if the flow-cytometry based assay could be used to distinguish between different classes of topo II inhibitors. While neither compound that acted prior to the cleavage step led to an increase in cells with stabilized topo II, both bisdioxopiperzines and topo II poisons showed linear or curvilinear increases in cells with stabilized cleavage complexes in our initial studies with the magnitude or response with topo II poisons being the considerably higher of the two. To see if there were any additional differences between the two classes of compounds, we decided to look at how time

110

of exposure to the compounds might influence the induction of stabilized cleavage complexes. The concentrations used in the time course experiments were chosen as those where significant increases in both MN and cells with SCCs were seen without excessive cytotoxicity. For both topo II poisons, etoposide and mitoxantrone, the increase in cells with SCCs that were seen at 4, 8, and 12 hours were actually higher than the responses seen at the same concentration at 24 hours (100 nM for both compounds) (fig 4-3). We also observed a decreasing trend, which may have been due to resolution of the SCCs with time or increased cytotoxicity with longer exposure to both compounds.

The time course of SCC formation in cells treated with ICRF-154 and -187 exhibited different patterns when compared to the topo II poisons. For ICRF-154, the number of cells with SCCs remained relatively constant at the 4 time points measured when treated continuously at a concentration of 25 μM. When cells were treated with 5 μM of ICRF-187, the number of cells with SCCs increased throughout the time course starting at approximate 4.5% at 4 hours and doubling to over 9% by the final 24 hour time point.

Fisetin and Genistein

The concentrations for fisetin and genistein were selected based on previously published studies for both compounds where significant increases in micronucleus induction occurred. With fisetin, no significant increases in cells with stabilized cleavage complexes were observed at either concentration tested. Cells treated with

genistein, on the other hand, exhibited increases in cells with SCCs at levels of approximately 7.5% of cells at 25µM and 18% at 50 µM (fig 4-4)

Discussion

The induction of topo II stabilized cleavage complexes by the compounds tested in the current study are consistent with the mechanisms by which the compounds have been reported to inhibit the enzyme. For instance, aclarubicin and merbarone have both been shown to affect the topo II catalytic cycle prior to formation of the double strand break but through different mechanisms. Aclarubicin is believed to act through intercalation, thereby preventing topo II from binding to DNA (18-19), whereas merbarone has been shown to act by preventing enzyme-mediated scission by topo II without intercalating or binding in the minor groove. Consistent with their proposed mechanisms, no significant increases in SCC were detected across the dose range tested for these two compounds. The fact that both of these compounds have been shown previously to have clastogenic effects is of particular interest. In regards to aclarubicin, it has been reported that the compound may affect multiple targets in the cell, such as histones, and topo II may not be the only enzyme or target affected (19). With merbarone, there are some conflicting reports as to whether the compound is indeed a topo II catalytic inhibitor or is actually a topo II poison with Snyder (20) proposing that it is a poison, based on his results that merbarone-induced micronucleus formation can be antagonized in V79 cells by known topo II catalytic inhibitors. Further mechanistic studies by Pastor *et al* (21) showed that merbarone-induced chromosome breakage occurs

during DNA replication supporting a proposed mechanism where stalled and collapsed replication forks, due to the inability of topo II to initiate cleavage of DNA to relieve topological strain, leads to formation of double stranded breaks. In the present study we show that merbarone does not stabilize the cleavage complex, a defining characteristic of topo II catalytic inhibtors , which is consistent with its proposed mechanism of action.

The topo II poisons tested in the current study included etoposide and mitoxantrone. The mechanism underlying the clastogenic effects induced by topo II poisons is well understood and involves stabilization of the cleavage complex and interference with religation, which would also lead to stabilization of the otherwise transient double stranded break that occurs during the enzyme's catalytic cycle. Subsequent removal of the covalently bound topo II by various mechanisms including proteasomal degradation then exposes or releases the double strand breaks (22-25). These can result in micronuclei or can be repaired through either the non-homologous end joining (NHEJ) or homologous recombination (HR) pathways. As expected, our current studies showed significant increases in cells with stabilized cleavage complexes at all concentrations and lengths of exposure to either etoposide or mitoxantrone.

The last class of topo II catalytic inhibitors tested were the bisdioxopiperazines, ICRF-154 and ICRF-187. These compounds are believed to trap topo II in a "closed-clamp" formation where the double strand break has been properly ligated and the enzyme is no longer covalently bound to the DNA but is

113

unable to be converted back to a catalytically active form (5-7). Much like the mechanism described above for merbarone, the resulting depletion of active topo II caused by these compounds could then lead to clastogenic responses as the enzyme is no longer available to relieve the torsional strain associated with DNA replication, transcription, and decatenation of sister chromatids during mitosis. The increase in cells with SCC's when treated with the catalytic inhibitors ICRF-154 and ICRF-187 in the current study is particularly interesting, and the low levels of stabilized cleavage complexes observed may explain some of the previously reported clastogenic effects observed by these compounds (6-7). Again much like with other catalytic inhibitors, there are some conflicting reports as to whether bisdioxopiperazines are indeed catalytic inhibitors or act as topo II poisons. Similar to their findngs with merbarone, Snyder and associates (20) showed decreases in micronuclei induced by both ICRF-154 and -187 when cells were also treated with known catalytic inhibitors. In addition, the structurally similar ICRF-193 has also been shown to induce concentration dependent increases in DNA-topo II crosslinks (26); and Cowell *et al* (27) reference unpublished results using the TARDIS assay, a microscopy based assay to detect SCC's in cells, suggesting that ICRF-193 both stabilizes the cleavage complex and can also act as catalytic inhibitor.

Another possible explanation is that the small increases in topo II SCCs are due to a potential reversible equilibrium that exists between the cleavage complex and the closed-clamp formations as previously described by our lab (28). Here, accumulated levels of the enzyme in the closed clamp could cause a shift of some

114

"trapped" but non-covalently bound enzyme back to the cleavage complex state, meaning that the SCCs observed occur secondary to inhibition of the step leading to release of the enzyme and not directly to inhibition of the religation step. The persistence or slight increase in cells with SCCs when treated with bisdioxopiperazines in our time course experiments might also support this hypothesis. Cells treated topo II poisons accumulate large amounts SCC's, which are then quickly resolved leading to double stranded breaks that are either repaired or accumulate to trigger cell death, whereas the cells treated with bisdioxopiperazines slowly deplete available topo II, shifting the equilibrium back towards the cleavage complex. This proposed reversible nature of this step of the topo II catalytic cycle requires further investigation.

In addition to the model topo II inhibitors tested, we also studied cells treated with the flavonoids fisetin and genistein. Both have been shown in cell free systems to inhibit topo II, but little evidence exists to show that the same inhibitory effects are seen in cells exposed to these compounds. The slight increases in cells with stabilized topo II when treated with genistein coupled with previously reported evidence that it induces micronucelei caused mostly by chromosome breakage, suggests that genistein does in fact act as a topo II poison in cells. Treating cells with fisetin, on the other hand, did not lead to an increase in cells with stabilized cleavage complexes, similar to the pre-cleavage acting catalytic inhibitors aclarubicin and merbarone, or to chemicals that do not act through topo II inhibition. Unlike the two catalytic inhibitors that act prior to DNA cleavage that induce

micronuclei due to chromosome breakage, fisetin has been shown to induce micrconuclei caused almost entirely by chromosome loss (29).

While many catalytic inhibitors have been shown to cause clastogenic effects with increases in micronucleus formation, the current method may be useful to screen for and differentiate between agents that act prior to, or after, the cleavage step of the catalytic cycle. In our studies, we were able to see clear differences between aclarubicin and merbarone compared to the other four topo II inhibitors that act following formation of the cleavage complex. Though stabilization of the cleavage complex occurs prior to formation of micronuclei, the current assay to detect SCCs was not necessarily more sensitive in detecting topo II poisons. In cells treated with etoposide, significant increases were seen in both MN and SCCs at the lowest concentration tested. Nevertheless, data from this assay may be useful in properly identifying and classifying compounds that have been shown to inhibit topo II in cell-free assays with isolated enzymes versus compounds that target topo II in intact cells, though further studies will be required to more thoroughly validate this approach and will need to focus on a broader range of suspected topo II inhibitors beyond fisetin and genestein.

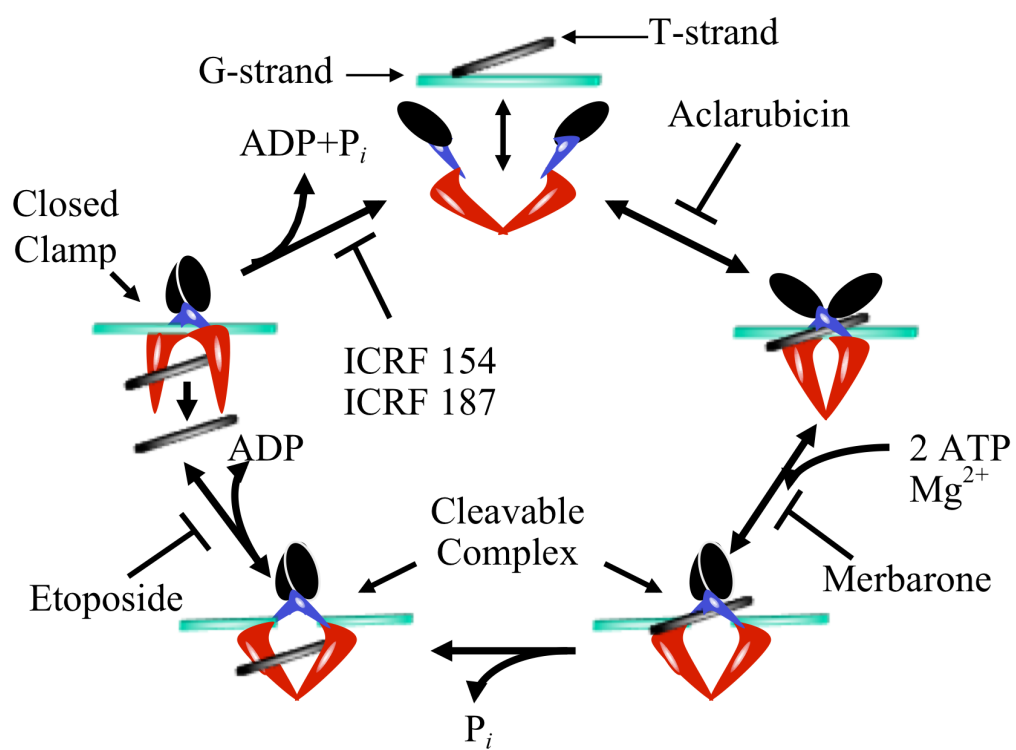**Figure 4-1 Topoisomerase II Catalytic Cycle**

Figure 4-1. Topo II catalytic cycle. The sites of action of the topo II inhibitors used in current study are shown. Adapted from Mondrala S and Eastmond DA. (5)
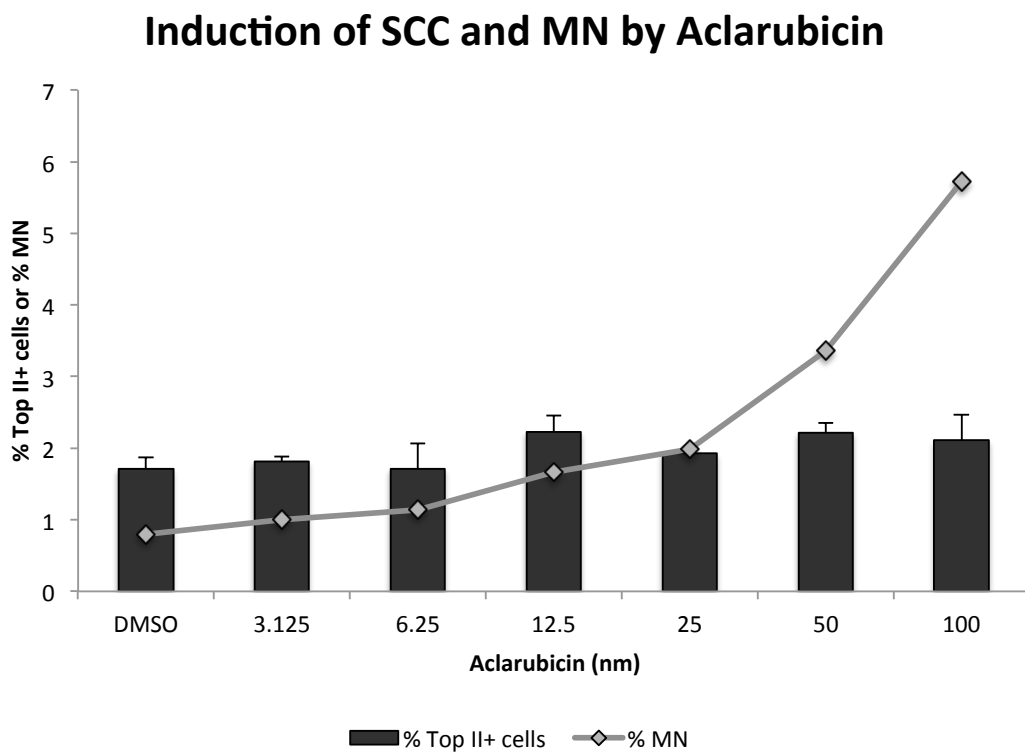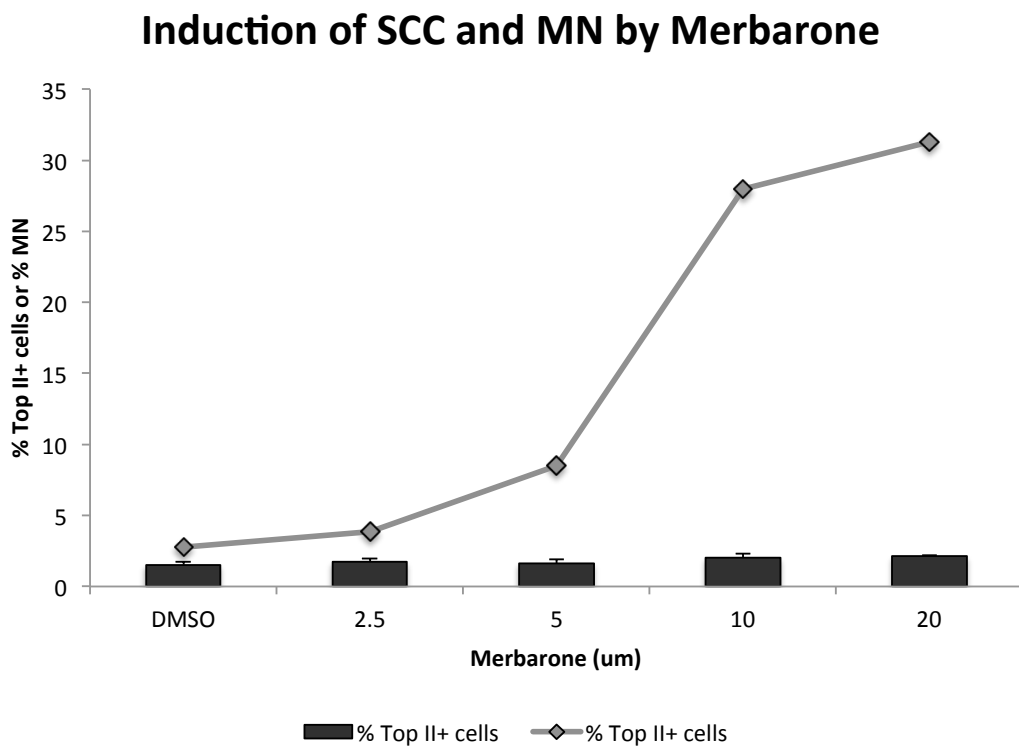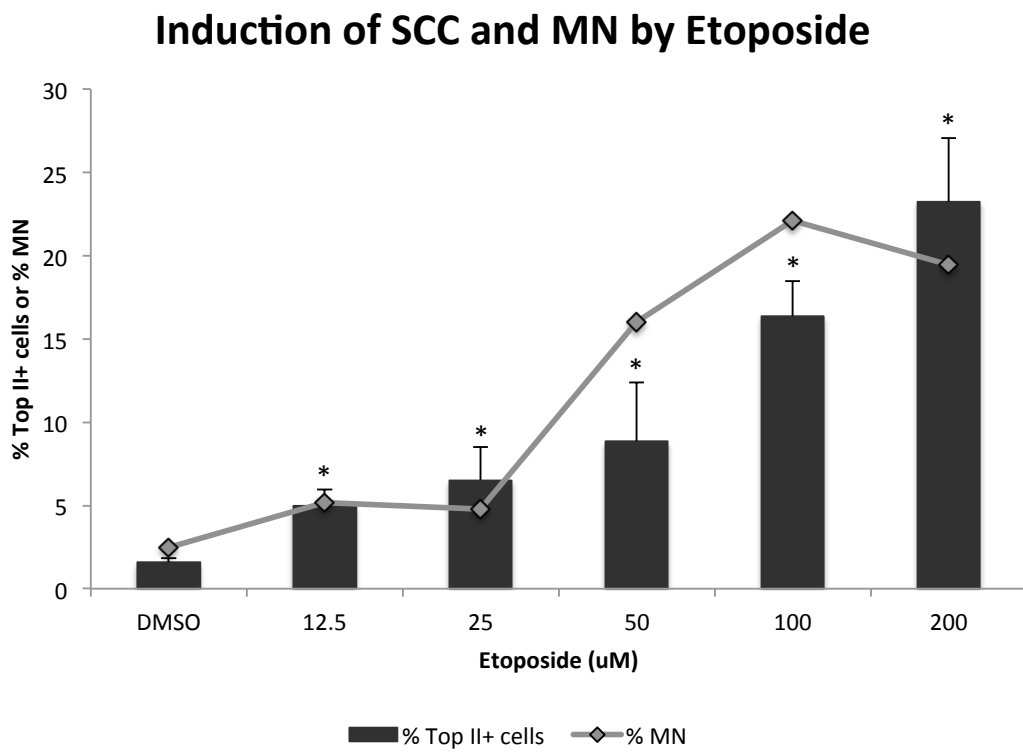
Figure 4-2a

Induction of SCC and MN by Aclarubicin

Figure 4-2b

Induction of SCC and MN by Merbarone

Figure 4-2c

Induction of SCC and MN by Etoposide

Figure 4-2d

Induction of SCC and MN by Mitoxantrone

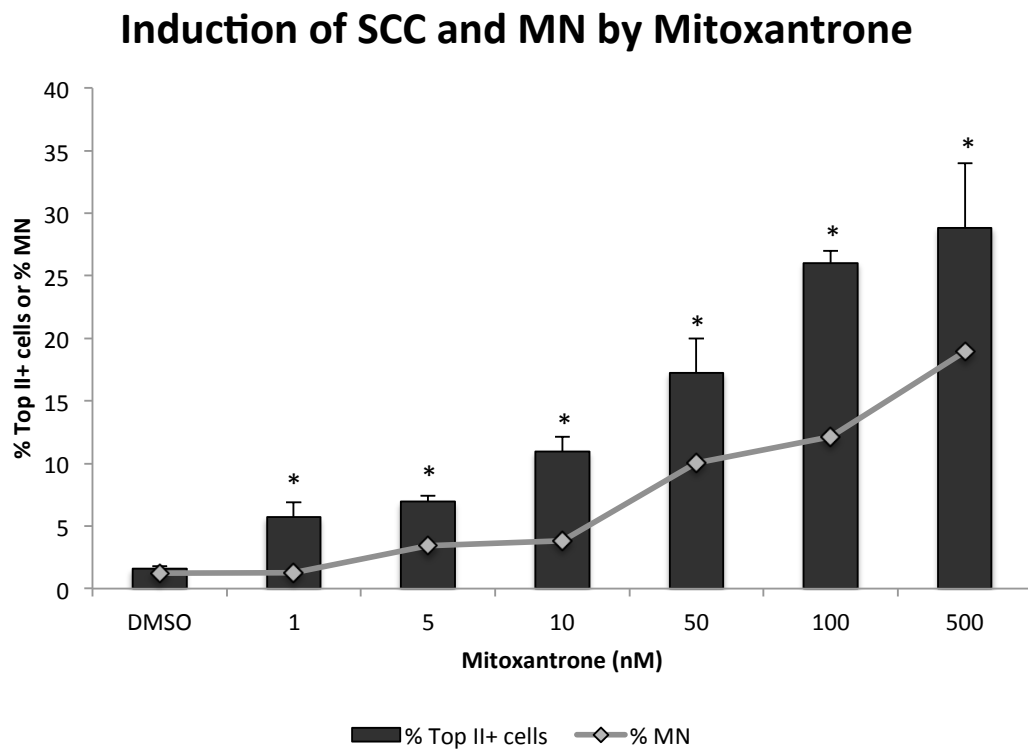**Figure 4-2e**

Induction of SCC and MN by ICRF-154
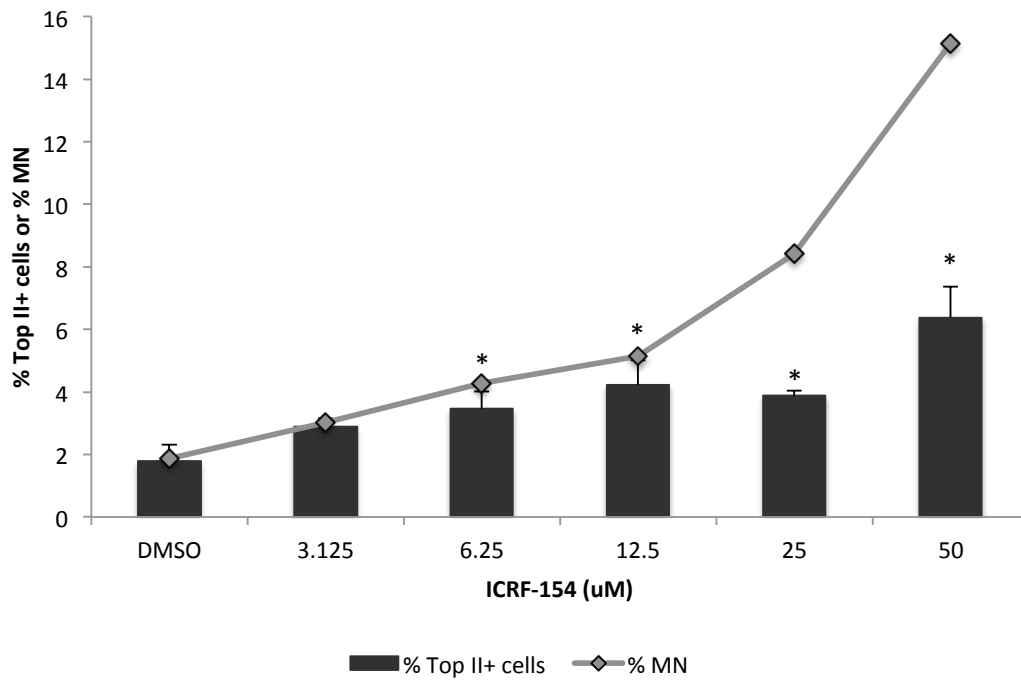
Figure 4-2f

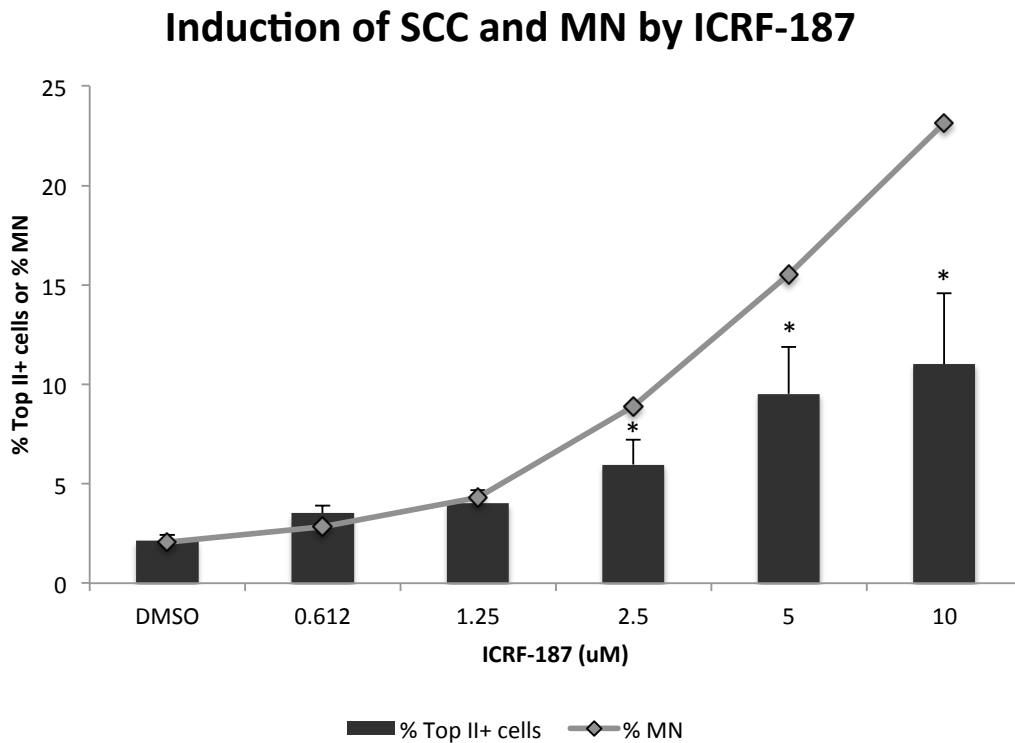**Induction of SCC and MN by ICRF-187**

Figure 4-2 Induction of stabilized cleavae complexes (SCC) and micronuclei (MN) by a) aclarubicin, b) merbarone, c) etoposide, d) mitoxantrone, e) ICRF-154, and f) ICRF-187. Percentages of topo II+ cells are shown using the columns and data is represented as means and standard deviations. For direct comparison, percent micronuclei measured by flow cytometry at the same concentrations are overlayed with the line graph using the same axes.

Figure 4-3

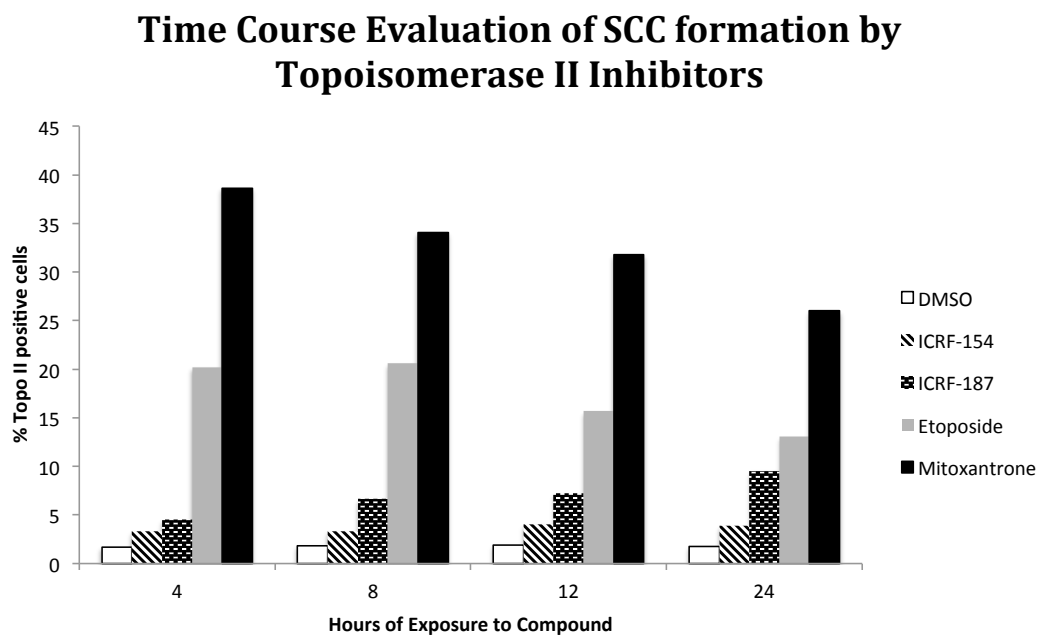## Time Course Evaluation of SCC formation by Topoisomerase II Inhibitors

Figure 4-3. Time course evaluation of stabilized cleavage complex formation in cells treated with bisdioxopiperazines, ICRF-154 and ICRF-187, and topo II poisons, etoposide and mitoxantrone.
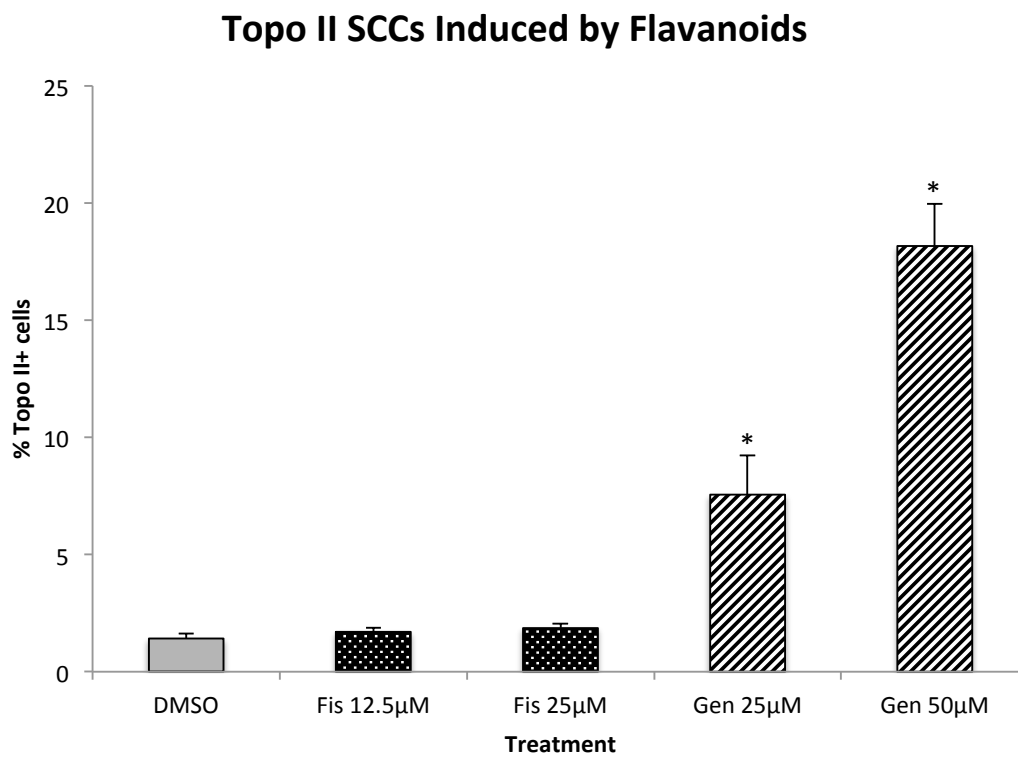
Figure 4-4

Figure 4-4 Percentages of topo II positive cells induced by flavonoids fisetin and genistein. Data represents means and standard deviations.

References

1. Pendleton M, Lindsey RH Jr, Felix CA, Grimwade D, Osheroff N. Topoisomerase II and leukemia. Ann N Y Acad Sci. 2014;1310: 98–110.

2. McClendon AK, Osheroff N. DNA topoisomerase II, genotoxicity, and cancer. Mutat Res. 2007;623: 83–97.

3. Deweese JE, Osheroff N. The DNA cleavage reaction of topoisomerase II: wolf in sheep's clothing. Nucleic Acids Res. 2009;37: 738–748.

4. Vos SM, Tretter EM, Schmidt BH, Berger JM. All tangled up: how cells direct, manage and exploit topoisomerase function. Nat Rev Mol Cell Biol. 2011;12: 827–841

5. Nitiss JL. 2009. DNA topoisomerase II and its growing repertoire of biological functions. *Nat Rev Cancer.* 9**:** 327– 337

6. Vuong MC, Hasegawa LS, and Eastmond DA. 2013. A comparative study of the cytotoxic and genotoxic effects of ICRF-154 and bimolane, two catalytic inhibitors of topoisomerase II. *Mut Res.* 750(1-2):73-71

7. Wang L and Eastmond D.A. 2002. Catalytic inhibitors of topoisomerase II are DNA-damaging agents: induction of chromosomal damage by merbarone and ICRF-187. *Envrion Mol Mutagen.* 39(4):348-56

8. Mauritzson N, Albin M, Rylander L, Billström R, Ahlgren T, Mikoczy Z, et al. Pooled analysis of clinical and cytogenetic features in treatment-related and de novo adult acute myeloid leukemia and myelodysplastic syndromes based on a consecutive series of 761 patients analyzed 1976-1993 and on 5098 unselected cases reported in the literature 1974-2001. Leukemia. 2002;16: 2366–2378.

9. Joannides M, Mays AN, Mistry AR, *et al.* 2011. Molecular pathogenesis of secondary acute promyelocytic leukemia. *Mediterr J Hematol Infect Dis.* 3**:** e2011045.

10. Park SH, Chi HS, Cho YU, *et al.* 2013. Evaluation of prognostic factors in patients with therapy-related acute myeloid leukemia. *Blood Res.* 48: 185–192.

11. Rashidi A and Fisher IS. 2013. Therapy-related acute promyelocytic leukemia: a systematic review. *Med Oncol.* 30**:** 625.

12. Strick R, Strissel PL, Borgers S, Smith SL, Rowley JD. Dietary bioflavonoids induce cleavage in the MLL gene and may contribute to infant leukemia. Proc Natl Acad Sci U S A. 2000;97: 4790–4795.

13. Spector LG, Xie Y, Robison LL, Heerema NA, Hilden JM, Lange B, et al. Maternal diet and infant leukemia: the DNA topoisomerase II inhibitor hypothesis: a report from the children's oncology group. Cancer Epidemiol Biomarkers Prev. 2005;14: 651–655.

14. Y.S. Li, Y.L. Zhao, Q.P. Jiang, C.L. Yang Specific chromosome changes and nonoccupational exposure to potentially carcinogenic agents in acute leukemia in China Leuk. Res., 13 (1989), pp. 367-376

15. Y. Xue, D. Lu, Y. Guo, B. LinSpecific chromosomal translocations and therapy-related leukemia induced by bimolane therapy for psoriasis Leuk. Res., 16 (1992), pp. 1113-1123

16. Lynch A, Harvey J, Aylott M, Nicholas E, Burman M, Siddiqui A, et al. Investigations into the concept of a threshold for topoisomerase inhibitor-induced clastogenicity. Mutagenesis. 2003;18: 345–353.

17. de Campos-Nebel M, Palmitelli M, González-Cid M. A flow cytometry-based method for a high-throughput analysis of drug-stabilized topoisomerase II cleavage complexes in human cells. Cytometry A. 2016;89: 852–860.

18. Pang B, de Jong J, Qiao X, Wessels LF, Neefjes J. Chemical profiling of the genome with anti-cancer drugs defines target specificities. Nat Chem Biol. 2015 Jul;11(7):472-80. Epub 2015 May 11

19. Pang B, Qiao X, Janssen L, Velds A, Groothuis T, Kerkhoven R, et al. Drug-induced histone eviction from open chromatin contributes to the chemotherapeutic effects of doxorubicin. Nat Commun. 2013;4: 1908.

20. Snyder RD. Evidence from studies with intact mammalian cells that merbarone and bis(dioxopiperazine)s are topoisomerase II poisons. Drug Chem Toxicol. 2003;26: 15–22.

21. Pastor N, Domínguez I, Orta ML, Campanella C, Mateos S, Cortés F. The DNA topoisomerase II catalytic inhibitor merbarone is genotoxic and induces endoreduplication. Mutat Res. 2012;738-739: 45–51.

22. Mao Y, Desai SD, Ting CY, Hwang J, Liu LF. 26 S proteasome-mediated degradation of topoisomerase II cleavable complexes. J Biol Chem 2001;276:40652–40658.

23. Hartsuiker E, Neale MJ, Carr AM. Distinct requirements for the Rad32(Mre11) nuclease and Ctp1(CtIP) in the removal of covalently bound topoisomerase I and II from DNA. Mol Cell 2009;33:117–123.

24. Cortes Ledesma F, El Khamisy SF, Zuma MC, Osborn K, Caldecott KW. A human $5'$ - tyrosyl DNA phosphodiesterase that repairs topoisomerase-mediated DNA damage. Nature 2009;461:674–678.

25. 18. Borda MA, Palmitelli M, Vero n G, Gonz alez-Cid M, de Campos-Nebel M. Tyrosyl- DNA-Phosphodiesterase I (TDP1) participates in the removal and repair of stabilized-Top2a cleavage complexes in human cells. Mutat Res 2015;781:37–48.

26. Huang KC, Gao H, Yamasaki EF, Grabowski DR, Liu S, Shen LL, et al. Topoisomerase II poisoning by ICRF-193. J Biol Chem. 2001;276: 44488–44494.

27. Cowell IG, Tilby MJ, Austin CA. An overview of the visualisation and quantitation of low and high MW DNA adducts using the trapped in agarose DNA immunostaining (TARDIS) assay. Mutagenesis. 2011;26: 253–260.

28. Mondrala S, Eastmond DA. Topoisomerase II inhibition by the bioactivated benzene metabolite hydroquinone involves multiple mechanisms. Chem Biol Interact. 2010;184: 259–268.

29. Gollapudi P, Hasegawa LS, Eastmond DA. A comparative study of the aneugenic and polyploidy-inducing effects of fisetin and two model Aurora kinase inhibitors. Mutat Res Genet Toxicol Environ Mutagen. 2014;767: 37–43.

Conclusions

This research was initiated to investigate the genotoxicity of different types of enzyme inhibitors, in particular those that are known or suspected to inhibit either Aurora kinases or topoisomerase II. The initial chapter compared the aneugenic and clastogenic properties of two Aurora kinase inhibitors and compared those effects seen to a plant flavonoid, fisetin, which had previous been reported to inhibit Aurora kinases as well as topo II in different studies. Based on the differences seen between fisetin and the two kinase inhibitors, this project was followed by a more thorough investigation of the genotoxic effects caused by topo II inhibitors, with a focus on understanding how different mechanisms of inhibition of the enzyme affects both the types of chromosomal damage that can occur as well dose-response for those compounds. Lastly, we sought to investigate whether detection and quantification of stabilized topo II cleavage complexes, a precursor lesion that occurs prior to formation of double stranded breaks and micronuclei, could be used as a more sensitive endpoint for characterizing genotoxicity for topo II inhibitors and be used to identify where in the enzymes catalytic cycle a compound would act. A summary of the major findings of this research are listed below:

1) Aurora kinase inhibitors VX-680 and ZM-447439 are effective aneuploidy and polyploidy-inducing agents *in vitro*, and indicate that numerical chromosomal alterations result from the inhibition of Aurora kinases in human cells. The chromosomal changes seen at low nanomolar concentrations of VX-680 and ZM-

447939 likely to contribute to anti-neoplastic effects attributed to these Aurora kinase inhibitors.

2) Similar to Aurora kinase inhibitors, the plant flavonoid induced increases in micronuclei due to chromosome loss at non-cytotoxic concentrations. While increases polyploidy were also observed using a flow-cytometry based assay, these effects were only seen when cells after the compound was removed from the culture and cells were allowed to recover for 12-24 hours, indicating that fisetin also induces cell cycle delay, unlike Aurora kinase inhibitors.

3) Topoisomerase II inhibitors induce concentration dependent increases in micronuclei. These micronuclei were largely formed due to chromosome breakage, though small increases in chromosome loss were observed as well. These effects were seen in both topo II poisons, which act to stabilize the cleavage complex (etoposide and mitoxantrone), as well as topo II catalytic inhibitors that act both prior to cleavage (aclarubicin and merbarone) and after religation of the double stranded break (ICRF-154 and ICRF-187)

4) In terms of potency of topo II inhibitors, bisdioxopiperazines ICRF-154 and ICRF-187 as well as merbarone induced significant increases in MN at low micromolar concentrations. Effects seen with aclarubicin occurred at similar nanomolar concentrations as the topo II poison etoposide. The cytotoxicity and magnitude of

micronucleus induction suggest that effects seen with aclarubicin may be due to effects on other cellular targets.

5) While topo II poisons are known to cause chromosome breakage by stabilization of the enzyme-DNA cleavage complex, treatment of cells with post-religation catalytic inhibitors ICRF-154 and ICRF-187 also led to increases in cells with SCCs when measured using a recently developed flow-cytometry based assay. In contrast, treatment with either aclarubicin or merbarone led to no increases in cells with SCCs.

6) While several flavonoids have been reported to poison topo II in cell free enzyme activity assays, it was unclear if these compounds actually targeted or inhibited topo II in intact cells. The slight increases in cells with stabilized topo II when treated with genistein coupled with previously reported evidence that it induces micronucelei caused mostly by chromosome breakage, suggests that genistein does in fact act as a topo II poison in cells. Treating cells with fisetin, on the other hand, did not lead to an increase in cells with stabilized cleavage complexes, similar to the pre-cleavage acting catalytic inhibitors aclarubicin and merbarone.

The research projects included in this dissertation also utilized several recently developed flow cytometry based assays for rapid evaluation of various endpoints including aneuploidy, polyploidy, micronucleus induction, and evaluation

of stabilized of topo II cleavage complexes. While traditional microscopy based assays are limited in terms of the number of cells that can be scored, scoring biases, and other inconsistencies, flow cytometry allows for robust data collection from large numbers of cells, in some cases up to 20,000 cells per treatment. Evaluation of large numbers of cells often is often advantageous, particularly in dose-response evaluation. While this research was largely focused on characterizing the genotoxic effects of unique classes of enzyme inhibitors, we were also interested in evaluating the usefulness and validating the use of these flow-cytometry based assay. Our results showed that:

1) The flow-based aneuploidy assay useful for simultaneous evaluation of numerical chromosomal aberrations, though it was limited in regards to detection of small amounts of chromosome loss. Aurora kinase inhibitors as well as fisetin were associated with statistically significant increases in micronuclei due to chromosome loss, though no such increases in hypodiploidy were observed using the flow-based assay.

2) The flow based *in vitro* micronucleus assay was slightly less sensitive than it's traditional microscopy based counterpart. Among five topoisomerase II inhibitors compared using the two assays, all had at least one concentration at which no significant increase in micronuclei was observed using flow-cytometry that was significant when assessed by microscopy.

3) Flow cytometric analysis of large number of cells presents unique statistical challenges when trying to assess dose-response relationships and identify possible NOGELs or LOGELs. These limitations can be overcome with use of modeling approaches such as benchmark dose modeling.

4) The flow cytometry based assay for detection of the stabilized topo II cleavage complexes does not appear to be any more sensitive than traditional genotoxicity endpoints such as induction of micronuclei. This assay, however, was useful in discriminating between topo II inhibitors that act prior to the cleavage step of the enzyme's catalytic cycle and those that act either by poisoning the enzyme or after religation of the double strand break.

Appendix

Studies Related to Detection of Mitoxantrone-Induced Translocations in TK6 and HL-60 Cells

This appendix contains information on the research approaches, methods, limited results, and recommendations related to a project intended to identify mitoxantrone-induced translocations *in vitro* using PCR.

The mechanisms of leukemia-specific translocations caused by the topo II poison etoposide have been fairly well established in several key studies both *in vivo* and *in vitro* [1-3]. While it appears mitoxantrone may act in a similar manner, there appear to be key differences. In particular, mitoxantrone leads to the generation of a distinct balanced translocation, t(15,17), unique from the 11q23 translocations associated with other topo II poisons [4]. In addition, translocation break points that have been mapped in patients correspond to very specific points on the chromosome, including an 8bp hotspot on chromosome 15 [4-6]. *In vitro* studies detailing the mechanisms by which mitoxantrone acts and ultimately leads to development of leukemia in humans would be useful in understanding the risk associated with topo II inhibitors.

The first part of this project involved characterization of the effects of concentration and exposure time on cytotoxicity and DNA damage. To this extent, various time course experiments were conducted in order to identify treatment conditions with mitoxantrone that were most likely to give rise to translocations in cells.

Since breakpoint hotspots have been identified for t-APL, particularly within chromosome 15, polymerase chain reaction (PCR) with *PML-RARA* specific primers was attempted to confirm the occurrence of translocations *in vitro* following

chromosomal breakage. Because PCR-based approaches are commonly used in clinical settings for the diagnosis of APL, the sensitivity of PCR should allow for detection of even rare occurrences of t(15,17) tranlocations.

Primary studies were carried out using TK6 human lymphoblastoid cells, with follow-up studies in HL-60 cells, as a myeloid cell line may be a more representative surrogate for the precursor from which t-APL would arise due to the expression and activity of RAR-alpha in these cells.

Cytotoxity and Micronucleus induction in mitoxantrone treated cells

Primary studies characterizing the cytotoxic and genotoxic effect of mitoxantrone were conducted in TK6 cells (Figures A-1 and A-2). Results indicate that short-term exposures of 6 hours to mitoxantrone are enough to induce DNA damage as seen by increases in micronuclei using flow-cytometry. In addition, these increases are accompanied by less cytotoxicity compared to longer exposure times. Further studies were carried out in which treatment cultures were washed out and cells were suspended in fresh media and allowed to recover. In these experiments, cells exposed to mitoxantrone for shorter periods of 6-12 hours were able to recover and cell growth was comparable to DMSO treated cells (data not shown).

A comparison of micronucleus induction in TK6 and HL-60 cells was also performed (Figure A-3). Mitoxantrone induced similar levels of MN in both cell types across most of the concentration range tested. HL-60 cells also behaved similarly to TK6 cells when treated for periods shorter than 24hours (Figure A-4).

Figure A-1: Relative Increase in Cell Counts (RICC) of Cells Treated with Mitoxantrone
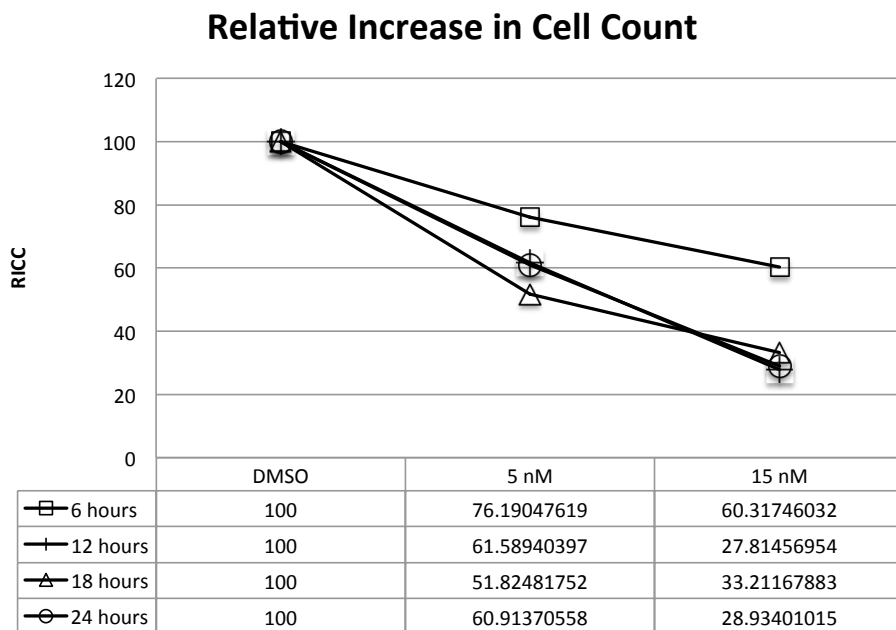
Relative Increase in Cell Count

	DMSO	5 nM	15 nM
6 hours	100	76.19047619	60.31746032
12 hours	100	61.58940397	27.81456954
18 hours	100	51.82481752	33.21167883
24 hours	100	60.91370558	28.93401015

Figure A-1 Graph and corresponding table below indicate relative increases in cell counts, a measure of cytotoxicity. RICC was calculated by [(increase in # of cells treated)/(increase in # of control cells)]*100.

Figure A-2: Induction of MN by mitoxantrone in TK6 cells at multiple time points
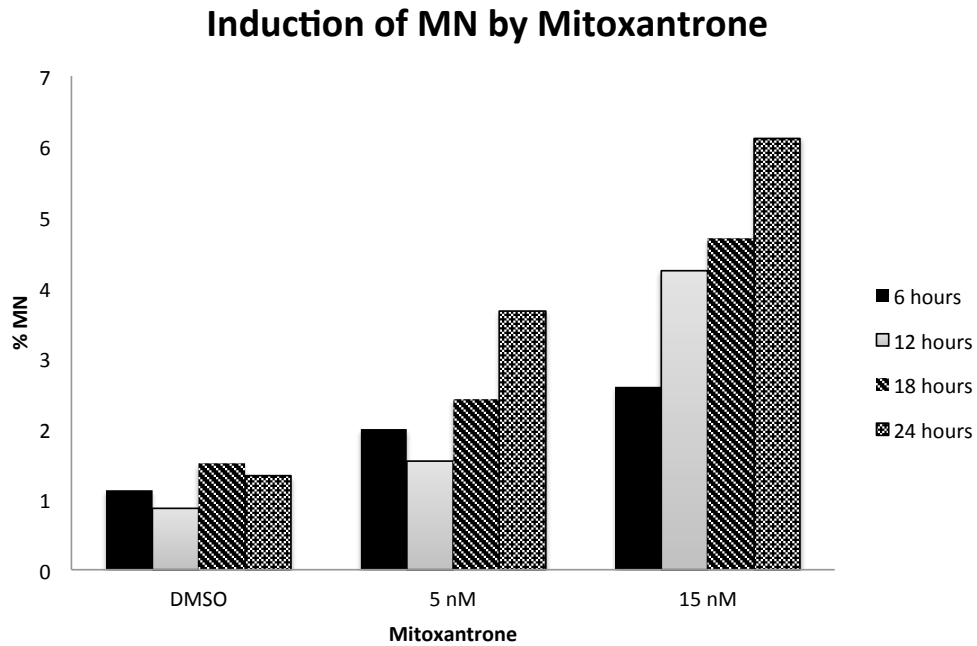
Induction of MN by Mitoxantrone

Figure A-2 Frequencies of micronuclei (MN) in TK6 cells treated with mitoxantrone or control (DMSO) for either 6, 12, 18, or 24 hours. Data from 20,000 nuclei were collected using flow-cytometry.

Figure A-3 Comparison of MN induction by mitoxantrone in TK6 and HL-60 cells
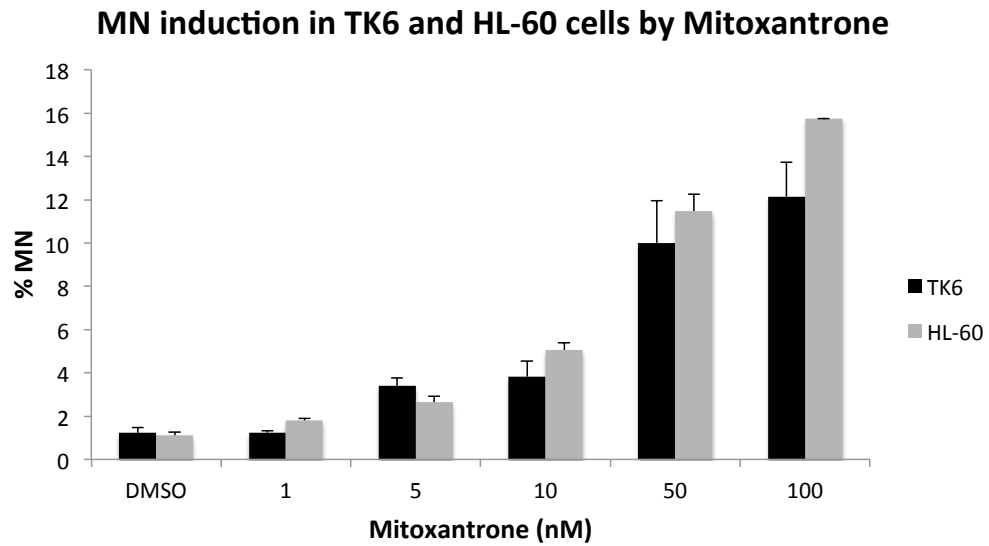

Figure A-3 Percentages of micronuclei in TK6 and HL-60 cells treated mitoxantrone measured using a flow cytometry-based *in vitro* micronucleus assay. Data represents means and standard deviation.

Figure A-4: Induction of MN by mitoxantrone in HL-60 cells at multiple time points
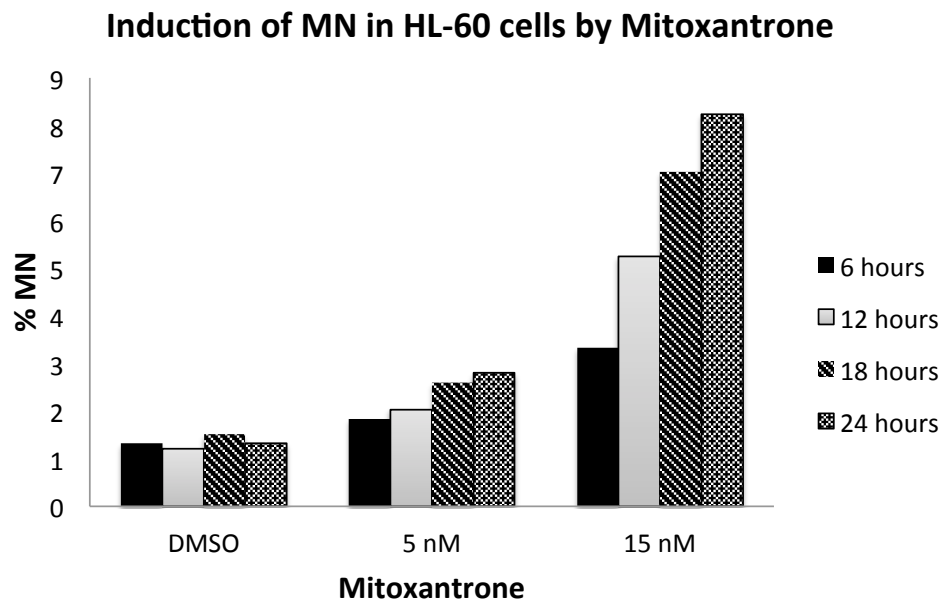

Figure A-4 Frequencies of micronuclei (MN) in HL-60 cells treated with mitoxantrone or control (DMSO) for either 6, 12, 18, or 24 hours. Data from 20,000 nuclei were collected using flow-cytometry.

PCR based detection of mitoxantrone-induced translocations

Based on results from cytotoxicity and genotoxicity studies described above, both TK6 and HL-60 cells were treated using two different strategies in attempt to maximize the number of cells with DNA damage that would lead to detectable amounts of translocations. The first was a continuous 24-hour treatment of cells in culture at 15 nM, as the longest time periods consistently resulted in the largest increases in MN. The second was a multiple treatment scheme with a shorter exposure time (12 hours) followed by a washout of the compound and recovery time of 72 hours, with this cycle repeated three times consecutively. The reasoning for the second exposure strategy was that 1) the lower cytotoxic conditions would be more favorable for our studies, 2) recovery time between treatments would allow cells with translocations to divide and expand in number, and 3) the multiple treatments would more closely resemble a chemotherapy model in which multiple courses of the drug are administered.

PCR primers and conditions for the PML-RARA fusion product that results from the t(15,17) translocation had previously been published by McHale *et al* [7] and are listed in Table A-1. In repeated experiments using both treatment strategies in both TK6 and HL60 cells, no visible PCR bands were detected.

Table A-1 PCR Primers and reaction conditions

Primer	Sequence	PCR Conditions
Forward Primer (Exon 3)	5'-GGACCTCAGCTCTTGCATCAC-3'	50°C for 2min, followed by 50 cycles of 15 s at 95°C, 30 s at 60°C, and 30s at 72°C
Forward Primer (Exon 6)	5'-TCTTCCTGCCCAACAGCAA-3'	
Reverse Primer	5-CATAGTGGTAGCCTGAGGACTTGT-3'	

Recommendations

The PCR based strategies employed in these experiments were unable to detect mitoxantrone-induced translocations resulting in expression of the PML-RARA fusion product. There are several possibilities why this might be the case. The first is that the occurrence of such translocations is incredibly rare and even if a very small number of cells in culture do contain any translocations, it is possible that those transcripts were not harvested during mRNA extraction. To that extent, tweaks to the multiple exposure strategy used here, including starting with lower cell concentration allowing affected cells to clonally expand further might increase the likelihood of detection of rare translocations. In addition, it is possible that neither HL60 nor TK6 cells are the ideal models for detection of these rare events and perhaps working in even further undifferentiated cell types such as human derived pluripotent stem cells would be more appropriate. If able to detect translocations *in vitro,* qPCR methods could be utilized to quantify another critical lesion related to topo II poison induced leukemia.

References

1. Pendleton M, Lindsey RH Jr, Felix CA, *et al*. 2014. Topoisomerase II and leukemia. *Ann N Y Acad Sci.* 1310:98-110

2. McClendon AK & Osheroff N. 2007. DNA topoisomerase II, genotoxicity, and cancer. *Mutat Res.* 623**:** 83–97.

3. Deweese JE & Osheroff N. 2009. The DNA cleavage reaction of topoisomerase II: wolf in sheep's clothing. *Nucleic Acids Res.* 37**:** 738–748.

4. Mauritzson N, Albin M, Rylander L, *et al.* 2002. Pooled analysis of clinical and cytogenetic features in treatment- related and *de novo* adult acute myeloid leukemia and myelodysplastic syndromes based on a consecutive series of 761 patients analyzed 1976–1993 and on 5098 unselected cases reported in the literature 1974–2001. *Leukemia* 16**:** 2366–2378.

5. Joannides M, Mays AN, Mistry AR, *et al.* 2011. Molecular pathogenesis of secondary acute promyelocytic leukemia. *Mediterr J Hematol Infect Dis.* 3**:** e2011045.

6. Rashidi A and Fisher IS. 2013. Therapy-related acute promyelocytic leukemia: a systematic review. *Med Oncol.* 30**:** 625.

7. McHale CM, Lan Q, Corso C, Li G, Zhang L, Vermeulen R, et al. Chromosome Translocations in Workers Exposed to Benzene. J Natl Cancer Inst Monogr. Oxford University Press; 2008;2008: 74–77.